

# **Novel analytical biosensors for Point-of-Need applications**

Juanjuan Liu

Bioengineering Department

McGill University, Montreal

June 2021

A thesis submitted to McGill University in partial fulfillment of the requirements of the degree of Doctor of Philosophy in Biological and Biomedical Engineering

© Juanjuan Liu 2021

## Abstract

Sensors developed for Point-of-Need (PON) applications such as health care and food safety are closely related to our daily life. They offer an analytical way to detect disease-related biomarkers or food contaminants, which helps with the follow-up decision or solution making. The development of PON sensors is still challenging regarding many factors such as sensitivity, portability, and cost. To address these problems, different sensor parameters are discussed and elaborated. Based on different transducers, there are various types of sensors, among which, plasmonic and ElectroChemical (EC) sensors are commonly used and studied due to their high sensitivity and specificity. Therefore, sensors based on these two transducing techniques, more specifically, Surface Enhanced Raman Spectroscopy (SERS) and EC, are thoroughly reviewed with discussion on fundamental properties, materials, techniques, and applications, allowing for a better understanding and promoting the development of biosensors at PON.

Further, to explore sensors that address the limitation of portability and cost for practical applications, a multimodal biosensing platform is developed at low cost and evaluated for PON applications that are related to health and food quality monitoring. More specifically, a substrate is fabricated by electrochemically depositing silver nanoparticles (AgNPs) on a commercial glucose test strip. The proposed biosensing platform is then applied for EC detection of urea that is important for health monitoring and food safety. The linear detection range of urea concentration within the physiological range is studied. Further, other sensing performances such as reproducibility and stability are studied. Additional measurements of urea in reconstituted plasma and milk samples are also conducted to show the potential of the substrate for practical applications. Moreover, this platform is adapted for the detection of chlorfenapyr, which is an insecticide used in agriculture. It is a potential food contaminant in vegetables such as chives. Compared to the application to urea detection, this platform is used here as a multimodal sensor that combines EC and SERS to provide complementary information for the detection of chlorfenapyr. It is used as a working electrode for chlorfenapyr detection via EC, and as a SERS substrate for detection via Raman spectroscopy. The results show the potential of the multifunctional sensor for applications to food quality monitoring.

As the demand for PON applications is increasing, the development of sensors at PON is attracting more and more attention. The exploration of various factors that play an important role for sensors

in this thesis advances this field. The fabrication and evaluation of this inexpensive biosensing device based on an AgNP-coated glucose test strip open up a novel way towards cost-effective applications in different areas.

## Résumé

Les capteurs développés pour les applications au point de besoin (PON) telles que les soins de santé et la sécurité alimentaire sont étroitement liés à notre vie quotidienne. Ils offrent un moyen analytique de détecter des biomarqueurs ou des contaminants alimentaires liés à des maladies, ce qui aide à la décision de suivi ou à la prise de solutions. Le développement des capteurs PON est toujours difficile en ce qui concerne de nombreux facteurs tels que la sensibilité, la portabilité et le coût. Pour résoudre ces problèmes, différents paramètres du capteur sont discutés et élaborés. Sur la base de différents transducteurs, il existe différents types de capteurs, parmi lesquels les capteurs plasmoniques et électrochimiques (EC) sont couramment utilisés et étudiés en raison de leur sensibilité et de leur spécificité élevées. Par conséquent, les capteurs basés sur ces deux techniques de transduction, plus spécifiquement, la spectroscopie Raman améliorée de surface (SERS) et l'EC, sont soigneusement examinés avec une discussion sur les propriétés fondamentales, les matériaux, les techniques et les applications, permettant une meilleure compréhension et la promotion du développement de biocapteurs chez PON.

En outre, pour explorer des capteurs qui abordent la limitation de la portabilité et le coût des applications pratiques, une plate-forme de biodétection multimodale est développée à faible coût et évaluée pour les applications PON liées à la surveillance de la santé et de la qualité des aliments. Plus spécifiquement, un substrat est fabriqué par dépôt électrochimique de nanoparticules d'argent (AgNPs) sur une bandelette de test de glucose du commerce. La plate-forme de biodétection proposée est ensuite appliquée pour la détection EC de l'urée qui est importante pour la surveillance de la santé et la sécurité alimentaire. La plage de détection linéaire de la concentration d'urée dans la plage physiologique est étudiée. En outre, d'autres performances de détection telles que la reproductibilité et la stabilité sont étudiées. Des mesures supplémentaires d'urée dans des échantillons de plasma et de lait reconstitués sont également effectuées pour montrer le potentiel du substrat pour des applications pratiques.

De plus, cette plateforme est adaptée pour la détection du chlorfénapyr, qui est un insecticide utilisé en agriculture. C'est un contaminant alimentaire potentiel dans les légumes comme la ciboulette. Par rapport à l'application à la détection d'urée, cette plateforme est ici utilisée comme un capteur multimodal qui combine EC et SERS pour fournir des informations complémentaires pour la détection du chlorfénapyr. Il est utilisé comme électrode de travail pour la détection du

chlorfénapyr via EC et comme substrat SERS pour la détection par spectroscopie Raman. Les résultats montrent le potentiel du capteur multifonctionnel pour les applications de surveillance de la qualité des aliments.

Alors que la demande d'applications PON augmente, le développement des capteurs chez PON attire de plus en plus l'attention. L'exploration de divers aspects qui jouent un rôle important pour les capteurs dans cette thèse fait progresser ce domaine. La fabrication et l'évaluation de ce dispositif de biodétection peu coûteux basé sur une bandelette de test de glucose revêtue d'AgNP ouvrent une nouvelle voie vers des applications rentables dans différents domaines.

## Acknowledgement

Life can be so different when looking back. PhD study is like a long journey full of excitement but also frustration. It would be impossible for me to finish this journey on my own. There are so many people around me that helps me to keep going on and on even with all the up and downs.

First of all, I would like to thank my supervisor **Prof. Sebastian Wachsmann-Hogiu**, for helping me to adapt into the program and my research when I first came here, for providing everything needed to support the project, for offering opportunities to expand my vision in research by attending the conferences and research exchange, for the patient guidance provided when there are problems rising up, and for the invaluable advice on not only work but also life. The supervisor can be so important for a PhD student and I am truly grateful to have Sebastian as my supervisor since he is not only a knowledgeable professor but also a great supervisor who is always there to help.

I would also like to thank **Dr. Roozbeh Siavash Moakhar** and **Dr. Ayyappasamy Sudalaiyadum Perumal** for their significant help on my project. Ayyappasamy helped me a lot when I first joined the lab and started experiments. Roozbeh provided so much precious advice about electrochemistry and helped me extract useful information from numerous data so that my work can continue. I also want to thank my PhD committee, **Prof. Sara Mahshid, Prof. Andrew Kirk, and Prof. David Rudko**, for all the suggestions they gave that keep me on good track. In addition, I would also like to express my gratitude to McGill Engineering Doctoral Award (**MEDA**) for the financial support during my PhD studies.

No one is an isolated island. And most of the PhD time seems so frustrating, I wouldn't go through it without the support from all the lovely friends. I would firstly thank **Rong** and **Chengyao**, even you are far away from me with 12 hours time difference. I always feel your support and love. Rong is like an angel who helps me so much, not only in my PhD but since we met each other, and I know it will last life long. Chengyao is such a great friend who can always discuss research life with and root for me when I am depressed. I would also thank **Han**, who is like a life saver when I first came here, for the kindness, the help in work and life, and not unfriending me when I was annoying you cross the internet :).

I would also thank the lovely friends I make here in the lab, **Sara, Mona, Mahsa, Jackie, Mira, Sorina, and Reza**. Sara and Mona are like sisters to me and life is always getting better when we share happiness and sadness with each other. Mona is always so caring and loving with complete

understanding and support and she always brings unexpected surprise for me. Sara is the first one I knew in the lab and I will always be so grateful for all her help and patience. We had such great time together and even after Sara left, the connections are never broken. Thanks to Mahsa and Jackie, my PhD life is getting more colorful with the shopping, the tea time, the movie time, and all the Chinese dumplings and noodles that make me less homesick. And of course, last but not least, my lovely friends Mira, Sorina, and Reza as SWH group, the academic life becomes less stressing since they join. Mira is so considerate and thoughtful. I remember all the laugh we had in the microscopy room, and not to mention how much fun we had during the trip to Davis. Sorina and I shared a lot of memories in discovering this city during the pandemic. And I would definitely have been depressed without her. Reza is a great friend who is always ready to help. It is amazing that time always flied so fast when conducting experiments with him. This pandemic makes me realize how much I appreciate all the friends and how important they are for me. I would say thank you to all the members in BBME program that make the lab life more vivid.

In the end, **I would devote this thesis, along with my love, to my family for their infinite support and love:** to my parents who barely talk about it but I know how much you love me, to my brother who will always spare hours and hours to talk to me when I need you, to my sister in law and my lovely nieces and nephew who are making this family full of cheerfulness. Even we don't talk too much about love, I know you are always there for me, when I cried behind the phone, when I cheered on the screen, and when the future comes.

Finally, I would like to stop here, in the same way as for my master thesis, to keep motivating myself by quoting a poem from *Long Live Youth* by Meng Wang, because I know the end of PhD is far away from the end of the life journey:

*All the days passing by, just go on,  
I'm happily moving forward in life,  
I won't cave no matter how heavy the burdens are,  
I won't be disgraced no matter how austere the battles are;  
One day, after wiping the gun, the machine, and the sweats,  
I will miss you, greet you,  
And with pride, watch you.*

## **Contributions to original knowledge**

During my PhD studies, I focused on addressing design considerations for the development of point-of-need (PON) sensors. In specific, first, discussions on the factors that play vital roles for PON applications and how they are important for different applications are presented. It provides a comprehensive references of sensor parameters for the future development of sensors at PON. Second, a multifunctional sensing platform is designed, fabricated, and explored for PON applications. These work has been published as three manuscripts (as first author). In addition, I have also worked on the development of sensing substrates for, as contribution to two more publications as a co-author. More information of the manuscripts will be introduced in the later section. More details about each work in my first author publications are presented as below.

In the first publication [1], a comprehensive review of plasmonic biosensors detailing most recent developments and applications is presented. Sensors based on Surface Plasmon Resonance (SPR), Localized Surface Plasmon Resonance (LSPR), and SERS are introduced and classified based on their materials and structure. Further, most recent applications to environment monitoring, health diagnosis, and food safety are presented. With the discussion of current progress, potential, and challenge for PON applications using plasmonic biosensors, this review offers the prospective to expand the range of applications utilizing plasmonic biosensors into use cases outside labs, bringing more possibility for real life applications, especially at the point of need.

In the second publication [2], a novel non-enzymatic electrochemical (EC) biosensor for urea detection is designed and fabricated. It utilizes a commercial glucose test strip with bimetallic channels, on which silver nanoparticles are electrochemically deposited on the surface. The platform is used for urea detection, which can be a potential biomarker for medical diagnosis for kidney related diseases, as well as a potential analyte for food safety. It shows high sensitivity and specificity for urea detection in physiological concentration range. Compared to other methods, this sensor is able to improve simplicity for urea detection by avoiding the use of enzymes, and also shows advantages of low cost and ease of fabrication. The development of this inexpensive platform opens up an innovative tactic for the design of sensing substrates with the utilization of commercial test strips as a half ready platform with electrical properties and the portability. This platform for urea detection provides a prototype for non-enzymatic detection of urea, which can

be used for personnel to monitor either urea level or food safety such as in milk, and it paves the way for commercial home test assay for urea monitoring.

In the third first author publication [3], the substrate fabricated in the second paper, prepared by electrodepositing AgNPs on the commercial glucose test strip, is explored for multimodal detection of a pesticide known as chlorfenapyr via both EC and SERS for the first time. It is the first time to detect chlorfenapyr electrochemically, thus it provides a new strategy for chlorfenapyr detection via EC. The combination of EC and SERS guarantees the quantitative (EC) and qualitative (SERS) at the same time. Since there is no report on EC detection of chlorfenapyr yet, the identification using SERS is of significance. On the other hand, the analytical measurements using EC overcomes the drawbacks of SERS when the hot spots on the substrate are not reproducible. This in turn gives a boost to the multifunctional sensing substrates. Compared to traditional techniques used for chlorfenapyr detection, this multimodal detection is more promising for cost-effective applications.

## Contributions of authors

- **Chapter II**

This chapter is based on my first publication [1]. In this chapter, a review of plasmonic biosensors is presented. Specifically, fundamentals, materials, detection techniques are introduced. Then, emphasis is put on recent developments and applications of plasmonic biosensors. Moreover, PON applications are highlighted with thorough discussion on the current status and considerations. The contributions of the authors are listed as follows: Juanjuan Liu wrote the manuscript except for section 2.3 that is written by Mahsa Jalali. Sebastian Wachsmann-Hogiu designed the outline of the manuscript and reviewed the manuscript. All authors made substantial intellectual contributions to the manuscript.

Specifically, my contribution is detailed below.

I reviewed the literature in the field of plasmonic biosensors for PON applications, and provided a comprehensive summary including the basic concepts, materials, and structures used for plasmonic biosensors. In addition, I reviewed main methods for the functionalization of the substrates with focus on improved sensing performance, as well as plasmonic-based detection methods. I reviewed the current status of PON plasmonic biosensors and described applications of plasmonic biosensors in different areas, with emphasis on PON applications. Finally, I discussed the parameters that are important for the design of PON biosensors in detail.

- **Chapter III**

This chapter is based on my second publication [2]. In this chapter, a flexible sensing platform for urea detection is developed on a AgNP-deposited commercial glucose test strip. The sensing performance of this platform is explored for urea detection via electrochemistry (EC) including sensitivity, selectivity, and reproducibility. Real sample analysis in reconstituted plasma and milk samples are also performed to show its potential for the use in real applications. The contributions of the authors are: Juanjuan Liu, Roozbeh Siavash Moakhar, and Sebastian Wachsmann-Hogiu conceived the experiments, Juanjuan Liu conducted the experiments, Juanjuan Liu and Roozbeh Siavash Moakhar analyzed the results. Juanjuan Liu wrote the main manuscript with input from all the authors. All authors made substantial intellectual contributions to the manuscript. Sebastian Wachsmann-Hogiu supervised the whole project.

Specifically, my contribution is detailed below.

I fabricated the AgNP-coated test strips by using electrodeposition of AgNPs on a commercial test strip, followed by the morphology characterization of the substrate by SEM, along with EDS, to confirm the deposition, distribution, and size of AgNPs. After the fabrication and characterization of the test strip, I performed CV to confirm the electroactivity of this substrate. For the application, I conducted a series of CV measurements to explore the catalytic activity for urea detection, the limit of detection, and other sensing performance such as the reproducibility, reusability, stability, as well as selectivity. I measured a linear detection range of 1- 8 mM with a limit of detection of 0.14 mM, which is applicable for the physiological concentration range of urea ranging from 2.5 – 7.5 mM in human blood. In addition, I also detected urea in real samples including plasma and milk to evaluate its potential for practical applications for medical diagnosis and food safety, and demonstrated that this substrate can be used for urea detection in real life applications with further improvements.

- **Chapter IV**

This chapter is based on my third publication [3]. This chapter presents multimodal detection of chlorfenapyr via EC and SERS on the AgNP-deposited substrate. Quantitative EC measurements are conducted to explore analytical detection for chlorfenapyr, while SERS measurements are recorded to show characteristic identification. The contributions of authors are: Juanjuan Liu contributed to the design of the experiments, performed the experiments, data analysis, and wrote the manuscript. Roozbeh Siavash Moakhar contributed to the design of the experiments and data analysis. Sara Mahshid provided feedback on the experiments. Fartash Vasefi contributed to the use case and provided the samples. Sebastian Wachsmann-Hogiu contributed to the design, data analysis, writing of the manuscript, and overall supervised and managed the project. All authors reviewed and provided feedback to the manuscript.

More specifically, my contribution is outlined below.

I fabricated the AgNP-deposited test strip and then adapted it for the multimodal detection of chlorfenapyr. I performed CV measurements to explore its ability for chlorfenapyr detection via EC as well as SERS measurements to confirm its ability for enhancing Raman signals for chlorfenapyr detection after the morphology characterization and evaluation for EC and SERS performance. I collected SERS spectra of chlorfenapyr on the fabricated substrate, and

compared with other control samples to confirm the characteristic peak for identification of chlorfenapyr. I evaluated the reproducibility and the selectivity towards other pesticides. After the identification of chlorfenapyr using SERS, I performed CV measurements for chlorfenapyr to evaluate the ability of the substrate to provide quantitative results. I measured a limit of detection of 4.2 ppm within a linear detection range of 20-50 ppm. Further, I conducted real sample analysis of chlorfenapyr with chives via both SERS and EC, and demonstrated the potential to be used for real life applications.

## List of Publications

### First-author publications (related to this thesis)

Published: **Juanjuan Liu**, Mahsa Jalali, Sara Mahshid, Sebastian Wachsmann-Hogiu, Are plasmonic optical biosensors ready for use in point-of-need applications?, *Analyst*, 2020, DOI: 10.1039/C9AN02149C (**IF: 3.978, citations: 54**)

Published: **Juanjuan Liu**, Roozbeh Siavash Moakhar, Ayyappasamy Sudalaiyadum Perumal, Horia Roman, Sara Mahshid & Sebastian Wachsmann-Hogiu (2020). An AgNP-deposited commercial electrochemistry test strip as a platform for urea detection. *Scientific Reports* 10(1): 9527. <https://doi.org/10.1038/s41598-020-66422-x> (**IF: 4.379, citations: 12**)

Published: **Juanjuan Liu**, Roozbeh Siavash Moakhar, Sara Mahshid, Fartash Vasefi, Sebastian Wachsmann-Hogiu, Multimodal Electrochemical and SERS platform for chlorfenapyr detection, *Applied Surface Science*, 2021, <https://doi.org/10.1016/j.apsusc.2021.150617> (**IF: 6.707**)

### Co-author publications (contributions to other projects)

Published: Sorina Suarasan, **Juanjuan Liu**, Meruyert Imanbekova, Tatu Rojalin, Silvia Hilt, John C. Voss and Sebastian Wachsmann-Hogiu (2020). Superhydrophobic bowl-like SERS substrates patterned from CMOS sensors for extracellular vesicle characterization. *Journal of Materials Chemistry B* 8(38): 8845-8852. (**IF: 5.344, citations: 4**)

Published: Tatu Rojalin, Hanna J. Koster, **Juanjuan Liu**, Rachel R. Mizenko, Di Tran, Sebastian Wachsmann-Hogiu, and Randy P. Carney (2020). Hybrid Nanoplasmonic Porous Biomaterial Scaffold for Liquid Biopsy Diagnostics Using Extracellular Vesicles. *ACS Sensors* 5(9): 2820-2833. (**IF: 6.944, citations: 6**)

## Conferences

### 2018:

Poster presentation: A novel biosilica-based plasmonic substrate on adhesive tapes

Authors: **Juanjuan Liu**, Ayyappasamy Sudalaiyadum Perumal, Aysun Korkmaz, Maya Kenton, Gulsen Aksin, Sara Kheireddine, Mehmet Kahraman, Sebastian Wachsmann-Hogiu

Conference: Photonics North, Montreal, Quebec, Canada

Date: June 6, 2018

### 2019:

Oral presentation: A flexible and portable nanocomposite-based substrate for electrochemical biosensing

Authors: **Juanjuan Liu**, Ayyappasamy S. Perumal, François R. Doucet, Kheireddine Rifai, Lütfü Özcan, Sara Kheireddine, Dan V. Nicolau, and Sebastian Wachsmann-Hogiu

Conference: SPIE Photonics West, San Francisco, California, United States

Date: February 3, 2019

### 2020:

Presentation: AgNP-decorated 3D nano-bowl structures for SERS detection of urea and exosome

Authors: **Juanjuan Liu**, Sorina Suarasan, Meruyert Imanbekova, Sebastian Wachsmann-Hogiu  
(Presented by SWH due to inability to travel)

Date: February 2, 2020

### **Research exchange**

I participated in a short-term research exchange in August 2019 at the University of California Davis in the lab of Prof. James Chan. In this context, I had the opportunity to learn various optical techniques related to Raman spectroscopy such as line scan Raman imaging and multifocal Raman imaging. This research exchange enhanced my knowledge in the area of Raman spectroscopy as well as expanded my horizon, providing me more understanding and available sensing techniques for my projects. In addition, this research exchange also helped us to establish further collaboration with their group on the development of SERS substrates where we contribute to materials development part. This research exchange was funded by Graduate Mobility Award (GMA).

## List of figures and tables

### *List of figures*

**Figure 1.1 Schematic diagram of the development of the multi-functional biosensor:** (left) main components used for the biosensor including the commercial test strip and metallic nanoparticles; (right) dual detection methods via EC and SERS

**Figure 1.2 Schematics of electrochemical three-electrode system.** (i) Photograph of an EC cell with three-electrode system; (ii-iii) electrochemical system on a strip and in a cell; (iv) equivalent circuit of a three electrode system.

**Figure 1.3 Working principle of cyclic voltammetry:** Triangular potential waveform (left) and duck shaped voltammogram (right)

**Figure 1.4 Working principle of chronoamperometry:** constant potential input (left) and current output (right)

**Figure 1.5 Working principle of DPV:** applied potential staircase (top left), current-potential response for an oxidation (top right), sampling and the mechanism of response curve (bottom)

**Figure 1.6 Working principle of EIS:** EIS response (left) and an idealized Randles electrical equivalent circuit (right)

**Figure 1.7 Schematic representation of biosensing based on electrochemistry:** The working flow of measurements including experimental setup (top) and detection methods, and different materials and structures developed for working electrodes (bottom)

**Figure 1.8 Schematics of Raman spectroscopy.** (A) Basic principle of Raman scattering. (B) schematics of experimental setup for Raman spectroscopy

**Figure 2.1. The fundamental optoelectrical properties of metallic nanostructures and graphene.** Schematic illustration of a localized surface plasmon resonance (a). Plasmon tuning ranges of the common plasmonic metallic materials, Au, Ag, and Al (b). Extinction spectra of a gold monomer, and gold hepatmers with different interparticle gap separations (c). Schematic of an ion-gelgated graphene monolayer on a fused silica substrate covered by ion-gel and voltage biased by the top gate (d). Fermi level variation of single-layer graphene modulated with electrical

field (e). Figure 2.1a is adapted from reference [46] with permission from The Royal Society of Chemistry, Copyright (2016). Figure 2.1b is adapted from reference [47] with permission from American Chemical Society, Copyright (2014). Figure 2.1c is adapted from reference [25] with permission from American Chemical Society, Copyright (2010). Figure 2.1d and 2.1e are adapted from References [40] and [39] with permission from Springer Nature, Nature Photonics, Copyright (2018) and American Chemical Society, Copyright (2011), respectively.

**Figure 2.2. Schematics of biosensing based on plasmonic materials.** The preparation of measurements: functionalized substrates (based on antibody/antigen, aptamers, and molecular imprinting) of different materials and structures (a) and various detection methods (b).

**Figure 2.3.** EM images of AuNPs deposited on carbonized paper(a), Side view of a SERS sensor consisting of nanoporous PS-b-P2VP nanorods functionalized with AuNPs connected to a nanoporous PS-b-P2VP membrane (b), Au Nanorods (c), MoS<sub>2</sub>/silver nanodisk hybrid structure on a Si/SiO<sub>2</sub> substrate (d), and Au-deposited quasi-3D plasmonic crystal (e). Figure 2.3a is adapted from reference [60] with permission from Elsevier Copyright (2017). Figure 2.3b is adapted from reference [99] with permission from John Wiley and Sons, Copyright (2017). Figure 2.3c is adapted from reference [69] with permission from The Royal Society of Chemistry, Copyright (2013). Figure 2.3d is adapted from reference [100] with permission from American Chemical Society, Copyright (2016). Figure 2.3e is adapted by from reference [81] with permission from Springer Nature, Nature Communications, Copyright (2011).

**Figure 2.4.** The schematic of the mechanism of SPR (a-c) and LSPR (d-f). Figure 2.4a, b, e and f are adapted from reference [120] with permission from Elsevier, Copyright (2016).

**Figure 2.5. Representative examples of utilizing natural materials as supporting substrate:** (a) AgNPs deposited on *Mytilus coruscus* (M.c) shell; (b) AgNPs sputtered on dragonfly wing; (c) Graphene oxide (GO) and AuNPs deposited on cicada wing. Figure 2.5a and b are adapted from reference [93] and [94] with permission under Copyright Clearance Center, Inc, Copyright (2019). Figure 5c is adapted from reference [178] with permission from Elsevier B.V., Copyright (2018).

**Figure 3.1. Schematic representation of the workflow.** (i) preparation of the test strip before modification (by removing the enzyme layer). (ii) electrodeposition of AgNPs directly on the test

strip by applying a potential at -0.6 V for 30 s between the working and reference electrodes in presence of  $\text{AgNO}_3$  and  $\text{KNO}_3$ . (iii) drop casting of the sample on the sensing area of the test strip for detection. (iv) EC measurements.

**Figure 3.2 The fabrication and characterization of the test strip.** (A) the photo (i) and optical imaging (ii) of commercial glucose test strip before (i) and after (ii) electrodeposition of AgNPs (inset: 1-working electrode; 2-counter electrode; 3-reference electrode); (B) SEM images of bare test strip (i) and AgNP-coated test strip (ii).

**Figure 3.3. EDS characterization of the test strip.** (A) EDS spectrum and (B) EDS mapping of the AgNP-coated commercial glucose test strip.

**Figure 3.4. EC evaluation of the AgNP-coated test strip.** (A) Electrochemical evaluation with  $\text{K}_3\text{Fe}(\text{CN})_6$  and (B) EIS of bare and AgNP-coated glucose test strip. Electrolyte: 0.1 M KCl for  $\text{K}_3\text{Fe}(\text{CN})_6$  (5 mM), and 0.1 M NaOH for EIS; scan rate for CV: 20 mV/s.

**Figure 3.5. Sensing performance of the AgNP-coated test strip for urea detection.** (A) CV response and (B) EIS of AgNP-coated glucose test strip in the absence and presence of urea; (C) CV response of AgNP-coated glucose test strip in the presence of urea at different scan rates (10-50 mV/s), and (D) corresponding calibration plot of peak current vs. square root of scan rates. (E) CV response of AgNP-coated glucose test strip in the presence of urea at different concentrations (1-8 mM) and (F) corresponding calibration plot of peak current vs. urea concentration.

**Figure 3.6. CV response of AgNP-coated glucose test strips in the presence of urea.** (A) with different strips, (B) different cycles with the same strip, (C) with strips stored for different times, and (D) with interference of other substances glucose and AA. Electrolyte: 0.1 M NaOH; Scan rate: 50 mV/s.

**Figure 4.1. Schematic representation of the dual detection of chlorfenapyr via EC and SERS on AgNP-coated test strips prepared by electrodeposition:** sample preparation of chlorfenapyr (left), fabrication of dual functional sensing platform based on bimetallic test strip, including the nucleation and growth of AgNPs during electrodeposition (middle), and dual detection of chlorfenapyr via SERS (identification) and EC (calibration).

**Figure 4.2. Characterization of AgNP-strip via SEM and EC:** SEM image of bare strip without AgNP deposition (A) and AgNP-strip after AgNP deposition (B), inset: enlarged image of the area indicated in red box. CV curves of the bare strip and AgNP-strip in the response to potassium ferricyanide (C) and Raman spectra of the bare strip (black, 60s) and AgNP-strip in the presence of 4ATP (red, 10s) (D).

**Figure 4.3 Chlorfenapyr detection via SERS:** (A) Raman spectra of chlorfenapyr 100 ppm (3 $\mu$ Lx3) on unmodified (bare strip, black) and modified (AgNP-strip, red) strips; integrations time: 300s. (B) SERS spectra of control sample (DMSO alone, black, 10s) and chlorfenapyr (in DMSO, red, 300s) on AgNP-strip and the Raman spectrum of chlorfenapyr powder on cover slip (blue, 60s). (C) SERS spectra of chlorfenapyr on AgNP-strip at different concentrations (in DMSO, 300s). (D) SERS spectra of control sample (DMSO alone, black, 10s) and chlorfenapyr (in DMSO, red, 10s) on AgNP-strip and the Raman spectrum of chlorfenapyr powder on cover slip (blue, 60s).

**Figure 4.4 Reproducibility of SERS measurements for chlorfenapyr on AgNP-coated strip:** (A) 10 SERS spectra of chlorfenapyr at 50 ppm from different spots on AgNP-strip; integrations time: 60s; (B) Averaged SERS spectra of 10 SERS spectra from different spots with standard deviation. (C) 8 averaged SERS spectra (of 10 spots) of chlorfenapyr at 50 ppm on different AgNP-strips; integration time: 60s; (D) Averaged SERS spectra of 8 SERS spectra from different strips with standard deviation.

**Figure 4.5 Chlorfenapyr detection on AgNP-strip via EC:** (A) CV curves of chlorfenapyr on bare strips. (B) CV curves of the drop cast AgNP-strip in the absence and presence of chlorfenapyr at different concentrations. (C) CV curves of the electrodeposited AgNP-strip in the absence and presence of chlorfenapyr at different concentrations, scan rate: 50 mV/s. (D) the relation of the potential shift in the presence of chlorfenapyr compared to the blank measurement versus the concentration of chlorfenapyr detected on electrodeposited AgNP-strip. (E) Relative standard deviation of the peak potential shifts on different substrates (n=3~7) for chlorfenapyr detection at different concentrations. (F) CV curves of the electrodeposited AgNP-strip in the absence and presence of chlorfenapyr, in the presence of imidacloprid and triadimefon with chlorfenapyr at 20 ppm.

**Figure 5.1 Components of Accu-chek aviva test strips:** Photograph of the unmodified test strip before (left) and after (right) peeling off the protecting cover and removing the enzyme (middle)

**Figure 5.2 Morphology and elemental characterization of bare strip:** EDS spectrum (A) and EDS mapping (B) of bare commercial glucose test strip.

**Figure 5.3 Optimization of parameters used for electrodeposition:** CV response of the bare test strip for silver nitrate (A) and SEM images (B-F) of AgNP-coated test strips via electrodeposition with different applied voltage and duration times.

**Figure 5.4. CV response of the bare test strip (without AgNP deposition) in the absence and presence of urea.** Electrolyte: NaOH 0.1M, scan rate: 20 mV/s

**Figure 5.5. Urea detection in real samples on the AgNP-coated test strip:** CV response for the detection of urea in milk (A) and plasma (B) samples

**Figure 5.6 Schematic representation of the fabrication of AgNP-coated test strips via drop casting colloidal AgNPs.** (i) The synthesis and concentration of the colloidal AgNPs; (ii) The deposition of colloidal AgNPs on the test strip via drop casting

**Figure 5.7 Morphology characterization of colloidal AgNPs.** (Left) Absorbance spectrum of colloidal AgNPs reduced by sodium citrate; (Right) SEM image of colloidal AgNPs reduced by sodium citrate

### *List of Tables*

**Table 2.1** Basic concepts for the characterization of plasmonic biosensors

**Table 2.2.** Summary of applications of plasmonic biosensors. Applications that are close to PON situations are highlighted in bold.

**Table 3.1.** Comparison of electrochemical electrodes reported in the literature for urea detection

**Table 3.2.** Detection of urea in milk and plasma sample

**Table 4.1** Chlorfenapyr detection using various techniques

**Table 4.2** chlorfenapyr detection in vegetable samples

## Table of Contents

<b>Abstract</b> .....	2
<b>Résumé</b> .....	4
<b>Acknowledgement</b> .....	6
<b>Contributions to original knowledge</b> .....	8
<b>Contributions of authors</b> .....	10
<b>List of Publications</b> .....	13
<b>Conferences</b> .....	13
<b>Research exchange</b> .....	14
<b>List of figures and tables</b> .....	15
<b>Chapter I: Introduction</b> .....	24
<b>1.1 Background and motivation</b> .....	24
<b>1.2 Hypothesis and objectives</b> .....	26
<b>1.3 Rationale and innovation</b> .....	27
<b>1.4 Electrochemical sensors</b> .....	29
<b>1.4.1 Basic fundamentals of electrochemistry</b> .....	29
<b>1.4.2 Electrochemical techniques</b> .....	34
<b>1.4.3 Electrochemical (bio)sensors</b> .....	39
<b>1.5 Surface enhanced Raman spectroscopy (SERS)</b> .....	45
<b>1.5.1 Raman spectroscopy</b> .....	46
<b>1.5.2 AgNP-based substrates for SERS</b> .....	47
<b>Chapter II: Are plasmonic optical biosensors ready for use in point-of-need applications?</b> .....	51
<b>2.1 Abstract</b> .....	52
<b>2.2 Introduction</b> .....	52
<b>2.3 Fundamentals of plasmonic materials</b> .....	53
<b>2.4 Potential for improvement of plasmonic biosensors for applications at point of need</b> .....	59

2.4.1	Basic concepts of biosensing.....	60
2.4.2	Materials .....	61
2.4.3	Structures.....	63
2.4.4	Functionalization of substrates .....	66
2.4.5	Detection methods.....	67
2.5	Applications.....	76
2.5.1	Characterization of substrates and (bio)materials.....	76
2.5.2	Environment monitoring.....	77
2.5.3	Diagnosis for human health .....	78
2.5.4	Food safety.....	78
2.5.5	PON applications.....	79
2.6	Conclusions and outlook.....	86
2.7	Author contributions .....	87
2.8	Conflict of interest.....	87
2.9	Acknowledgements .....	87
2.10	References.....	87
<b>Chapter III: An AgNP-deposited commercial electrochemistry test strip as a platform for urea detection.....</b>		<b>100</b>
3.1	Abstract.....	102
3.2	Introduction.....	103
3.3	Results and discussion .....	105
3.3.1	Choice of Materials.....	106
3.3.2	Fabrication and characterizations of AgNP-coated electrode .....	107
3.3.3	Electrochemical evaluation of the electrode .....	109
3.3.4	Urea detection.....	110
3.3.5	Reproducibility, reusability, stability, and selectivity of the EC strip .....	115

3.3.6	Urea detection in reconstituted plasma solution and in milk samples .....	117
3.4	Conclusions .....	118
3.5	Materials and methods .....	119
3.6	Author contributions .....	121
3.7	Conflict of interest.....	121
3.8	Acknowledgements .....	121
3.9	References.....	122
<b>Chapter IV: Multimodal Electrochemical and SERS platform for chlorfenapyr detection.....</b>		<b>126</b>
4.1	Abstract.....	128
4.2	Introduction.....	128
4.3	Materials and methods .....	132
4.4	Results and discussions.....	135
4.4.1	Fabrication and characterization of AgNP-coated test strip .....	135
4.4.2	SERS performance.....	136
4.4.3	EC performance .....	136
4.4.4	Chlorfenapyr detection via SERS.....	136
4.4.5	Chlorfenapyr detection via EC .....	140
4.4.6	Chlorfenapyr detection in vegetable sample with chive solution.....	144
4.5	Conclusions.....	144
4.6	Author contributions .....	146
4.7	Conflict of interest.....	146
4.8	Acknowledgements .....	146
4.9	References.....	147
<b>Chapter V: Discussion .....</b>		<b>151</b>
5.1	Optimization of the biosensing platform.....	151
5.1.1	Selection and characterization of the commercial glucose test strip .....	152

---

5.1.2	Optimization of parameters used for the electrodeposition of AgNPs .....	154
5.1.3	Evaluation of EC and SERS performances on the AgNP-deposited test strip .....	157
5.2	Detection methods based on different transducers .....	157
5.3	Applications of the AgNP-deposited test strip.....	158
5.3.1	Urea detection via EC on the AgNP-deposited test strip.....	159
5.3.2	Chlorfenapyr detection via EC and SERS on the AgNP-deposited test strip.....	161
Chapter VI: Conclusions and perspectives.....		165
6.1	Conclusions.....	165
6.2	Outlook.....	167
References.....		169

## Chapter I: Introduction

Medical diagnostics and food safety are two important components of health care. Analytical identification of disease biomarkers or food contaminants using a sensor can help us to reduce the potential risk for disease. Therefore, to ensure our health and improve our life quality, it is beneficial to develop sensors, especially for Point-of-Need (PON) applications such as medical diagnosis, food safety, and environmental monitoring, which are closely related with our daily life [4]. Thus, the main goal of this thesis is to develop a multi-functional sensing platform with novel nanomaterials and to apply this platform in areas related to health care and food safety problems towards PON applications. In order to make it useful for these applications, the developed sensor is analytical, inexpensive, and easy to prepare. To achieve that, novel nanomaterials consisting of combinations of metallic nanoparticles and commercial test strips are utilized and explored to optimize its performance. In this chapter, a brief introduction to the background and motivation, hypothesis and objectives, and the rationale and innovation will be discussed.

### 1.1 Background and motivation

*Motivation.* Detection of disease biomarkers using non-invasive methods is important for early diagnosis of disease and for monitoring the health related conditions. On the other side, the presence of pesticide residue in food may trigger the development of diseases associated with the poor conditions of food safety. As a result, the monitoring of disease biomarkers or food contamination is closely related to our daily life and plays an important role in our health. Thus, to keep the quality of our life regarding health condition and food quality, it is significant to detect disease biomarkers or food contaminants at PON.

The development of sensors can facilitate the detection of food contaminants for food safety or specific biomarkers associated with the disease of interest in a direct and reliable manner. To make them more suitable for PON applications to diagnosis and food safety, it is important to develop sensors at low cost and with high accuracy for specific target analytes. Therefore, a novel nanomaterial composite is proposed to build a biosensing system that is inexpensive and easy to fabricate to detect health related biomarkers such as urea, which is associated with disease related to kidney or liver, and to detect the presence of pesticides such as chlorfenapyr, which is a potential food contaminant in vegetables. This device consists of an innovative blend of metallic

nanoparticles and a commercial glucose test strip that can be applied to multimodal detection approaches.

*Background.* Biosensors show great potential in many areas such as medical diagnostics, food safety and environmental monitoring [2-4]. Biosensors convert biological and/or chemical information of target analytes into detectable signals. With certain techniques, the transduced signals are then collected for further analysis to display the information of detected analytes. In this work, inexpensive and flexible substrates based on novel nanomaterial composite are designed and fabricated for PON applications to diagnosis and food safety. A series of characterization is conducted to confirm the morphology, followed by the evaluation of optical and electrochemical behavior with SERS and EC measurements. Detection of different analytes are then explored using this platform to evaluate its sensing performance and potential for practical applications, where two detection techniques, EC and SERS, are used due to their high specificity, and rapid detection response.

SERS is an emerging surface technique to enhance Raman signals for biosensing [5]. This technique utilizes plasmonic nanostructures or nanoparticles that enhance the emitted light signals of detection significantly compared to regular Raman detection [6]. SERS shows great potential in sensing due to its high sensitivity and the property of ‘finger printing’ to create unique spectra. Since SERS was discovered back in the 1970s, there are many reports about the application of SERS biosensors in various fields. Metallic nanoparticles are commonly used as SERS active materials because Raman signal can be significantly enhanced for molecules adsorbed on the metallic surface. Inexpensive SERS substrates can expand the use of this technique [7, 8].

On the other hand, EC methods can also be used for biosensing with the metallic substrates. Electrochemistry emerges as a powerful tool where electron transfer is involved. EC sensors directly convert biological and/or chemical information of the molecules to electrical responses due to the electron transfer generated during the redox reaction of the molecules on the surface of substrate, providing a straightforward way to detect the analyte of interest [9]. Usually, for EC measurements, a three-electrode system is used. In the three-electrode system, a working electrode is the sensing substrate where the reaction of interest occurs. A reference electrode is to provide the reference potential and a counter electrode is to complete the electrical circuit with working electrode [10]. In voltammetric measurements, by applying different forms of voltage,

corresponding current is recorded to get I-V curves (or voltammograms), through which the information of the analyte can be obtained. According to the waveforms of potential that are applied, there are a series of different EC techniques such as linear sweep voltammetry and normal pulse voltammetry, among which, cyclic voltammetry (CV) is widely used [9]. In this work, CV is used to demonstrate EC performance of the substrate.

## 1.2 Hypothesis and objectives

*Hypothesis.* In this thesis, I modified commercial glucose test strips with AgNPs to be adapted for a wide range of applications. The glucose test strip is composed of bimetallic channels coated with Au and Pd, onto which AgNPs are grown via electrodeposition. Bearing different properties of each material, we *hypothesize* that the combined nanomaterial composite consisting of AgNPs and bimetallic substrate will exhibit improved electrochemical and optical properties, i.e., catalytic activity and electroactivity for EC, and electromagnetic properties for Raman enhancement. These properties will make the nanomaterial-based substrate a good candidate for the detection of biomarkers for specific diseases such as urea and for the detection of pesticides such as chlorfenapyr via multimodal detection methods, which are electrochemistry (EC) and surface enhanced Raman Spectroscopy (SERS). The substrate will exhibit comparable sensitivity and specificity as other sensors for specific applications, but it can be fabricated in a simple way at low cost, which makes it more suitable for PON applications. There are two specific objects and they are described as below.

*Objective 1:* To develop an inexpensive sensing platform consisting of metallic nanoparticles, i.e., silver nanoparticles, and flexible commercial test strips. In order to achieve a sensing substrate that is cheap and can be fabricated in a simple way, nanomaterial composite composed of silver nanoparticles, and flexible commercial test strips are prepared via electrodeposition. To characterize the morphology of the fabricated substrate, Scanning Electron Microscopy (SEM) is conducted. Further, EC and SERS measurements for different test molecules are performed to evaluate the EC and SERS performance of the substrate.

*Objective 2:* To evaluate the sensing performance of the developed platform for PON applications. In order to achieve this objective, the substrate is used for the detection of different analytes that are related to medical diagnosis and food safety. The analytes detected here are urea and chlorfenapyr. Urea is a biological molecule of which the concentration is related to the condition

of kidney or liver, as well as to the food quality of dairy product. Chlorfenapyr, on the other hand, is a pesticide that could be a potential food contaminant in vegetables.

In order to achieve this objective, sensing performance such as sensitivity and limit of detection (LOD) are explored by running Cyclic Voltammetry (CV) and/or SERS measurements on the substrate with analytes. Further, to evaluate the potential of the substrate for practical applications, real sample analysis is also performed respectively for the analytes.

### 1.3 Rationale and innovation

To develop sensors that can be used for PON applications, it is important for the substrates to be inexpensive, and easy to manufacture. Therefore, in this project, a novel sensing platform based on nanomaterial composite consisting of different components is fabricated and explored in applications to health and food safety. The materials used for the sensing platform are composed of metallic nanoparticles and commercial test strips as the substrate (**Figure 1.1**). Each component of the materials exhibit properties and functionality that are beneficial for analyte detection at PON. More specifically, the rationale behind is described as following:

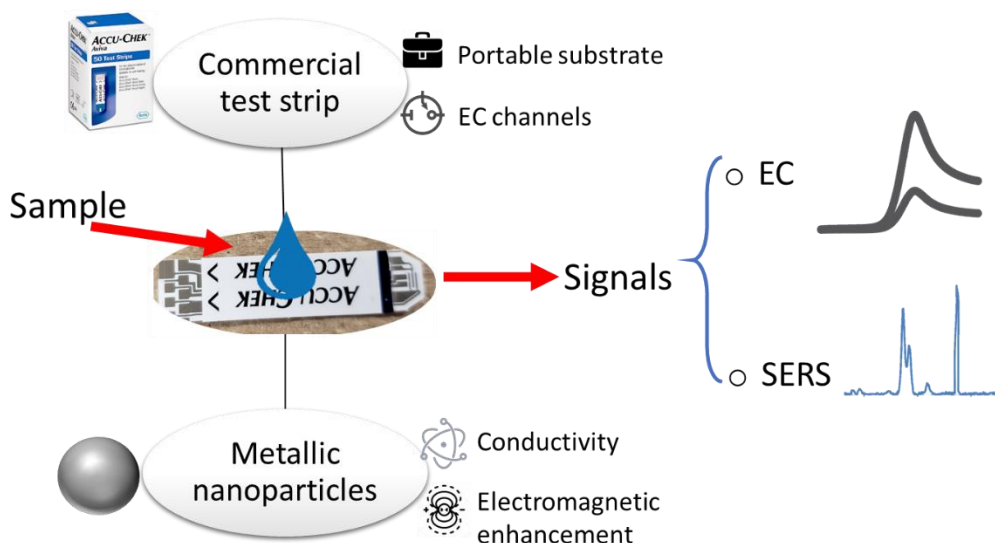


**Figure 1.1 Schematic diagram of the development of the multi-functional biosensor:** (left) main components used for the biosensor including the commercial test strip and metallic nanoparticles; (right) dual detection methods via EC and SERS

First of all, the materials selected here can be achieved at low-cost and prepared in a simple way. The commercial glucose test strip is a widely used product for monitoring blood glucose level. It

can be easily obtained from a local pharmacy with less than 1 CAD per strip. As for the modification of the test strip with metallic nanoparticles, AgNPs are synthesised in situ on the working electrode of the test strip by electrodeposition rapidly (~ 1 min). The precursor used here is silver nitrate ( $\text{AgNO}_3$ ) and a small amount (~ 50  $\mu\text{g}$  and the cost is negligible) of  $\text{AgNO}_3$  is needed for the modification of each test strip. In total, the cost of the materials for each substrate is less than 1 CAD, which is really cheap.

Second, the utilization of AgNPs improves the sensitivity and specificity that make the detection of analytes more precise using this substrate. AgNPs as plasmonic metallic nanoparticles have been an attractive candidate for SERS measurements since they can enhance the local electric field and thus enhance the detected signals [11]. On the other hand, AgNPs also draw a lot of attention as EC substrates since they exhibit the following properties: (a) high conductivity due to faster electron transfer; (b) catalytic activity; and (c) immobilization for some biomolecules [12]. These properties play an important role to facilitate the redox reaction happening on the modified electrode and improve the sensitivity. In addition, AgNPs also offer good biocompatibility, high surface-to-volume ratio compared to the traditional bulk materials.

Third, the utilization of the commercial glucose test strips improves the possibility of the substrate to be used at PON due to its flexibility and portability, as well as other features such as low cost mentioned above. Currently, there are many test strips for glucose detection that are commercially available. They are made of plastic or paper substrates on which metallic layers (electrodes) are deposited for EC functionality [13]. They are attractive for researchers in the area of biosensors because of their high sensitivity and rapid response towards detection. The commercial test strips are also portable and mostly flexible, which make them ideal candidates as biosensing substrates. Accu-Chek Aviva is one of them that is characterized by high accuracy and rapid detection for blood glucose estimation. The strip is composed of patterned Au-Pd electrodes (channels) deposited on a plastic substrate. Further modification with other materials such as AgNPs can result in significant improvement on the sensing performance towards specific analytes.

In conclusion, since both AgNPs and the commercial glucose test strip show potential in the field of biosensing, it is hypothesized that combining them will improve their sensing performance and open up a new way for PON applications. In fact, there are a significant number of papers exploring their various configurations of these materials [14]. Therefore, in this work, a sensing platform

based on nanomaterial composite that is made of different materials offering distinctive properties is designed, fabricated, and explored for PON applications.

## **1.4 Electrochemical sensors**

As one of the dual modal detection techniques used in this thesis, electrochemistry is a type of transducing technique that has high sensitivity and specificity. EC biosensors directly convert the reaction of biological/chemical molecules to electrical response, providing a straightforward way to detect the target of interest [9, 15]. A change in electrical current or potential is measured due to the reaction occurring on the electrode. There are many different techniques based on different modes of the input signal. For example, in the case of voltammetry, the analyte is detected by measuring the corresponding current obtained by applying a varying potential between the working and reference electrodes. In this section, EC biosensors will be introduced. The fundamentals of electrochemistry will be described so that a better understanding on the working principles of an EC biosensor can be obtained. It is followed by the introduction to different EC techniques. In the end, EC biosensors will be reviewed regarding the materials that are used for electrodes and the applications.

### **1.4.1 Basic fundamentals of electrochemistry**

To study electrochemical (bio)sensors, we first need to understand electrochemistry. Electrochemistry studies chemical reactions by physical phenomena that is involved with electron transfer. More specifically, it records the electrical changes, i.e., current (voltammetry), potential (potentiometry), or other conductive properties (conductometry), which are related with electron transfer occurring during chemical reactions [16]. When reduction or oxidation (redox) reaction happens, it involves the gaining or losing the electrons. And this process generates the movement of electrons, which creates electrical signals that are measurable. Considering the fact that the redox reactions can create electricity, one of the most common applications of electrochemistry is battery. The working principle of a battery can be explained in a galvanic cell. A galvanic cell is an electrochemical cell that utilize the redox reactions of two metals to generate current [17]. Another common application of electrochemistry is electrochemical (EC) (bio)sensor. Different from a galvanic cell, an electrochemical sensor is to study the species/analytes of interest on the electrodes (typically the working electrodes). Based on the species that are reduced or oxidized, the chemical potential needed are different, as well as the generated signals. Therefore, the

quantitative electrical signal responses upon applied voltage or current will give us the information about the species or analytes in the electrochemical process.

### *EC setup: a three-electrode system*

To realize EC measurements which involves the movement of electrons and current flow, an EC cell is necessary to implement the circuit. The EC cell is usually composed of a two- or three-electrode system in electrolyte. The electrodes are the electronic conductors and the electrolyte are working as the ionic conductors. A two-electrode system includes a working electrode and a counter electrode (also works as a reference electrode), while a three-electrode system includes an external reference electrode except for working electrode and counter electrode [17]. The external reference electrode offers a stable reference potential during measurements. For the development and exploration of EC biosensors, the emphasis is on the working electrode since the reaction of target analyte occurs on the surface of a working electrode. Therefore, it is important to make sure that the performance of the working electrode will be free from the change of the counter electrode. As a result, compared to the two-electrode system, a three-electrode system is preferable in this use case.

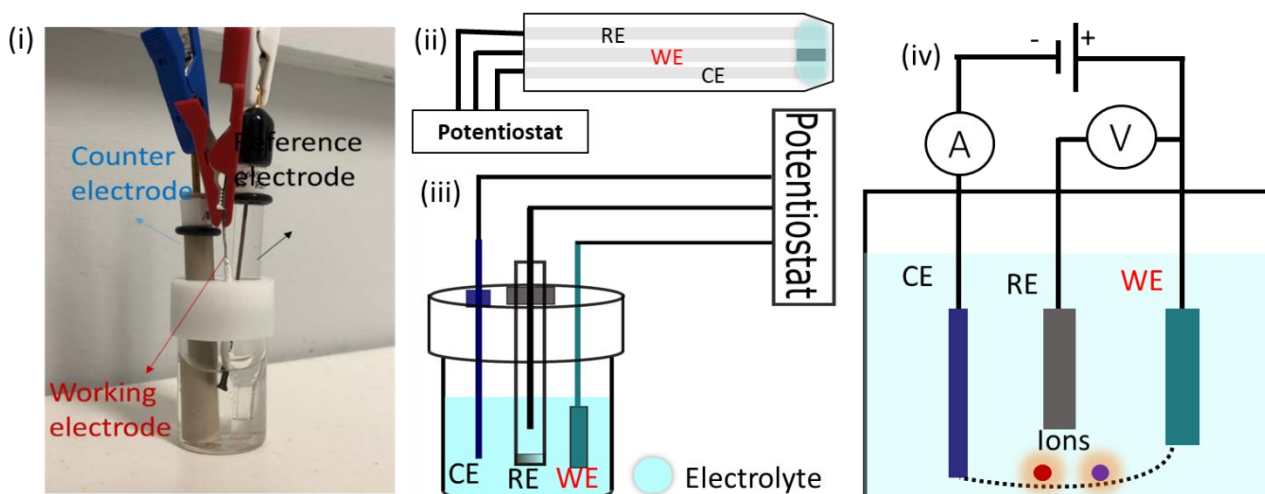


**Figure 1.2 Schematics of electrochemical three-electrode system.** (i) Photograph of an EC cell with three-electrode system; (ii-iii) electrochemical system on a strip and in a cell; (iv) equivalent circuit of a three electrode system.

A potentiostat is also needed for EC measurement. It not only provides the power supply at different forms but also records the responses from the EC cell via the respective software that is installed on a computer, which is connected with the potentiostat. With the potentiostat and the software, it allows us to apply different EC techniques, such as CV and impedance spectroscopy

as well. Then the recorded responses (signals) can be analyzed to characterize the chemical change on the interface of the working electrode that are related with the redox reactions. The information of the analyte can thus be extracted from the data analysis.

For the three-electrode system, on one end, the three electrodes are connected to a potentiostat. On the other end, the electrodes are also connected to each other as a circuit since they are immersed in the electrolyte in a cell, or surrounded/covered by a droplet of the electrolyte that usually contains the analyte of interest. The whole setup for a three-electrode system is as shown in **Figure 1.2**, where the equivalent circuit of the EC setup is also presented. As shown by the equivalent circuit, the potential is adjusted and measured between reference electrode and working electrode, while the current is flowing and recorded between counter and working electrode. And between the working and counter electrodes, the current/charge is conducted by the ions in the electrolyte. More description and interpretation of the roles of the three electrodes are as follows:

**The reference electrode (RE):** the reference electrode is to provide a steady and well-known potential reference for the measurement of the potential of the working electrode. During the measurement, with the reaction occurring on the surface of the working electrode, the potential at working electrode might be affected by the reaction. Thus, it is very important to adjust the potential of the working electrode with respect to a constant value provided by a reference electrode. To maintain the constant value of the electrode potential, a reference electrode is usually composed of a half-cell structure with an electrode and surrounding electrolyte. And the species involved in the redox reaction are at constant concentrations that are typically buffered or saturated [18].

Standard hydrogen electrode (SHE) is the simplest reference electrode and it is used as the standard reference ( $E = 0$  V) for well-known potential values of the other reference electrodes. Similarly, as other reference electrodes, it is composed of a conductive electrode and electrolyte. The electrolyte is an acid solution containing hydrogen ions ( $H^+$ ) at 1 M and the electrode is made of platinum that is platinized [19]. On the surface of the platinum, the reduction of hydrogen occurs:



In addition, to maintain the constant concentration of hydrogen ions (oxidized form), the reduced form of hydrogen ( $H_2$ ), i.e., hydrogen gas, at 1 bar (100 kPa) needs to be bubbled into the electrolyte near the electrode. This results in the difficult maintenance and preparation for the

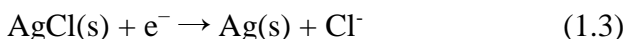
application in EC biosensors. Therefore, reference electrodes that are easy to be prepared are needed when developing EC biosensors.

Saturated calomel electrode (SCE) and Silver chloride electrode (Ag/AgCl) are two of the most commonly used reference electrodes for EC biosensors. SCE is based on the redox reaction of elemental mercury (Hg) and mercury (I) chloride (Hg<sub>2</sub>Cl<sub>2</sub>) and Ag/AgCl is based on the redox reaction between elemental silver and silver chloride. Compared to the universal SHE, the preparation and storage of SCE and Ag/AgCl are simpler. Therefore, they are more commonly used for electrochemical measurements.

The electrode potential of SCE is + 0.241 V (saturated) referring to SHE. It consists of a Pt wire that is linked to Hg and the paste of Hg/Hg<sub>2</sub>Cl<sub>2</sub>/KCl. The surrounding solution is potassium chloride (KCl). The half cell reaction happens on SCE is as below [20]:



However, SCE is now widely replaced with Ag/AgCl due to the environment consideration. As a result, Ag/AgCl is now widely used as reference electrode in electrochemical measurements since it is easy for preparation/maintenance and environment friendly. Ag/AgCl consists of a silver wire coated with AgCl and the wire is immersed in the chloride salt solution. The salt solution is normally 3 M KCl or sodium chloride (NaCl). The electrode potential of Ag/AgCl is +0.197 V (saturated) with respect to SHE. And the half-cell reaction is based on the redox reaction between Ag and AgCl, which is described as below [20]:



Moreover, the reference electrode can also be adapted from other materials. For example, in this work, the whole strip with three bimetallic electrodes is directly adapted to the three-electrode for urea detection. In other words, the reference electrode used in that case is the electrode of gold and palladium (the bimetallic channels). It might suffer the loss of stability, but it benefits the manufacturing for minimized portable electrodes system.

**The counter electrode (CE):** the counter electrode is the electrode to complete the circuit with working electrode. It is also known as auxiliary electrode. The current flows through working and counter electrode via electrolyte and then is recorded as the response signal during electrochemical measurements. The implementation of the counter electrode ensures that the current will not pass

through the reference electrode, hence the stability of reference electrode will not be affected by the current. The materials used for counter electrodes should have good conductivity so the current passing through will not be limited. Usually, platinum (Pt) is used as a counter electrode. In some situations, other conductive materials such as carbon material, Au, and Ag can also be used as a counter electrode.

**The working electrode (WE):** the working electrode is where the redox reactions occur [21]. It is the part we are most interested in when developing an EC biosensor. It is the transducing area that convert the chemical or biological information of the target molecule into measurable electrical signals. The materials used for working electrodes need bare good conductivity and also the ability to not interfere the redox reaction of the target analyte within the applied potential range [22]. Metallic materials such as Au, Ag, and Pt are commonly used as working electrodes [23-25]. Carbon materials such as graphene and glassy carbon and also widely used for the development of the working electrodes [26, 27]. In addition, it is also important to consider the catalytic reactivity of the electrode for the specificity of the target molecule. Therefore, considering different aspects, the development of the working electrode as (bio)sensor often combine different materials. For example, modification of nanomaterials, based on commonly used working electrodes made from bulk materials (such as GCE, Au, etc.) is commonly performed to achieve better performance for electrochemical sensing [2, 28, 29]. A more detailed introduction to the EC (bio)sensors (which are basically the development and application of working electrodes) will be given later.

Now we will dive deeper into the micro scale to have a close look at the fundamental mechanism behind the redox reactions on the interface of the working electrode.

#### *Electric double layer:*

As mentioned before, the whole electrochemical system can be described by an equivalent circuit. Similarly, the reaction related with molecules happens on the surface of the working electrode can also be described by electrical components. More specifically, the interface between the working electrode and the electrolyte is described by an electrical double layer. This theoretical model was firstly proposed by Helmholtz [30, 31]. Briefly, the interface between the electrode and the bulk solution (the electrolyte) can be considered to consist of two layers. The first layer is composed of specifically absorbed ions and solvated ions. It is also known as compact layer. In more details, the center of the specifically absorbed ions on the surface via chemical attraction is called inner

Helmholtz plane (IHP), while the solvated ions that are surrounded by the solvent particles next to IHP is called outer Helmholtz plane (OHP) [18]. Next to OHP, the other layer is formed by the ions that are attracted to the first layer because of the surface charge. Compared to the compact layer, the ions forming the second layer have higher mobility. Thus, the second layer is also known as the “diffuse layer”, and it ranges from OHP to the bulk solution.

#### *Faradaic current and charging current:*

To improve the sensitivity of the (bio)sensor, i.e., the working electrode for the detection of target and/or probe molecule, it is important to understand the details when redox reaction occur on the surface of the working electrode. The signal, or the current that we are interested in should be directly caused by or related to electron transfer induced by the redox reaction, which is also known as the Faradaic current. However, in addition to Faradaic current, there is also non-Faradaic current generated during the electrochemical process that is not related with the redox reaction but with the polarization and the capacitance of the electrode, which is called charging current [32]. During the measurement of the current signal, especially with the analytes that have been well studied with their redox reactions, we always try to record the Faradaic current but minimize the non-Faradaic current so that the non-Faradaic current which is not relevant with the redox reaction of the analyte will not overshadow the Faradaic current, which results in the inaccurate interpretation of the data analysis and a bad sensitivity.

### **1.4.2 Electrochemical techniques**

There are a series of different techniques in electrochemical measurement based on different input and output, classified into voltammetric, potentiometric, and electrochemical impedance spectroscopy. In this section, several methods including cyclic voltammetry (CV), chronoamperometry (CA), differential pulse voltammetry (DPV), and Electrochemical impedance spectroscopy (EIS). All of these methods can be used for electrochemical detection in (bio)sensing. CA and CV can also be used for deposition. For example, in our work, CA is used to electrochemically deposit AgNPs onto working electrode.

In Cyclic Voltammetry (CV) form, the potential changes at a constant rate. After it reaches the limit, it will change the scanning direction at the same rate. Researches are reported using electrochemical methods to detect biological molecules with metallic nanoparticle- and/or carbon-

based electrode via CV as a readout [33, 34]. Differential Pulsed Voltammetry (DPV) is another technique much different from CV. It is a type of pulse voltammetry with a staircase after each period. DPV is one of the most important and widely used pulse voltammetry [35]. It is more sensitive to the low-concentration analyte since the interference of capacitive current is subtracted. As a result, the Faradaic current can be recorded more accurately to indicate the reaction that occurs on the working electrode surface [36]. However, for an analyte that is not well studied, it is also important to explore its reaction mechanism via CV. Additionally, Electrochemical Impedance Spectroscopy (EIS) performs direct impedance measurement. Compared to CV or DPV, EIS gives us a more direct idea about the conductivity of the materials used for the working electrode [37].

**CV:** CV is a powerful technique that helps to study the redox reaction of molecules and is one of the most popular EC technique [38]. It applies a triangular waveform of voltage and recording the responding current. The detection of target analyte is achieved by analyzing the I-V curve (CV curve). As shown in the **Figure 1.3**, the input potential is scanned between two different values ( $E_1$  and  $E_2$ ) at a constant scan rate. In the forward scan, it starts from  $E_1$  to  $E_2$ , then it scans back to  $E_1$  at the same scan rate in the reverse scan. This is considered as one cycle and multiple cycles can be applied during EC measurements. Based on IUPAC convention, when the increasing voltage reaches the standard potential of the analyte, the analyte (in reduced form) will be oxidized, thus Faradaic current is generated. Therefore, an increase in the current is observed. At the same time, the analyte is consumed. When it reaches the point when there is not much analytes left, the reaction process will be limited by the diffusion of the analyte from the bulk solution to the electrode surface. As a result, the current starts to drop due to the limited amount of reactants. The peak in the forward scan thus indicates the oxidation of the analyte. During the reverse scan, a similar process happens, but instead of oxidation, the oxidized analytes are reduced (in a reversible reaction), following by the formation of reduction peak [39].

CV is most commonly used EC technique, especially when dealing with unknown analytes since it applies a range of voltage and the forward and reverse scans enable the investigation of both oxidation and reduction processes. It is beneficial to explore the possible reactions of the analyte. Based on the change in the peak potential or current, CV responses provide analytical measurements for (bio)sensing. In this work, we used CV because the catalyst for analyte reaction

is the oxidized silver, and the redox reaction of analyte is occurring in the reverse scan, which can only be realized by CV.

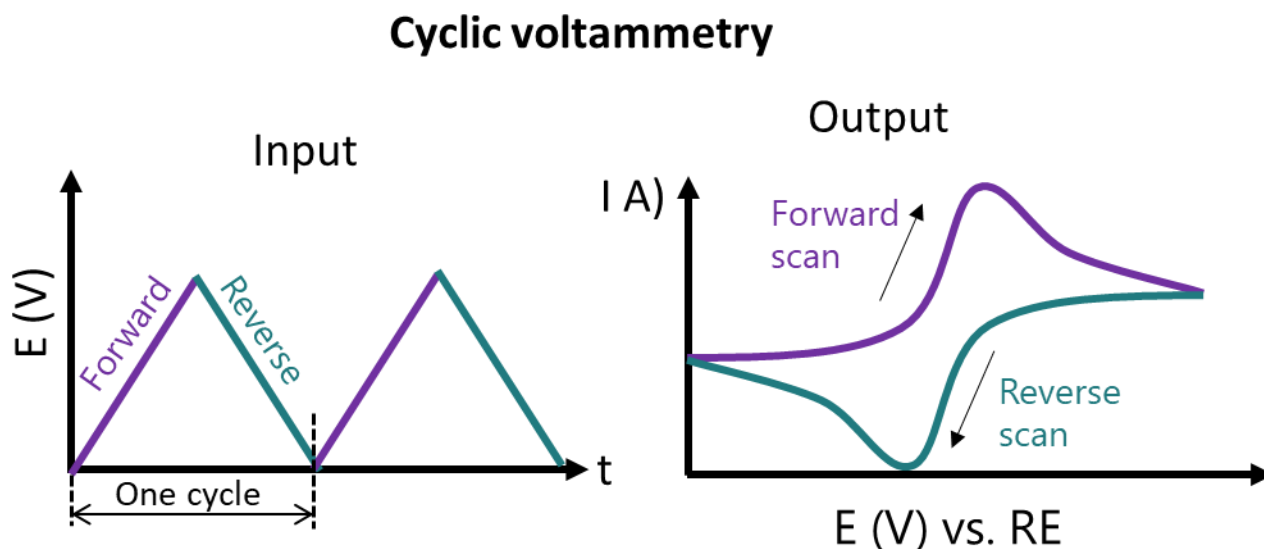


**Figure 1.3 Working principle of cyclic voltammetry:** Triangular potential waveform (left) and duck shaped voltammogram (right)

**CA:** CA is a voltammetric method. A constant potential is applied for a certain period of time, and the current is measured versus time. For CA, the choice of the constant potential is important. Usually, CV is conducted before applying CA so that the constant potential that enables the redox reactions will be applied. The current is then generated when the potential is stepped and decreased with time since there is no change in the potential. However, the charging current is also recorded with the Faradaic current, which will affect the sensitivity for (bio)sensing.

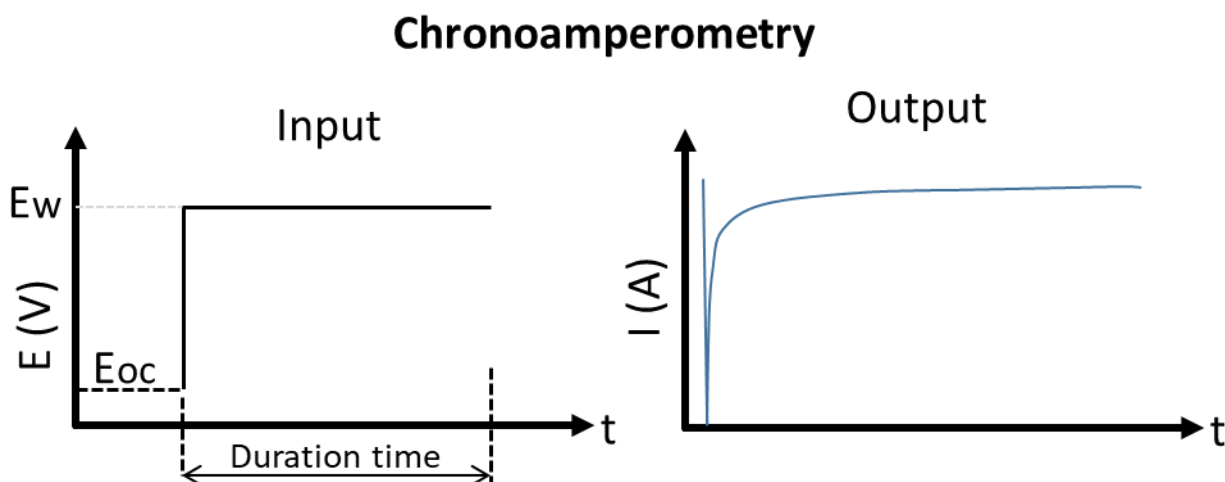


**Figure 1.4 Working principle of chronoamperometry:** constant potential input (left) and current output (right)

**DPV:** DPV is a pulse technique that applies pulse voltage, but with a differential step increase. It combines a pulse waveform with a linear sweep voltammetry (LSV) by superimposing a pulse potential on a linearly increased voltage. For pulse techniques, the measured signal is based on the difference between two sampling currents. One ( $i_1$ ) is sampled in the end of a pulse and the other one ( $i_2$ ) is sampled right before the starting of the next pulse (**Figure 1.5**). The recorded signal is calculated as  $\Delta i = i_1 - i_2$  [35]. The applying of the pulse induces a high charging current due to the capacitance of the electrode. The charging current decays exponentially with time, which is much faster than the decrease of Faradaic current. Then a measurement ( $i_1$ ) is taken when the charging current decays a lot. Similarly to this process, when the pulse is relaxing, the charging current on the opposite direction still decays faster than the Faradaic current. The second sampled current ( $i_2$ ) is thus much smaller but closer to the first sampled current. Thus, the difference between them is very small. By taking the difference between these two measurements, the effect of charging current is reduced (**Figure 1.5**). For DPV, the implementation of a linear sweep potential increases the applied voltage gradually. When the potential is still low, the charging current takes over the signals since there is no electrochemical reaction, leading to the result that no Faradaic current is generated. Consequently, the recorded current from the difference of the charging currents is small. With the increase of the linear potential, the redox reaction occurs, resulting in Faradaic current taking over the measurement since it is much higher than the charging current. Because the reaction just begins, there is still plenty of reactants. Thus, the decrease of Faradaic currents upon both sampling are slow, the difference is large. It increases with the increase of the applied voltage. When it reaches the diffusion-controlled stage where the consumption of the reactants is too much, the decrease of each sampled Faradaic current becomes faster due to the fast consumption of reactants on the surface and the limit of reactant diffusion from bulk to the electrode interface. As a result, the signal from the difference of the Faradaic currents start to decrease. Eventually, a peak indicating the redox reaction is generated with time. Considering the sampling method, a major advantage of DPV is that it minimizes the interference from the charging current, thus the results represented more Faradaic currents caused by the electrochemical reactions. Hence the sensitivity for detection is improved.

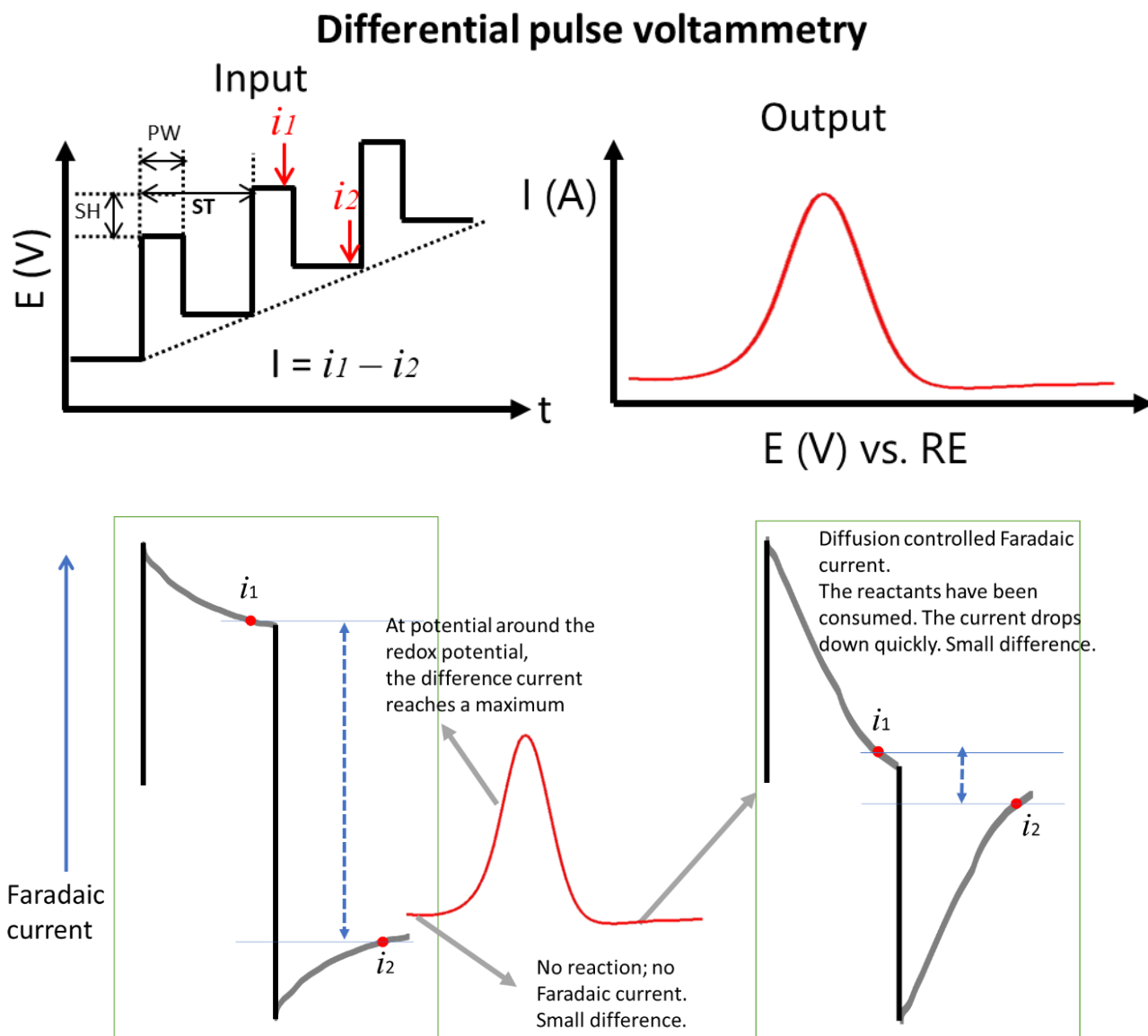


**Figure 1.5 Working principle of DPV:** applied potential staircase (top left), current-potential response for an oxidation (top right), sampling and the mechanism of response curve (bottom)

**EIS:** EIS is also an important EC technique that characterizes the change of the impedance on the surface of the working electrode and in the electrolyte. The interface of the working electrode can be considered as a capacitor in parallel with two impedances in series. In addition, the bulk solution next to the interface is considered as an impedance. This is described by an idealized Randles electrical equivalent circuit (Figure 1.6) [40]. Explanation of each component is introduced as below:

- **Cd** indicates the **capacitor** that is formed by the double layer.

- $R_{CT}$  is known as charge transfer impedance/resistance. It is related with the Faradaic reaction and the charge transfer that happens between the electrode and electrolyte.
- $R_s$  indicates the impedance of the electrolyte (the solution).
- $Z_w$  is caused by the diffusion of reactants. It is known as **Warburg impedance**. It is affected by the frequency of the applied potential. At low frequency,  $Z_w$  is larger since the diffusion of reactants is farther, while at high frequency,  $Z_w$  is smaller since time is limited for the reactants to diffuse far.

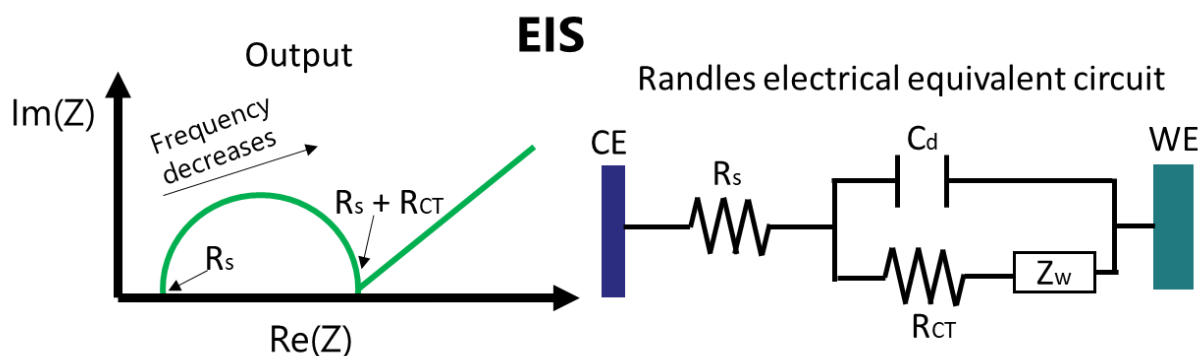


Figure 1.6 Working principle of EIS: EIS response (left) and an idealized Randles electrical equivalent circuit (right)

### 1.4.3 Electrochemical (bio)sensors

(Bio)sensors are devices that convert chemical or biological information related to target molecules into detectable signals. Based on different transducers that are used for the (bio)sensors, there are many different types of (bio)sensors such as optical and mechanical. Electrochemical (bio)sensors are one type of (bio)sensors that investigate the chemical and/or biological reaction and/or binding of the target analytes and turn them into measurable electrical signals on a working electrode, typically within a three-electrode system. EC (bio)sensors are widely used in various applications such as medical diagnosis [41], food safety [42], and environmental monitoring [43] due to their high specificity, high sensitivity, low cost, small sampling volume, simple preparation, and rapid response [16, 44, 45].

The development of an EC (bio)sensor typically refers to the development of the working electrode, on which the surface reaction occurs, and where the transducing of signal happens. As introduced in previous sections, the materials used for a working electrode should offer good electrical

conductivity, thus facilitate the electron transfer during electrochemical reaction. Two main classes selected for EC biosensors, mainly working electrodes, are metallic and carbon materials due to their electrical and mechanical properties that help to improve electrochemical activities and fabrication of the electrodes [46].

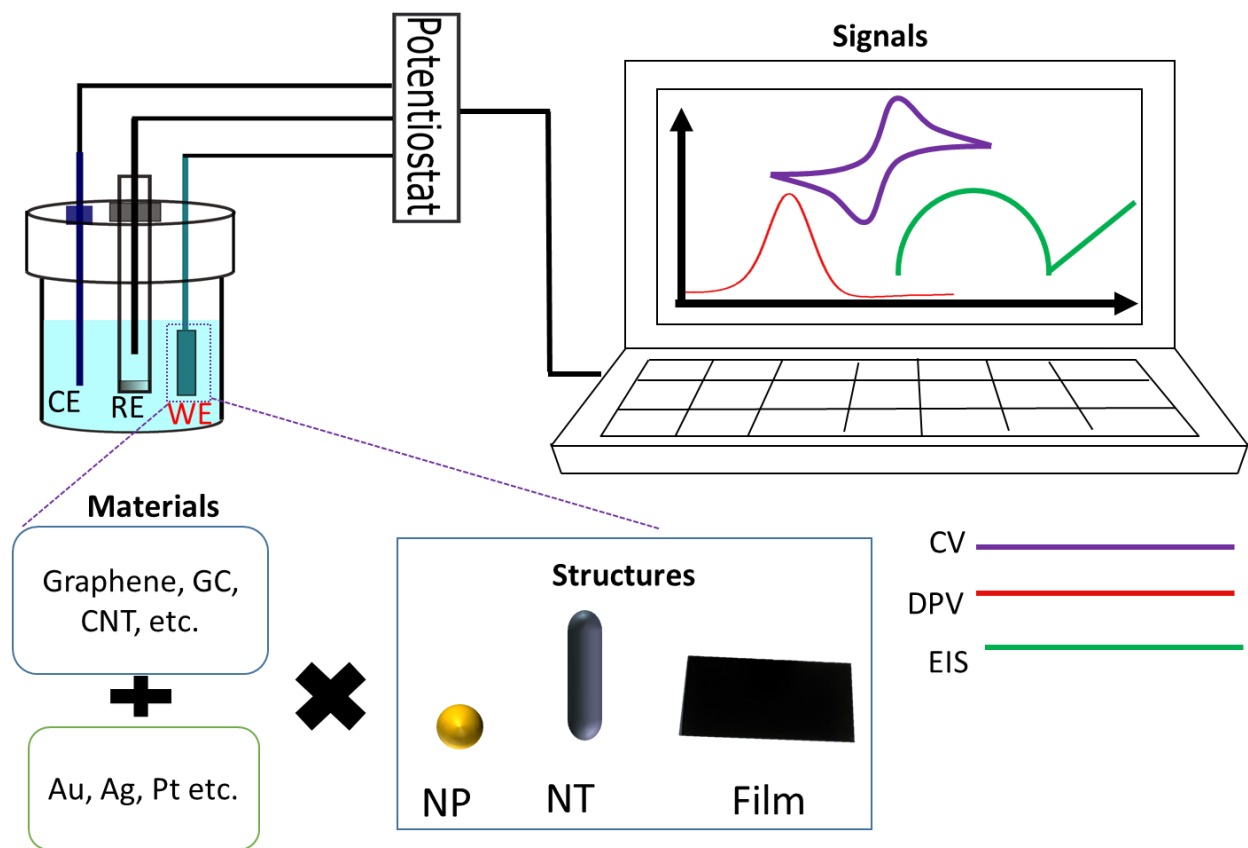


**Figure 1.7 Schematic representation of biosensing based on electrochemistry:** The working flow of measurements including experimental setup (top) and detection methods, and different materials and structures developed for working electrodes (bottom)

**Metallic Materials:** it is expected to think of metals when constructing EC (bio)sensors since they are natural electrical conductors. There are several commonly used metallic materials used for EC (bio)sensors such as Au, Pt, and Ag etc.. In addition to the materials, the morphology also plays an important role in the design of a working electrode. In general, the metallic materials used for the (bio)sensors can be categorized into nanoporous metal, and metallic nanoparticles [47, 48].

For nanoporous metal electrodes, the key parameters are the pore structure inside. The diameter of the pores ranges from nanometer to micrometer scale [49]. The pore structures increases the surface to volume area, and also allows for a better permeability [50].

Different materials such as Pd and Cu are manufactured as nanoporous metallic electrodes. The most commonly used one is Au. One typical example of nanoporous Au based electrodes are glucose meters [51, 52]. Compared to other materials, Au is well studied and has been shown to work in neutral or alkali conditions [53], thus leading to the safe preparation for EC system and better understanding towards the investigation of electrochemical process. It is also stable against regular storage. As a result, it is widely used as the candidate for commercial EC (bio)sensors such as blood glucose monitor [2]. Another metal Pt is also popular as for the fabrication of EC (bio)sensors since it offers good electrocatalytic property as well as high stability [54].

The fabrication of the nanoporous metal electrodes can be achieved by different methods. For example, electrochemical anodization, or oxidation, and chemical dealloying are two techniques commonly used for the manufacturing of nanoporous metals [47, 55]. Electrochemical anodization is a surface technique used to deposit metal on the substrate. By adjusting the conditions used for this method, such as the electrolyte and applied voltage, controllable porous structures can be obtained [56]. A typical size of 20 nm is achieved for nanoporous Au electrode via anodization methods. However, based on different protocols, different pore sizes will be managed, and larger pore size that enables more surface area interacting with analytes reaching up to hundreds and thousands of nanometers can be obtained by involving a hard template [57]. On the other hand, for less noble and alloy metals, chemical dealloying is a good option to fabricate the porous structures. Though nanoporous metal electrodes have been widely developed and used in different applications [58-60], the fabrication is still complicated and potentially limits some applications.

Metallic nanoparticles (MNPs), on the other hand, are attracting more and more attention due to their unique properties such that the sensitivity and selectivity can be improved [61]. In addition, MNPs are widely explored in biomedical applications due to their high surface area that allows for not only the analytes to interact but also functionalization such as the immobilization of antibodies [62], enzymes [63], aptamers [64] and so on. Moreover, the implementation of nanoparticles in general facilities the minimization and portability of the sensing device, expanding the applications towards point-of-care.

MNPs can be deposited on a support substrate or can be modified on an existing electrode. The deposition or coating of MNPs on substrates or electrodes can be conducted in different ways. One of the simplest methods is drop casting [65]. It is performed by simply drop casting a certain

amount of MNP solution on the surface of the substrate and then wait for the evaporation of solvent so that the MNPs will be left and coated on the substrate. MNPs in solution can be synthesised prior to drop casting by different methods such as by chemical reaction [66]. For drop casting, the amount of MNPs cast on the substrate is the main factor that matters. However, regardless the simplicity of preparation by this approach, uniform distribution of MNPs might be problem. This is because the nanoparticles tend to aggregate during the drying process. In other words, MNP deposition prepared in this method suffers from poor reproducibility [67].

Another commonly used approach for deposition of MNPs is electrochemical deposition (electrodeposition). Methods based electrodeposition are typically performed in an EC system where the target substrate that needs to be deposited is immersed in the electrolyte. The electrolyte contains the metal salt (precursor) of the desired MNPs. Then voltage or current will be applied on the target substrate at different waveforms for a certain period of time. During this process, the metal salt will be reduced. Nucleation occurs on the substrate, followed by the size growth [68]. Compared to drop casting, methods based on electrodeposition are more controllable over the distribution of MNPs. Also, the size and shape of MNPs can also be manipulated by playing with the different parameters such as the concentration of the precursor in the electrolyte, the applied voltage or current, and the duration time of them. Different EC techniques can be used for electrodeposition, such as CA, CV, as well as pulse voltammetry (pulse electrodeposition) [67]. However, electrodeposition methods are only applicable for the modification of a working electrode that is already conductive because the deposition along with the synthesis of MNPs requires a complete circuit to accomplish the reduction of the precursor.

**Carbon Materials:** Carbon materials are another main class of the electrodes used for EC (bio)sensors. They are widely used due to their electrical property, low-cost, wide working potential range, as well as electrocatalytic activities [69, 70]. There is wide series of different types of carbon-based materials harboring different morphology and structures. And the chemical properties can also be very different for different types of carbon materials. Two well-known carbon allotropes are graphite and diamond [69], among which, graphite based carbon materials such as graphene is often used in electrochemistry.

*Graphene* is a monolayer graphite with lattice structure of  $sp^2$  bonded carbon atoms [69, 71]. It has attracted significant attention for electrochemical (bio)sensing due to its extraordinary

properties in different aspects, including electrical, optical, thermal, and mechanical [72, 73]. Besides, as a 2D material, it also shows high surface area [74].

The synthesis method of Graphene plays an important role on the synthesized products and their structural properties [75]. Several methods have been reported to synthesize Graphene such as mechanical exfoliation of graphite [76], chemical vapor deposition (CVD) [77], and chemical or thermal reduction of graphite oxide (GO) [78].

Exfoliation of graphite is the first reported repeatable method for Graphene synthesis since 2004 by Novoselov et al. [76]. They discovered graphene films that were few atoms thick and obtained them by mechanical exfoliation of highly oriented pyrolytic graphite (HOPG). This method utilizes a scotch tape to repeatedly peel off layers from HOPG after they are broken into small mesas. Since then, the interest in Graphene has been significantly increased due to this reliable synthesis method of Graphene films [79, 80]. Their method has been followed and modified to reach large-area production [81, 82]. These methods generate single- or few- layer Graphene that are typically applied in electronics [83].

CVD is another approach for Graphene synthesis that was first proposed in 2006 [77]. Graphene sheets were synthesized on Ni foils from the precursor camphor via a reaction induced by heating and cooling procedure. Graphene sheets prepared by this approach usually have several layers and large areas. However, using this technique doesn't allow for controllable number of layers [83].

In addition to Graphene introduced above, *carbon nanotubes (CNTs)*, including single-walled and multiple-walled carbon nanotubes (SWCNTs and MWCNTs) is also exploited for EC (bio)sensing [47]. CNTs are 1D materials that are shaped as a cylinder with a wall of Graphene. Thus they share some similar properties such as large surface area, good conductivity, and chemical properties [46], which make them good candidates as well for EC (bio)sensors.

On the other hand, *glassy carbon* is a glass-like carbon material. It can be synthesized by heating polymers such as polyacrylonitrile at high temperature (1000-3000 °C) under pressure [84]. It can stand high temperature. It is a widely known electrode material. In fact, Glassy carbon electrode (GCE) is one of the most widely used electrodes owing to its high electrical conductivity, electrochemical inertness, wide potential window, and low cost [85, 86].

As known now, both metallic materials and carbon materials are commonly used types of electrode materials for EC (bio)sensing, and it is worth noting that some materials especially nanomaterials such as MNPs or CNTs need support substrate when implemented into EC system as working electrodes, while some other materials can be used as electrodes directly without supporting substrate, such as GCE or bulk metal materials. Consequently, to combine the advantages of different materials, the combination of different materials is explored a lot. For example, GCE is frequently modified with MNPs [87], carbon nanomaterials [88], or both [89].

### ***Applications***

As introduced before, there are many different implementations into EC techniques such as CV and DPV that can be used in an EC (bio)sensor. There are also different electrodes of different materials and modifications to improve the performance for EC (bio)sensors. Based on these, numerous EC (bio)sensors have been proposed and reported for analytes in various applications such as medical diagnosis, food safety, and environmental monitoring [90-92]. In addition, EC (bio)sensors also show great potential for PON applications in particular due to their utilization of portable sensing device.

*Environmental* problems have been a significant global issue for decades, especially with pollution issues such as water pollution and air pollution. Among different types of (bio)sensors, EC (bio)sensors are explored widely for environmental monitoring because of their characteristics such as high sensitivity, low cost and rapid response [43]. Except for those advantages, the fact that EC sensors can work with small volume of samples down to micro liter reduces the risk of working with hazardous pollutants at large quantity [93]. Moreover, EC sensing device can also be portable, which is significant for applications at PON, so the sensing device can be carried and used easily [94].

The market of EC biosensors or devices for *medical diagnosis or health monitoring* are progressing rapidly for the detection of biomarkers that are specific or related to different diseases. For example, glucose meter is a common product now in the market, and it can be used for diabetes monitoring [13]. To improve the specificity for biomarker detection, different bio-recognition elements like nucleic acid [95], antibodies [96], or other components such as enzyme are utilized. Enzymatic biosensors can catalyze the redox reaction of the analytes which will improve the sensitivity and specificity. However, the functionalization of enzymes also brings drawbacks, such

as more complicated preparation of electrodes and shorter lifetime of the sensor due to instability of enzymes. Therefore, the development of non-enzymatic biosensors draw more and more attention for medical applications, especially for PON applications [97, 98]. The ability to maintain a comparable sensitivity and specificity as enzymatic sensors is still challenging but the key point when developing non-enzymatic EC sensors.

*Food safety* is another important issue that greatly affects our life quality. Rapid analytical detection of the potential food contaminants including toxins, bacteria, or pesticides residues is critical for the monitoring of food quality [99]. EC (bio)sensors exhibit advantages such as in situ analysis and rapid detection over conventional techniques [42]. In addition, EC biosensors are also reported to be combined with other techniques such as microfluidics in order to improve sensitivity [100]. In the particular case of pesticide detection, which is a potential food contaminant, chromatographic methods are typically used such as gas chromatography or high-performance liquid chromatography (HPLC) [101]. However, their expensive cost and complicated sample preparation limit their use at PON. EC biosensors, on the other side, address those limitations and thus make a good candidate for pesticide detection at PON. The limit of detection for pesticide residues via EC can reach as low as nM level in fruit or vegetable samples [102].

In summary, the characteristics of EC (bio) sensors such as high sensitivity, high specificity, low cost, and fast response make them possible for PON applications which involve point of care and also provide more information for follow up. So far, EC (bio) sensors have already been commercially available in medical application such as glucose meters. In this thesis, a sensing platform that works for EC will be used for the detection of urea and chlorfenapyr to demonstrate the potential in applications to food safety and diagnostics.

### **1.5 Surface enhanced Raman spectroscopy (SERS)**

As another sensing technique used in this work, SERS, is a highly sensitive approach that enhances Raman signal significantly for molecules adsorbed or absorbed on plasmonic substrates such as metallic nanoparticles or nanostructures [103]. As a beginning, an introduction to the basic fundamentals on Raman spectroscopy will be given, as well as the AgNP based substrates that are used for SERS. A more comprehensive review on plasmonic (bio)sensors will be presented in chapter II with emphasis on the discussion for PON applications.

### 1.5.1 Raman spectroscopy

Raman spectroscopy is an analytical technique that determines analytes based on an optical phenomenon known as Raman scattering. Raman scattering was discovered by Indian physicist Raman in 1928 [104]. It is an inelastic scattering, which means the frequency of the scattered light is different from the incident light. When the incident light, typically a laser, strikes on the target sample, most photons are scattered at the same energy level that leads to the same frequency. This is known as elastic scattering called Rayleigh scattering [105]. However, there is also a small fraction of photons that are scattered at different frequency after interaction with the target samples and this is Raman scattering. In Raman scattering the scattered photons have different energy as well as the frequency and wavelength compared to the incident photon. Based on how the energy level is shifted from the incident light, there are two different types of Raman scattering (**Figure 1.8A**). When the molecule of ground state moves to a more excited vibrational state, energy is needed and absorbed from the incident light. Thus it leads to a decrease in the energy for the scattered light, which further causes a decrease in frequency. This downshift in frequency for scattering is called Stokes scattering. On the opposite, when the molecule moves to a less vibrational state, it leads to an increase in energy and frequency for the scattering. And this upshift in frequency is called anti-Stokes scattering. Mostly Stokes scattering occurs, where the material absorbs energy and the emitted photon has a lower energy than the incident photons, thus has a larger wavelength and a lower frequency.

Raman spectroscopy utilizes Raman scattering for the identification at molecular level due to the distinctive energy shift in scattering after interaction with different chemical bonds according to their vibrational modes [106]. The shifts caused by different chemical bonds will be recorded as Raman spectra, indicated as peaks (**Figure 1.8A**, bottom). So for molecules with different chemical bonds, the Raman spectra specifically show chemical information, two molecules with different structures, each bond corresponds to different peaks, making different Raman spectra. According to the Raman spectra, the chemical structure of the molecule can be reconstructed [107].

Raman measurements can be achieved by a Raman system with different optical components. The experimental setup for a Raman system is shown in **Figure 1.8B**, the incident laser is focused on the target samples using an optical lens. The focused laser is then interacted with the target molecules, resulting in photons that are scattered at different frequencies that correspond to

different chemical bonds. The scattered photons will pass through the dichroic mirror and finally reach the grating, where the scattered light at different frequencies (wavelengths) will be grating and recorded as a Raman spectrum by the detector such as a CCD detector. Based on the recorded spectrum, the target molecule can be identified.

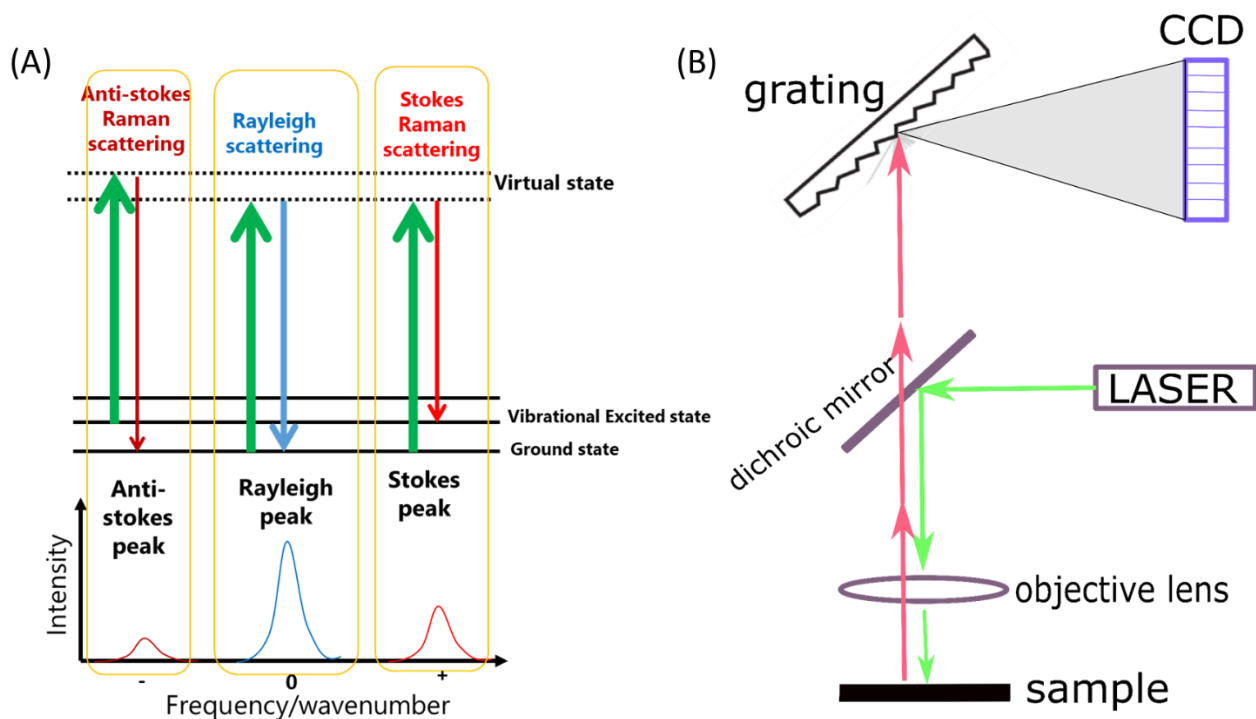


**Figure 1.8 Schematics of Raman spectroscopy.** (A) Basic principle of Raman scattering. (B) schematics of experimental setup for Raman spectroscopy

Raman spectroscopy is a plasmonic technique that provides identical detection method. Thus it is widely used for sensing applications. However, as mentioned above, only a very small fraction of photons is scattered in this way, so the Raman signals are usually very weak at low concentration. To improve the sensitivity for detection, the detected signals need to be enhanced to improve the limit of detection. SERS is such a technique to enhance Raman scattering by performing Raman measurements on plasmonic substrates such as metallic nanoparticles or nanostructures.

### 1.5.2 AgNP-based substrates for SERS

Two primary mechanisms are responsible for SERS enhancement: electromagnetic and chemical enhancements. Electromagnetic enhancement is considered as the dominant one. When the incident light strikes the surface, Localized Surface Plasmons (LSPs) are excited. It will enhance

the local electromagnetic field. The electromagnetic fields generated by Surface Plasmons (SPs) and LSPs at the surface of the metal will interact with the incoming photons and also with the Raman emitted photons to provide significant enhancement of the Raman scattered photons. SERS allows for highly sensitive structural detection of low-concentration analytes through the amplification of electromagnetic fields generated by the excitation of LSPs [108].

Among different plasmonic materials, noble metallic nanoparticles show good biocompatibility, high surface-to-volume ratio and unusual electrical, optical and magnetic properties compared to the traditional bulk materials [11]. As a result, numerous articles on noble metallic nanoparticles, especially AgNPs that are used for SERS substrates have been reported [109, 110]. On the other hand, the combination of AgNPs, working as SERS active materials, and nanostructured substrates enlightens directions for SERS measurements, especially on biological samples at small volume since the nanostructures help to concentrate target analytes in the samples and also can help to create “hot spots” of AgNPs.

SERS is one of the detection methods used here. As such, the preparation of the biosensing platforms for SERS is the first crucial step before moving forward to the applications. Therefore, this chapter is mainly focused on the (bio)sensing platforms/substrates that are developed for SERS.

AgNPs are widely used as SERS active materials, combining with different nanostructured substrates. The preparation and decoration of AgNPs are also various. In situ synthesis that grows AgNPs directly on the substrate is a simple and efficient method. For example, Suarasan et al. developed a superhydrophobic bowl-like SERS substrate for the characterization of extracellular vesicles (EVs) [111]. The substrate is made from PDMS that is molded on the CMOS chip that is already coated with polystyrene beads at 7  $\mu\text{m}$ . CMOS chip contains a micro-lenses array on the surface that are uniformly manufactured on the surface, which gives us a template of uniform nano-bowl structures. The bowl-like structured PDMS substrate exhibits superhydrophobicity that help to trap the EV samples. Later, this fabricated patterned PDMS is further functionalized with AgNPs that will enhance the local electromagnetic field for SERS signals, which is also where my major contribution comes, with the designing of in situ growth of silver nanoparticles on PDMS to enhance detected signals for SERS measurements [111]. A simple method is used to grow AgNPs in situ on the PDMS substrate under room temperature with short time. The synthesis of

AgNPs is adapted from a reported protocol [112]. A precursor of silver nitrite ( $\text{AgNO}_3$ ) is prepared at 25 mM, and the reducing agent selected are ascorbic acid (AA) and sodium citrate, which is also working as a protecting capping. They are also prepared at a concentration of 25 mM. The prepared solutions are then dropped on the surface patterned PDMS at the same volume of 20  $\mu\text{L}$ , and then pipetted gently to be mixed completely. The reaction happens once the mixture is done. A color change from transparent to light blue, and then to dark grey, indicating the growth of silver nanoparticles. The mixture is incubated under room temperature for 5 min to allow for a through reaction and bonding to structured PDMS. After then, the reacted solution is removed from PDMS with a pipette and then rinsed with Milli Q water to wash away the unbound nanoparticles.

In addition to the commonly used PDMS mentioned above, the combination of AgNPs with other materials such as biomaterials is also reported as ideal composites for SERS detection. Their inherent and natural properties can be utilized for biosensing. As a main group of unicellular microalgae [113], diatoms as a biomaterial exhibit a diversity of 3D structures with nanopores. These natural nanostructures provide diatoms with unique mechanical and optical properties. Compared to the complicated lithographic methods used to obtain patterned nanostructures to improve the reproducibility of SERS substrates, using diatoms as a natural template not only saves time and money but also provides a great diversity of nanostructures since there are more than 100,000 species of diatoms, each providing distinctive nanostructures [114]. Diatom cells are enclosed within a silica cell wall called a frustule. Frustules provide photonic crystal-like features. As naturally occurring photonic crystal structures, diatoms can be used to control and manipulate light as optical materials, which makes them quite attractive. In addition, due to their large areas and outstanding optical properties, diatoms are often used as a platform for biosensing [115].

Rojalin and Koster et al. proposed a simple, portable, and inexpensive plasmonic scaffold is proposed in this work for the identification of ovarian and endometrial cancer EVs. The plasmonic scaffold is nanobiocomposite coated strip that is prepared with AgNP coated biosilica, i.e., diatoms, on office tapes with a simple and low cost method. The substrate is then functionalized with cysteamine to better capture EVs in the hot spot area generated by the coated AgNPs [116]. The prepared (bio)sensing platform is characterized with EM imaging prior to the utilization in SERS analysis of EVs. The micro porous structure of the diatoms provides large surface area to capture target analytes, and its combination with AgNPs creates local electromagnetic field that enhances

the Raman detection for the EVs within the vicinity on the surface. This platform offers a rapid label-free method for the identification of EVs and shows promising potential for early stage cancer diagnostics [116].

Silver nanoparticles are widely used in the development of (bio)sensors or (bio)sensing platforms, working as SERS active materials and/or working electrodes for EC sensors. In this section, with different approaches, several (bio)sensing platforms are introduced using AgNPs that are deposited on different substrates based on the transducer and application. The simple preparation and low cost of the substrates make them promising substrates for PON applications. More discussion on plasmonic materials will be shown in the following chapter, as well as the fundamentals and applications, especially the discussion on the perspectives of plasmonic biosensors for PON applications.

## **Chapter II: Are plasmonic optical biosensors ready for use in point-of-need applications?**

As discussed in Chapter I, medical diagnosis and food safety are very important for our life. Sensors developed for PON applications provide straightforward ways for us to monitor either the disease biomarker or food contaminants that can potentially cause diseases. For the development of sensors for applications at PON, it is important to design and optimize sensor parameters that make their implementation close to practical. On the other side, plasmonic techniques, such as Raman spectroscopy, as one of optical methods, is commonly used for analytical biosensing due to their high sensitivity and specificity, potential for multiplexing, low noise background, and small volume sample [117], which makes it an ideal candidate for PON applications. Therefore, in this chapter, a literature review on plasmonic optical biosensors is given with emphasis on fundamental properties, materials, techniques, and applications. In addition, a thorough discussion on their use in PON applications is presented.

This chapter is based on my first publication as a first author [1]. The details of the publication are as following:

**Juanjuan Liu**, Mahsa Jalali, Sara Mahshid, Sebastian Wachsmann-Hogiu, *Are plasmonic optical biosensors ready for use in point-of-need applications?*, Analyst, 2020, DOI: 10.1039/C9AN02149C

The contributions of authors are: JL wrote the manuscript except for section 2.3 that is written by MJ. SWH designed the outline of the manuscript and reviewed the manuscript. All authors made substantial intellectual contributions to the manuscript.

Specifically, I reviewed the literature in the field of plasmonic biosensors for PON applications, and provided a comprehensive summary from fundamentals of the materials to the functionalization of the substrates and plasmonic-based detection methods. Further, I reviewed the current status of PON plasmonic biosensors in different areas. In the end, I discussed the parameters that are important for the design of PON biosensors in detail.

## **Are plasmonic optical biosensors ready for use in point-of-need applications?**

**Juanjuan Liu<sup>1</sup>, Mahsa Jalali<sup>1</sup>, Sara Mahshid<sup>1</sup>, Sebastian Wachsmann-Hogiu<sup>1\*</sup>**

<sup>1</sup>Department of Bioengineering, McGill University, Montreal, Quebec, Canada

**\* Correspondence:**

Sebastian Wachsmann-Hogiu

[Sebastian.wachsmannhogiu@mcgill.ca](mailto:Sebastian.wachsmannhogiu@mcgill.ca)

**Keywords: Optical Biosensors, Plasmonics, Nanostructures, Point-of-Need Applications**

### **2.1 Abstract**

Plasmonics has drawn significant attention in the area of biosensors for decades due to the unique optical properties of plasmonic resonant nanostructures. While the sensitivity and specificity of molecular detection relies significantly on the resonance conditions, significant attention has been dedicated to the design, fabrication, and optimization of plasmonic substrates. The adequate choice of materials, structures, and functionality goes hand in hand with a fundamental understanding of plasmonics to enable the development of practical biosensors that can be deployed in real life situations. Here we provide a brief review of plasmonic biosensors detailing most recent developments and applications. Besides metals, novel plasmonic materials such as graphene are highlighted. Sensors based on Surface Plasmon Resonance (SPR), Localized Surface Plasmon Resonance (LSPR), and Surface Enhanced Raman Spectroscopy (SERS) are presented and classified based on their materials and structure. In addition, most recent applications to environment monitoring, health diagnosis, and food safety are presented. Potential problems related to the implementation in such applications are discussed and an outlook is presented.

### **2.2 Introduction**

Biosensors show great potential in many areas such as medical diagnosis, food safety, and environmental monitoring [1-3]. When it comes to the detection of analytes such as disease biomarkers or contaminants, it is important to develop accurate biosensors that have high sensitivity and specificity. In general, biosensors utilize a bioreceptor as recognition element (a molecule capable of specifically binding to the analyte) and a transducer (an interface such as

electrodes or nanoparticles) to convert analyte binding events into readable signal. Analytical biosensors can provide accurate concentrations of the analyte due their linear relationship between the concentration and intensity of the detected signal. As a result, by means of a figure of merit, they provide an intuitive way to compare the sensitivity between different biosensors. [4]. Based on the detected signal, biosensors can be classified as optical (such as plasmonic biosensors), electrochemical, piezoelectric, or magnetic biosensors [5]. Among these biosensors, optical biosensors are one of the most commonly used techniques for analytical biosensing due to their high sensitivity and specificity, potential for multiplexing, low noise background, and small volume sample [4].

There are several review articles discussing the plasmonic biosensors which emphasize on different aspects of this field including the materials, fabrication method, and functionalization. For example, J. R. Mejía-Salazar et al. reviews the advances in plasmonic biosensing using new materials with unique properties focused on the manufacturing of portable devices [6]. Longhua Tang et al., on the other hand, specifically reviews the advances colorimetric biosensors for molecular diagnosis [7]. Other aspects such as chemical functionalization [8], and operating principles [9] of plasmonics-based biosensors have also been reviewed in recent years. More recently, review articles on the topics of comprehensive understanding and discussion on expectations for the near future development of SERS [10], plasmonic biosensors for point-of-care diagnosis applications [11], and carbon-based materials for SPR biosensors [12], were published. Here, we highlighted the potential of plasmonic biosensors in point-of-need applications with respect to the following aspects: (a) the fundamental principles and mechanisms that allow development of plasmonic biosensors, with emphasis on metallic structures and graphene (b) the materials and structures used to transduce the analyte binding events into an optical signal, (c) the applications to real life situations, and (d) their future potential and limitations

### **2.3 Fundamentals of plasmonic materials**

Plasmonics studies the interaction of light with metals or metallic nanostructures. Other materials such as graphene also exhibit plasmonic resonance due to the availability of conductive electrons. Plasmonics combines techniques from photonics and electronics at the nanoscale to perform optical measurements of spectra and refractive index changes (via reflection angles) that are related to the chemical structure, or binding events, and can help extract valuable information about the

presence, concentration, or identity of molecules of interest [13, 14]. The study of plasmonics relies on localized or propagating surface plasmons (SPs), which are collective (coherent) oscillations of electrons in the metal, and are generated by the coupling of the incident oscillating electric field of the electromagnetic wave with the electrons at the metal-dielectric interface [15]. The optical response of plasmonic materials can be described via the dielectric function (or complex permittivity),  $\epsilon(\omega)$ , where  $\omega$  is the angular frequency of the light. For plasmonic materials, the real part of the dielectric function is negative. Several phenomena can be observed when light interacts with plasmonic materials, such as the generation of surface plasmons (SPs) and surface plasmon polaritons (SPPs). SPs are collective oscillations of electrons generated at the interface between two materials where the sign of the dielectric function changes, such as in the case of metal-dielectric interfaces, where the dielectric is the positive-permittivity material and the metal is a negative-permittivity material. This charge oscillations generate an electromagnetic wave inside and outside the plasmonic material which is either localized (in the case of closed structures such as very small metallic particles) or delocalized (in the case of planar interfaces such as thin metallic films). The collective charge oscillation and the associated electromagnetic fields are called localized surface plasmons (in the first case) or surface plasmon polaritons (in the second case). The dispersion relation of different plasmonic materials including gold and silver can be investigated via Maxwell's equations. At visible wavelengths, the electromagnetic energy concentrates into subwavelength volumes at the surface of the metal and overcomes the diffraction limit constraint of classical optics [16]. The fundamentals of SPs and SPPs and their ability to guide and confine light into the ultra-small subwavelength scale has been extensively reviewed over the past two decades in the context of nanophotonics research [17-19]. In addition, these phenomena play a significant role in the design and function of plasmonic sensors, leading to two main techniques of plasmonic sensing: Surface Plasmon Resonance (SPR)-based and Localized surface Plasmon Resonance (LSPR)-based biosensing. Both SPR and LSPR are sensitive to the change in the dielectric environment [20]. The specific detection methods will be discussed in later section.

For the metallic materials, the Drude model is commonly used to characterize the dielectric function:  $\epsilon_{\text{Drude}} = 1 - \frac{\omega_p^2}{\omega^2 + i\gamma\omega}$ , where  $\gamma$  is the electron collision frequency in the bulk,  $i$  is the imaginary unit, and  $\omega_p$  is the bulk plasma frequency of the free electrons [21]. It indicates that the optical properties of the material will be affected by the incident light.

The interaction between a metallic nanoparticle and the incident light can lead to an increased photonic LDOS in the vicinity of the structures, leading to changes in the optical properties of nearby molecules such as the spontaneous emission rate [22]. Thus, these interactions can be effectively used in the enhancement and manipulation of light interaction with emitters, opening a variety of applications in biosensing [18, 23]. In addition, the resonant frequency of the surface plasmons is adjustable based on the size, geometry, dielectric environment, material composition (see Figure 2.1a and b) and separation distance of the metallic structures and will lead to opportunities in designing specific structures for specific applications [24].

Transition from single plasmonic particle to multiple particles arranged in complex geometries leads to strong interactions of plasmons in metallic nanostructures assemblies that can help with the optimization of plasmon resonance frequencies for applications in the field of plasmonic sensors. For example, in the case of pillars, as illustrated in Figure 1c, the optical response of the pillars is determined by the near-field interaction between neighboring elements. In the gold monomer, common dipolar plasmon resonances are observed, while in the heptamers with small enough interparticle gap distance, the transition from isolated to collective modes is observed. In addition, a pronounced Fano resonance dip is observed that can be characterized by destructive interference of oscillating plasmons of the central metallic structure and the ring-like hexamer surrounding it. The existence of the Fano resonance in metallic nanopillars aids tuning the plasmon resonances for enhanced biosensing [25].

In order to understand the interaction of the incident electromagnetic field with the plasmonic nanostructure pillars in close proximity, first, we demonstrate the strong electric field induced by the field of the light in the confined surface of the nanoparticle/ disc. Consider an incident laser beam with specific electric field  $E_0$  shining on the surface of a round-shaped metallic nanoparticle/ disc in an array. The metallic nanostructure first concentrates the light to an extremely small (subwavelength) volume, which gives rise to a strong electric field confinement at the surface of the single metallic disc,  $E_{surface}$ , which is greatly enhanced compared to the initial electric field of the beam,  $E_0$  [18]. The electric field at the surface of single metallic nanoparticle/ disc is derived using the following equation (2.1), and strongly depends on damping by absorptive processes within the metal nanostructure, such as electron-phonon oscillations and electron surface scattering, which can be described by the imaginary part of the dielectric function.

$$E_{Surface} = \frac{(1+\kappa)\varepsilon_m}{(\varepsilon+\kappa\varepsilon_m)} E_0 \quad (2.1)$$

Where,  $\kappa$  stands for the shape factor and  $\varepsilon$  and  $\varepsilon_m$  are dielectric function and medium dielectric constant, respectively. The real part of dielectric function is responsible for the frequency position of electron oscillation resonance, and the imaginary part controls absorptive dissipation of the resonance and broadening [21]. The nearfield electric field  $E_{nf}$  at distance  $r$  from the disc center can be approximated to be dipolar and quadrupolar decaying with the distance  $r$  according to the following equation:

$$E_{nf} = \frac{2\alpha E_0}{4\pi\varepsilon_0 r^3} + \frac{3\beta \ddot{E}_0}{4\pi\varepsilon_0 r^4} + \dots \quad (2.2)$$

where  $\alpha$  and  $\beta$  are polarizability tensors of dipole and quadrupole, respectively. The plasmonic nearfield directly affects the electronic transitions and consequently the emission properties of the optical emitters in close proximity [21].

By bringing two metal nanoparticle/ disc in proximity of each other, the nearfield of one can interact with the other one. In a way that the electric field felt by each nanoparticle/ disc is equal to  $E_0 + E_{nf}$  instead of  $E_0$ . As a result of this interaction the two, neighboring nanoparticle/ disc will be coupled. This coupling of oscillations is called plasmon coupling and is polarization-dependent which can be manifested in shifts of wavelength in absorption spectra [26, 27]. Consider a polarized incident light with direction parallel to the inter-particle/disc axis shine on nanoparticle/ disc pillar, the plasmon resonance will be red-shifted relative to the resonance of individual nanoparticle/ disc. Lowering the gap-size between the particles/discs will results in larger redshift. This polarization dependence of the plasmon coupling in nanostructure pillars is analogues to the absorption spectra shifts in organic molecules upon oligomerization [25]. While metals such as Au and Ag have been extensively studied as plasmonic materials and have been reviewed elsewhere [28-30], novel materials that exhibit two-dimensional plasmons such as graphene are currently explored as potential plasmonic materials in biosensors [31]. Graphene addresses issues such as limited tunability and large ohmic losses in coupling of electromagnetic waves to the charge excitation at the surface of sub-wavelength metallic nanostructures and offer tighter confinement and higher tunability via electrostatic gating compared to common metallic nanostructures along with longer propagation distances [32, 33]. Graphene plasmons have vastly

attracted investigations both in the area of fundamental properties [31, 34, 35] and their potential applications in biosensing [36].

An undoped graphene monolayer has a constant broadband absorption equal to 2.3% [37, 38]. The optical absorption of graphene is tunable via electrical gating by applying a voltage to shift the electronic Fermi level. Figure 1d shows a representative schematic demonstration of a fabricated ion-gel-gated monolayer graphene transistor covered by ion-gel and voltage biased by a top gate. In this example, gold was used as electrode material and fused silica was used as substrate. Figure 1e represents a schematic diagram demonstrating the modulation of the Fermi level of single-layer graphene via an applied electrical field. The positions of the Fermi level and Dirac point are equal in undoped monolayer graphene. When a negative/positive gate voltage is applied, the Fermi level of graphene will shift lower/upper vs the Dirac point, which results in negative/positive doping of the graphene monolayer. This further opens up the possibility of controlling of its optical properties in selected spectral regimes [39, 40]. Highly doped graphene has been recently investigated as a potential plasmonic material candidate because of its unique, tunable electrical properties [41]. It has shown promising plasmonic properties in the mid-infrared and terahertz spectral regions [41-43]. Graphene plasmon polaritons features stronger light-matter interaction, slow light propagation, high Purcell factor, and single photon non-linearities that have been fundamentally reviewed previously [31, 34, 44]. Tunable optical properties of graphene that enable tunable plasmonic properties of this material via the applied gate voltage leads to tunable light-matter interaction which can be used in ON/OFF switch sensors [45].

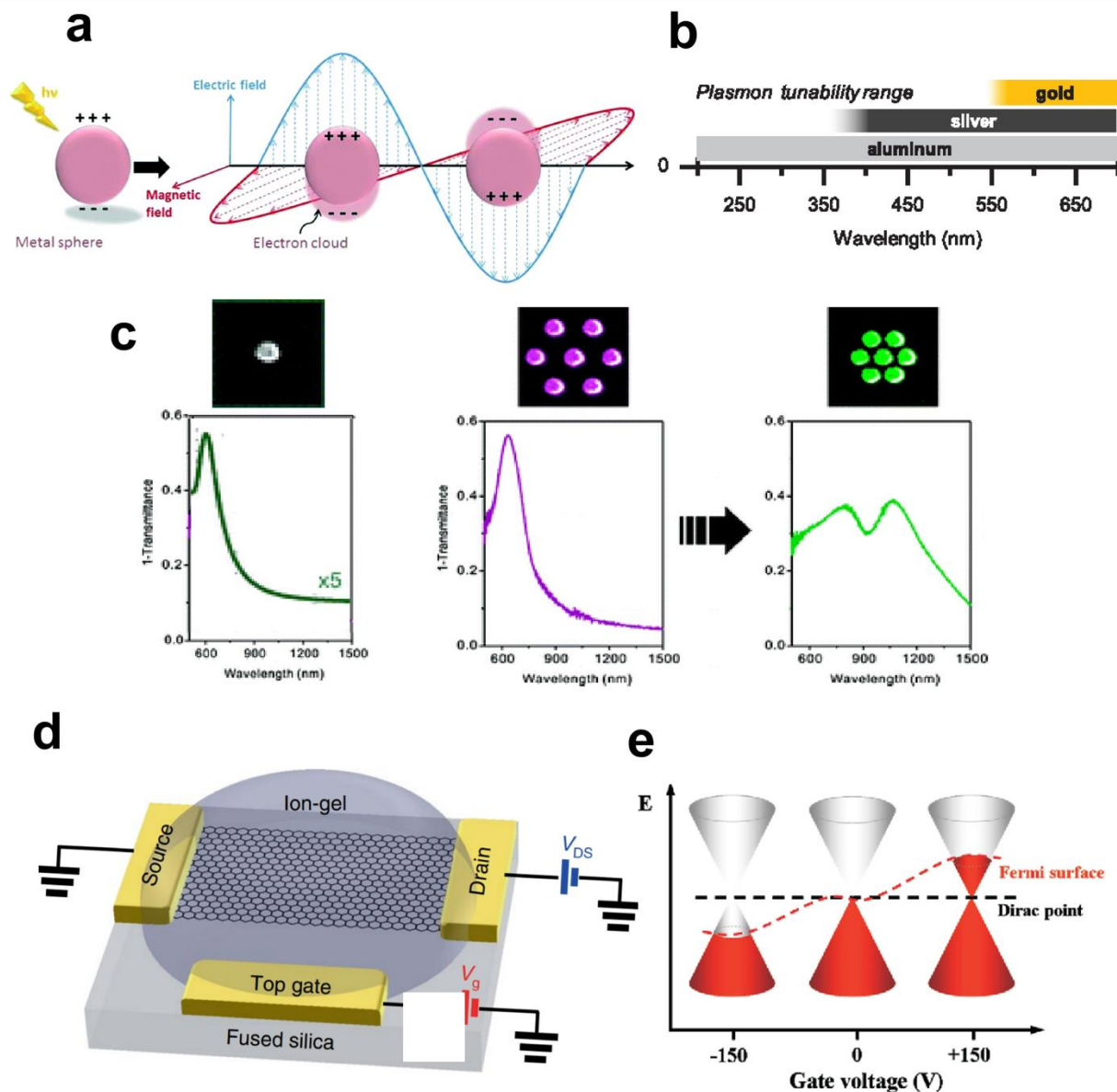


**Figure 2.1. The fundamental optoelectrical properties of metallic nanostructures and graphene.** Schematic illustration of a localized surface plasmon resonance (a). Plasmon tuning ranges of the common plasmonic metallic materials, Au, Ag, and Al (b). Extinction spectra of a gold monomer, and gold heptamers with different interparticle gap separations (c). Schematic of an ion-gel-gated graphene monolayer on a fused silica substrate covered by ion-gel and voltage biased by the top gate (d). Fermi level variation of single-layer graphene modulated with electrical field (e). Figure 2.1a is adapted from reference [46] with permission from The Royal Society of Chemistry, Copyright (2016). Figure 2.1b is adapted from reference [47] with permission from American Chemical Society, Copyright (2014). Figure 2.1c is adapted from reference [25] with permission from American Chemical Society, Copyright

(2010). Figure 2.1d and 2.1e are adapted from References [40] and [39] with permission from Springer Nature, Nature Photonics, Copyright (2018) and American Chemical Society, Copyright (2011), respectively.

## 2.4 Potential for improvement of plasmonic biosensors for applications at point of need

Over the past decades, plasmonic biosensors have been studied and their performance characterized for numerous applications in health, food safety, and environment monitoring. One particular area of interest is for point of need (PON) applications. PON applications, which include point of care, are applications where diagnosis or monitoring is needed, with recommendations for potential treatment, remediation, or follow up to a more specialized institution. Low cost, high sensitivity and specificity, fast response, possibility for multiplexed detection [48], and relative simplicity in operation make plasmonic biosensors more attractive for these applications over traditional biosensors.

The development and use of plasmonic biosensors for PON applications involves multiple steps, such as design and fabrication of substrates (Figure 2.2a), functionalization of substrates and preparation of samples, and detection of a signal indicating the presence and concentration of the analytes (Figure 2b). The working principles of these biosensors at each of these steps are described below, together with opportunities to improve their performance.

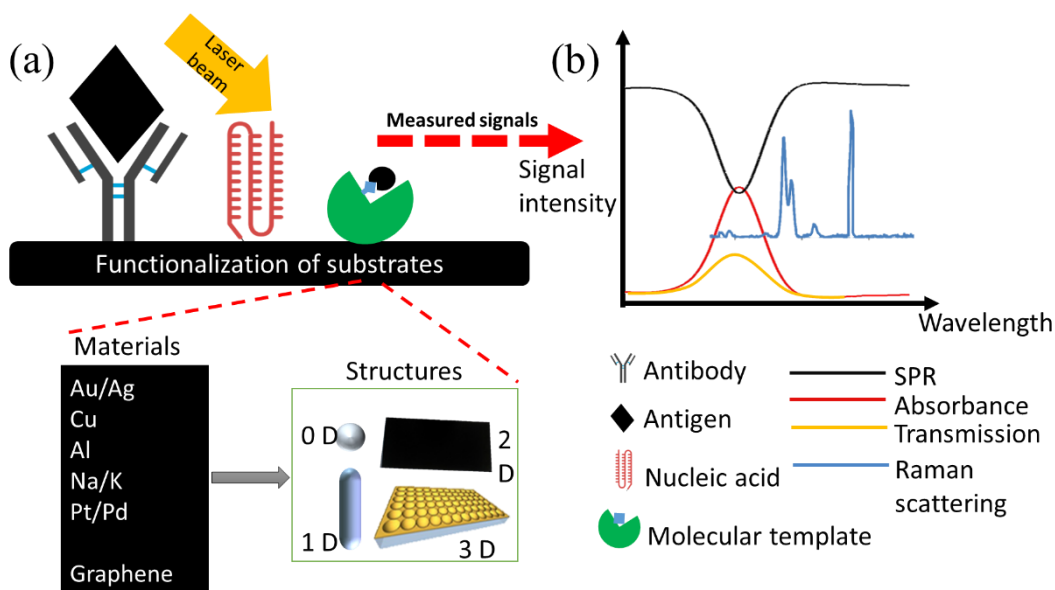


**Figure 2.2. Schematics of biosensing based on plasmonic materials.** The preparation of measurements: functionalized substrates (based on antibody/antigen, aptamers, and molecular imprinting) of different materials and structures (a) and various detection methods (b).

### 2.4.1 Basic concepts of biosensing

To evaluate the performance of biosensors, basic concepts are commonly used such as sensitivity, selectivity, receiver operating characteristic curve, limit of detection, figure of merit, and reproducibility. Here we provide a table summarizing their general definitions and the specific meaning in the context of plasmonic biosensing. The method of quantification (if applicable) is then provided in each specific case. In addition to these factors, specific factors related to plasmonic biosensors can be defined, such as the SERS *enhancement factor*, which is also discussed in the table below.

**Table 2.1 Basic concepts for the characterization of plasmonic biosensors**

Concept	General Definition	Plasmonic biosensor	Calculation
Sensitivity	For medical diagnosis: the probability of detecting the analyte (TPR) The term is also used as the minimum concentration of the analyte that can be detected	LOD, or How the measured signal changes in responding to varying concentration of the analyte	$TPR=TP/P$ for medical diagnosis, or the slope of the calibration plot
Specificity	For medical diagnosis: true negative rate The ability to distinguish the analyte in presence of other components	The biosensor is able to detect and differentiate the analyte of interest in the presence of other interfering substances	$TNR=TN/N$ for medical diagnosis
ROC	A tool to evaluate the classification performance	The performance balance between sensitivity and false positive rate	ROC curve is true positive rate versus false positive rate
LOD	The lowest quantity of the analyte that can be detected reliably	The minimum quantity/concentration of the analyte that can be detected reliably	The ratio of 3 times SD of blank to the slope of calibration plot [118]
FoM	A factor used to characterize the performance of a device, or materials, etc.	The parameter that can be used to characterize the biosensing performance such as sensitivity, LOD etc..	LSPR: The sensitivity of the refractive index in terms of change in resonance divided by resonance linewidth. SPR: sensitivity (Slope) divided by FWHM
Reproducibility	The consistency of measurements with same methodology	The ability to obtain identical measurements from sample to sample, time to time, spot to spot	RSD or CV

EF	The enhancement of SERS signal compared to Raman signal	The parameter to evaluate the enhancement of the Raman signal in the presence of plasmonic structures	The ratio between the signal detected in the presence of the plasmonic materials to the signal detected in the absence of it
----	---	---	--

\*Abbreviation in Table 2.1:

LOD: Limit of detection;

P: Positive; N: Negative; TP: True positive; TPR: true positive rate; TN: True negative; TNR: true negative rate;

FP: False positive; FN: False negative;

ROC: receiver operation characteristic;

FoM: Figure of merit;

FWHM: Full width at half maximum;

SD: standard deviation; RSD: Relative standard deviation; CV: coefficient of variation;

EF: Enhancement factor.

## 2.4.2 Materials

The selection of plasmonic materials as a medium for generating SPR or LSPR plays an important role in biosensing. As mentioned above, plasmonic phenomena emerge when light interacts at the interface between metals and dielectric materials. In order to choose the optimum plasmonic material, several factors need to be considered: *the loss, the reactivity, the resonant region (plasmon tuning range), and the tunability of optical properties.*

**Losses.** There are two types of losses in metals based on the specific mechanisms of interaction: ohmic loss indicating the resistance for flowing electrons (described by the carrier mobility, which needs to be high for good plasmonic materials), and optical loss rising from electronic transit (intra- and inter-band losses, which needs to be low). In addition, the carrier concentration is another material property that is important in the optimization of the material, as it determines the wavelength range the material is active. High carrier concentrations in metals leads to response in the visible and UV range, while low carrier concentration in semiconductor materials and graphene leads to a response in the infrared to THz range. Ohmic losses are the dominant loss at high frequencies [50]. At optical frequencies, the metals suffer from the optical losses caused by the interband and intraband transition. Optical losses in metals occur when free electrons transit from an occupied state to an unoccupied state [51]. For metals with high electrical conductivity such as silver, copper and gold, their ohmic losses are relatively low. Although most

metals have low ohmic losses and high electrical conductivities, the optical loss is still a challenge. For example, silver and gold have the best electrical conductivity, but the optical losses are still an important obstacle for their development in plasmonic device [52]. An ideal plasmonic material that would exhibit low ohmic and optical losses are not available yet, and therefore more research is dedicated to identify alternate materials (besides metals), such as graphene [53]. However, graphene has low carrier concentrations and therefore is typically active in the THz spectral range.

**Chemical activity.** This is also an important factor that affects the plasmonic materials. In terms of activity, these materials are divided into two groups based on their reactivity compared with hydrogen. Gold, silver, mercury, and copper are considered less reactive metals while other metals such as aluminum, iron and zinc are more reactive. The most relevant examples that highlight the significance of chemical activity are alkali metals such as sodium and potassium. They exhibit low losses that are comparable with silver and gold. However, their extreme reactivity makes it difficult to store or fabricate these materials [54]. Au is, on the other hand, very stable in air. In contrast, Ag and Cu are less stable when exposed to air as they oxidize easily in the presence of air [55]. Another important property of plasmonic materials is their potential catalytic activity that may be useful in certain applications. For example, platinum and palladium have been used as plasmonic materials in systems where the catalytic activity of the plasmonic material is important to the overall device functionality [54].

**Plasmon tuning range.** The plasmon tuning range is the optical spectral region where the plasmons generated at the metal interface can be resonant with the incident light. In addition to the carrier concentration of the material, tunability can be realized by adjusting the size, shape, and spatial distribution of the structures within the substrates [56]. The resonance can significantly enhance the desired signal when incident light interacts with the plasmonic materials in the resonance range. Once beyond the resonance range, the losses increase rapidly, making the materials lose their ability to enhance the signal. For practical purposes, with wider tuning range, more applications can be explored. Compared to gold, silver has larger plasmonic tunable range throughout the visible range and extends in the UV range down to 350 nm [13, 47]. The range can be further extended in the UV by using aluminum, which allows plasmonic resonances down to approximately 200nm [47].

Considering the drawbacks of metals, researchers are also searching for other materials as the substitute of metals. Due to low carrier concentration, it is difficult to observe plasmons in NIR or visible range for semiconductors [55]. However, graphene can potentially address this limitation due to their unique plasmon dispersion properties that describe the relation between carrier concentration and Fermi energy [55], which can be tuned by doping. Graphene has a very high absorption capability with linear dispersion of Dirac fermions enabling changing optical properties using electric gating [41, 57]. Koppens et al. showed that in doped graphene the electrical and mechanical properties entail partly from its Dirac fermions charge (charge carriers at zero effective mass), which allow micrometer-range travelling of charges without scattering. The surface plasmons bound to the surface of doped graphene facilitate strong light-matter interactions due to very small plasmon confinements in relation to the diffraction limit. In addition, extremely strong light-matter interaction is attainable at the quantum level [31]. Thus, an advantageous tunable surface plasmon spectra with hundreds of optical cycles can be achieved. With sufficient large doping, it is possible to achieve low losses at NIR frequencies [58].

Low et al. reviewed approaches to chemically, electrically and solid electrolyte gating of graphene to achieve higher concentration of free carriers per atom and using plasmonic graphene as substitute for plasmonic noble metals in various applications such as modulators, notch filters and mid-infrared photodetectors [43].

### 2.4.3 Structures

The plasmonic properties of the substrates in terms of the resonance frequency and strength of the electric field are affected not only by the materials but also by the structures of substrates such as size, shape and geometry. As mentioned in equation 2, the electric field near the surface is related to polarizability, which can be calculated using the dielectric function of medium and the size of the substrate [59]. Recent research has been devoted to the study of substrate structures, from 0D to 3D (Figure 2.2a, Figure 2.3), from nanoparticles with different shapes (spheres, semi-spheres, pyramids, nano-stars, etc.) to the deposition of plasmonic materials on a series of substrates with different nanostructures.

**0D and 1D materials.** Among the simplest structures widely used as plasmonic substrate are metallic nanoparticles (NPs), among the simplest structures widely used as plasmonic substrate are metallic nanoparticles (NPs), which are 0D and 1D materials that exhibit significant

enhancement of electromagnetic field due to localized surface plasmon resonance (LSPR) generated on the surface of NPs by electromagnetic fields [29].

When working with a nanosphere with a certain radius, the plasmonic properties are easy to understand by calculating the polarizability, which is related to the electric field. Among nanoparticles, noble metals such as silver nanoparticles (AgNPs) and gold nanoparticles (AuNPs) are most usually used since they can enhance SERS signals more significantly [13, 60, 61]. When nanoparticles are designed in other shapes that are more complex, such as nanostars nanofingers [62, 63], and nanorods [64-68], the plasmonic properties of the substrate are influenced by the shapes as well. For example, the plasmonic properties of nanorods depend very much on the ratio of the semi axes and head shape [69], while the characterization of nanostars and nanofingers have to consider the tips and the center parts at the same time [29]. On the other hand, core-shell structures [65, 70-72], can be considered as a single sphere with an equivalent radius [73].

**2D materials.** On the other hand, 2D substrates are made in thin 2D films or sheets. They utilize propagating surface plasmons and present very unique properties by means of confining the free electrons in proximity of metal surface [74]. Typically, SPR biosensors are mostly based on gold or silver films. This feature makes them more suitable for bulk analytes compared to molecules.

Other 2D structures include graphene and graphene oxide (GO), which show promising potential for SERS technology due to the high ratio of surface to volume, good electrical performance, and high affinity for some molecules [75, 76]. Graphene grown on Cu foils was used as the deposition substrate for Au nanoislands, which increases the enhancement factor [77].

In addition to graphene, silicon is also considered as a potential substrate for plasmonic materials. For example, silicon nanowires (SiNWs) exhibit a number of unique properties such as the biocompatibility, the fast response and the reproducibility that make it ideal alternative for the biosensors [78].

**3D materials.** Metals at nanoscale such as nanoparticles or nanorods are usually designed to generate so called 'hot spots', which create intense localization of surface plasmons and the enhancement is significantly increased. To generate more hot spots, high dimensional nanostructures are designed and fabricated recently, such as 3D structures. Wei et al. reviewed different types of nanostructures that give rise to hot spots [79, 80]. 3D nanostructure-based

plasmonic biosensors show increased sensitivity due increased availability of hot spots [81]. Based on a series of different structures as substrate or template such as latex particles array [82, 83], polystyrene beads [84], [85], nanospheres [84], polymer nanofingers [63] and compact disks [74] to form various structures such as 3D nanocups [86, 87] or 3D nanobowls (exosome detection) [88], metallic films are shaped to get high density of hot spots. With an etching mask providing quasi-periodic nanostructures, Au deposition generated hot spots of high density [89]. Alternatively, 3D structures can be designed and fabricated by combining nanoparticles with 3D substrates and templates. These materials can be made by deposition or other methods. For example, AgNPs or AuNPs can be deposited on paper/paper fiber [90, 91], silicon wafer [89], glass [92], or biological materials with unique structures such as cicada wing segment with patterned protrusion [93], dragonfly wing with disordered morpha [94], and *Mytilus coruscus* shell offering several types of micro/nano-structures [93], crystal biosilica diatoms [95-97] and even on modified nafion leafs [95]. In addition to deposition, metallic nanoparticles can also be encapsulated into mesoporous silica structure [98]. In these case, the plasmonic modes rise from the electromagnetic coupling of nanoparticles oriented on the nanostructured substrates [73].

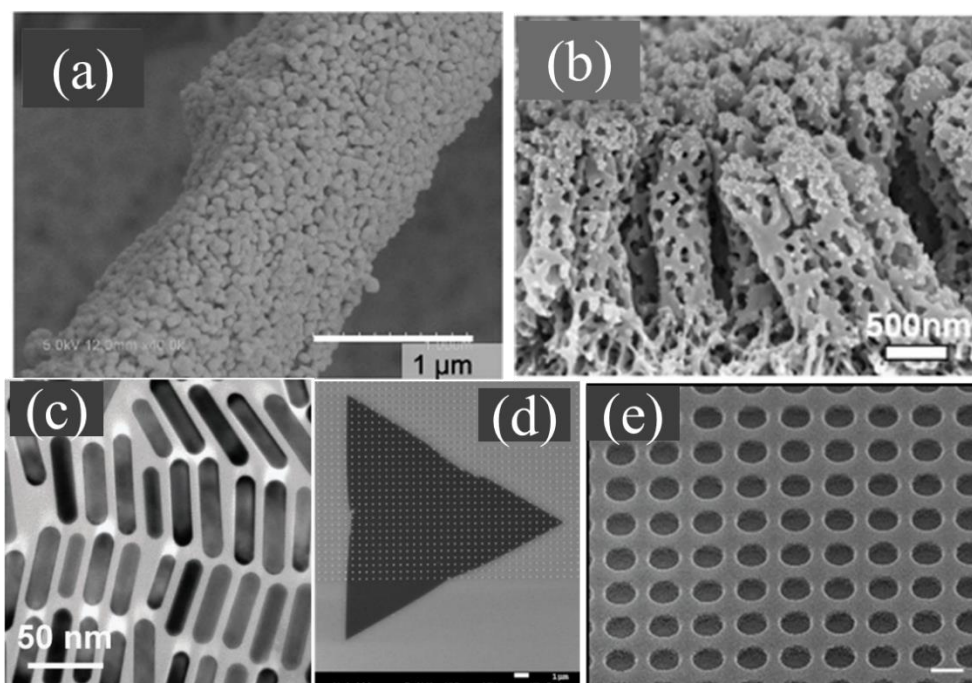


**Figure 2.3.** EM images of AuNPs deposited on carbonized paper(a), Side view of a SERS sensor consisting of nanoporous PS-b-P2VP nanorods functionalized with AuNPs connected to a nanoporous PS-b-P2VP membrane (b), Au Nanorods (c), MoS<sub>2</sub>/silver nanodisk hybrid structure on a Si/SiO<sub>2</sub> substrate (d), and Au-deposited quasi-3D

plasmonic crystal (e). Figure 2.3a is adapted from reference [60] with permission from Elsevier Copyright (2017). Figure 2.3b is adapted from reference [99] with permission from John Wiley and Sons, Copyright (2017). Figure 2.3c is adapted from reference [69] with permission from The Royal Society of Chemistry, Copyright (2013). Figure 2.3d is adapted from reference [100] with permission from American Chemical Society, Copyright (2016). Figure 2.3e is adapted by from reference [81] with permission from Springer Nature, Nature Communications, Copyright (2011).

A variety of methods has been used for the fabrication of plasmonic nanostructures depending on the dimensions of the plasmonic features. In general, there are two classes of fabrication techniques: bottom up and top down approaches. In the bottom up approach the plasmonic features are made via chemical/electrochemical methods from their precursors. For example, the metal nanoparticles (0D) can be produced through a chemical reaction, where the particle is reduced from metal ions by a reducing agent [101]. The shape, size and surface chemistry of the synthesized nanoparticles can be adjusted accordingly. On the other hand, the top down approach involves the breakdown of the materials from large-scale into nano-scale structures [102]. For instance, a variety of lithography techniques including soft lithography, nanosphere lithography [103], and electron beam lithography [104] have been used widely to fabricate different plasmonic features such as nanoholes, nanoposts, nano-cones, and nano-bowties [18]. In addition, fabrication of 3D plasmonic nanostructured materials usually involves a deposition step which can be performed using multiple techniques such as magnetic sputtering [94] and oblique angle deposition [64] for metallic plasmonic structures and chemical vapor deposition for graphene [36].

#### 2.4.4 Functionalization of substrates

Due to the nature of the signal enhancement, which depends on the electric field near the plasmonic structure, the signal intensity is very sensitive to the distance between samples and substrates. Therefore, careful design of the surface chemistry is very important in the detection of analytes of interest. Substrates can be classified into two broad types according to whether or not they are utilizing a biorecognition element: functionalized and non-functionalized. *Functionalized substrates* use molecular interactions for specific detection (such as antibodies, aptamers, or other small molecules designed to specifically attach to the targeted analyte), and the analyte binding to the biorecognition element will cause a change in the detected signal [105]. There are mainly three main types of functionalization based respectively on antibody, aptamer, and molecular template. Antibody/antigen-based functionalization is based on the specific noncovalent binding of the

antibody to the molecule of interest. To further improve the sensitivity, a secondary antibody construct can be applied to amplify the detection signal [106]. The drawback of this approach, though, is the fact that the analyte may be localized, after binding, too far from the plasmonic substrate to be detected. Aptamers, on the other hand, are oligonucleotides that have the ability to fold into smaller 3D structures that enable them to specifically bind to the analyte of interest via electrostatic interactions and localize the analyte closer to the substrate. However, these two methods mentioned above are usually not suitable for detecting small biological molecules [107]. One reason for this is the fact that the recognition site in the biorecognition element may be at a distance from the surface of the plasmonic structure. In this case, the signal generated by the small target molecule decays rapidly with the distance, as described by equation (2.2), and the signal may

be too weak to be detected. An alternative approach for small molecule detection is by using molecular imprinting technologies. The template molecule (the analyte to be detected) is used to generate a specific shape hole in the template polymer leading to specific detection of the analyte [107].

Another method to address the limitation of sensitivity is the use of non-functionalized substrates. In this approach, the molecules of interest may bind directly to the plasmonic structure and generate a measurable signal. Multiple binding analytes may pose a problem in this case that limits the specificity of detection. The advantage though is the fact that higher enhancement factors can be achieved due to closer proximity of the analyte to the plasmonic substrate [108].

#### 2.4.5 Detection methods

Based on the detection method, plasmonic biosensors can be divided into two types: SPR-based on flat thin film and LSPR-based including scattering detection such as SERS, and absorption, transmission, reflectance detection. In addition, fluorescence based detection also draws a lot of attention [109].

**SPR.** SPR is a label-free method that uses SPPs to quantify molecular interactions. When light interacts with thin metallic films (usually below 200 nm), SPPs are generated as described earlier [9]. When incident light at a certain angle (resonance angle) is absorbed by conduction electrons in thin metal film or other conducting materials, causing them to resonate. When

resonance occurs, the light is absorbed at this SPR angle. This results in the significant reduction of reflectivity [110]. SPR angle is dependent on the refractive index of the medium. Consequently, when the refractive index of the substrate, typically thin metallic films, changes, reflected light that are not absorbed will be detected, indicating the change of refractive index, which can be caused by the absorption of target molecules to the probes functionalized on the metallic films [111] (Figure 2.4 (a-c)). Therefore, SPR biosensors are very sensitive to the change of refractive index of dielectric due to the absorption event of analytes in the vicinity of the metal surface [104]. SPR biosensing is one of the mostly used techniques as label-free detection method that avoids using specific tags or dyes [112, 113].

Biosensing methods based on SPR use total internal reflection of incident light at the metaldielectric interface and the generation of SPPs at certain angles. While several configurations are possible, for an SPR system based on a prism coupler, the wavevector of the evanescent field in response to an electromagnetic wave of wavelength  $\lambda$  incident at an angle  $\theta$  propagating along (parallel to) the interface of prism-metal is related to the refractive index of the prism and incident angle [114].

$$k_{evan} = \frac{2\pi}{\lambda} n_p \sin(\theta) \quad (2.3)$$

where  $n_p$  is the refractive index of the prism.

Surface plasma wave (SPW) is an electromagnetic wave that propagates along the interface between metal and dielectric. The wavevector can be described as Eq. (4) [115]:

$$k_{SP} = \frac{\omega}{c} \sqrt{\frac{\epsilon_M \epsilon_D}{\epsilon_M + \epsilon_D}} \quad (2.4)$$

Where  $\omega$  is the angular frequency of the wave,  $c$  is the light speed under vacuum,  $\epsilon_M$  and  $\epsilon_D$  indicate the dielectric functions of metal and dielectric around metal, respectively. The dielectric function is related to the refractive index  $n$  by expression:  $n^2 = \epsilon\mu$ , where  $\mu$  indicates the relative permeability and the value is close to 1 at optical frequencies. Therefore, the dielectric function can be described as  $\epsilon = n^2$ .

Resonance occurs when  $k_{SP} = k_{evan}$ , thus, the incident angle, or the SPR angle necessary for resonance occurrence can be calculated by the equations mentioned above:

$$\theta_{SPR} = \arcsin\left(\frac{1}{n_p} \sqrt{\frac{n_D^2 \epsilon_M}{n_D^2 + \epsilon_M}}\right) \quad (2.5)$$

Where  $n_D$  is the refractive index of dielectric.

To improve the sensitivity of SPR biosensors, i.e., to increase the change in SPR angle or wavelength results from the change of refractive index due to the absorption of analyte on the interface of metal and dielectric [116], substrates as the sensing platform play an important role, as indicated in Eq. (5), where the dielectric functions of the metal is involved. Gold and silver thin films are most commonly used metals due to their low loss compared to other metals. Graphene also shows enhancement on SPR sensing [117]. Another way to improve the performance is to coat the substrates with dielectric layer [118]. On the other hand, SPR signal can also be amplified by utilizing plasmonic nanoparticles. By binding nanoparticles, such as Au, the detected SPR signal can be enhanced due to the localized and propagating surface plasmon [119].

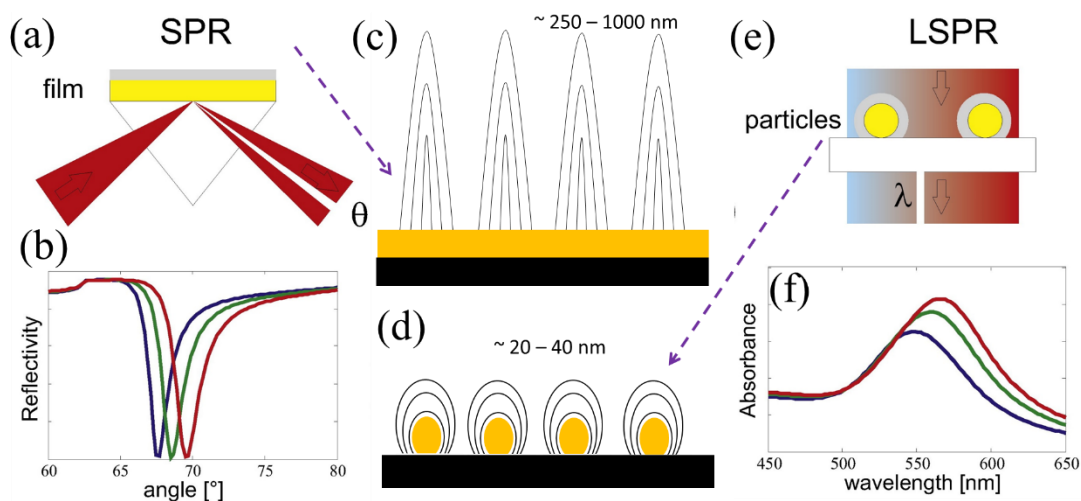


**Figure 2.4.** The schematic of the mechanism of SPR (a-c) and LSPR (d-f). Figure 2.4a, b, e and f are adapted from reference [120] with permission from Elsevier, Copyright (2016).

**LSPR.** Different from traditional SPR sensors that are based on metallic films, LSPR is generated usually on metallic nanoparticles or structures that generate localized electromagnetic fields where the decay length is much shorter (Figure 2.4 (d-f)). This confinement enhances the electric field at nanoscale around the metal nanoparticles, and such LSPR is sensitive to molecular binding especially for some small biological molecules [121].

**Absorption/transmission.** The way light interacts with matter is related to the medium it passes. Not only the reflectance and scattering are useful for the determination of samples on plasmonic

substrates, but other types of interactions of light with the material, such as absorption and transmission, also provide information about the samples, therefore raising interest from the research community as cheaper and simpler methods for real life applications [122].

**Surface Enhanced Raman Spectroscopy (SERS).** Another way for LSPR analyte detection is by using Raman spectroscopy, which is based on inelastic scattering of light when it interacts with vibrations of chemical bonds. The frequency of scattered photons is different from the frequency of the incident photons, and it can be detected via a spectrometer and a CCD detector. Normal Raman spectroscopy suffers from weak signal since the Raman scattering cross section is very low compared with fluorescence. One way to solve this problem is by using the phenomenon of enhancement or amplification of the Raman signal by strong electric fields, which leads to the technique of SERS. SERS utilizes plasmonic substrates such as metallic nanoparticles and nanostructures to enhance Raman scattering. Since the discovery of this amplification phenomenon [123], it has been used as a tool for sensing in a variety of applications. There are two primary mechanisms responsible for SERS enhancement: electromagnetic and chemical [124]. Electromagnetic enhancement is generally considered as the dominant mechanism.

Electromagnetic enhancement occurs due to the enhanced local electromagnetic field on the substrate surface. When incident electric field (light) is applied on the molecule of interest, a dipole is induced in the molecule. Meanwhile, the plasmonic substrate (e.g., particles) nearby the molecule also exhibits a dipole upon the interaction with light. The dipole moment of the molecule can then be calculated by the polarizability of both dipoles and the incident electric field, which then in turn contribute to the electric field leading to the increase in the effective Raman polarizability. Raman enhancement is determined by the derivatives of the dipole moment of the molecule and the dipole moment of the particle. It becomes stronger when resonant oscillations are generated on the surface of substrate. The scattering cross section positively related to the Raman polarizability is then improved [125], which then leads to stronger scattering intensity [126]. On the other hand, chemical enhancement is mainly dependent on the adsorption of chemical molecules to the proximity of substrate surface so that the interactions between electrons from the substrate and the molecule are allowed to happen [127].

Similar to SPR, for LSPR and SERS, the localized electric field relies on the dielectric and plasmonic nanostructures [20, 128]. The extinction spectrum for a sphere (with diameter  $a$ ) can be described as below [20]:

$$E(\lambda) = \frac{24\pi^2 N a^3 \varepsilon_D^{3/2}}{\lambda \ln(10)} \frac{\text{Im}[\varepsilon_M(\lambda)]}{(\text{Re}[\varepsilon_M(\lambda)] + \chi \varepsilon_D)^2 + \text{Im}[\varepsilon_M(\lambda)]^2} \quad (2.6)$$

Where  $\chi$  is the shape factor and  $N$  is the electron density. As shown here, the geometry, such as the shape and size, and the dielectric function of the nanostructures should be taken into consideration when developing a LSPR biosensor. As discussed before in **section 2.4.3** (Structures), various nanostructures including nanoparticles and nanostructures have been demonstrated [129]. In addition to the structures, bringing analytes as close as possible to the substrates is also important for both SPR and LSPR. Thus, the functionalization (as discussed before) is also explored by researchers.

Both SPR- and LSPR- based techniques show potential to be used towards PON applications due to their high sensitivity and specificity. From a practical perspective, more advances in fabrication methods are needed to reduce the fabrication complexity, achieve better defined and controlled nanostructures. Moreover, the use of portable spectrometers that can now be on the size of a cell phone also makes these techniques better candidates for PON applications.

**Photoluminescence.** Photoluminescence occurs when electrons are excited by the incident photons at a certain moment and then undergo radiative relaxation. During this process, photons are re-emitted [130]. The luminescence is from either the intrinsic properties of the analytes or the luminescent labels tagged to specific analytes. The intrinsic (endogenous) luminescence is mostly weak, thus it has low sensitivity. For this reason, there are not many biosensors that are developed based on intrinsic luminescence. Another option to avoid this issue is to use fluorophore tags (exogenous fluorophores) that have high fluorescence quantum yield. When the exogenous fluorophore is utilized, luminescence-based optical biosensors need to capture the analytes close to the fluorophore tags [130]. Fluorescence-based biosensors, as a type of luminescent biosensors (with shorter lifetimes in the ns or sub-ns range), have been widely used over the past decades [131]. The fluorescence signal of the analyte or label can also be enhanced by coupling with the confined surface plasmons generated on plasmonics active substrates [132]. The quantum yield of

fluorescence is determined by the radiative decay rate (when an electron goes back to ground state from excitation with photon emission) and non-radiative decay rate (when an electron goes back to ground state without photon emission). When a fluorophore is near the surface of the plasmonic materials that supports surface plasmons, both radiative and non-radiative decay rate would be changed due to the change of LDOS, which hence changes the quantum yield [131]. The interaction between the fluorophore and localized/propagating SPs can increase the intensity of the fluorescence by increasing the excitation rate and fluorescence quantum yield. However, when the fluorophore is too close to the plasmonic material surface, Förster energy transfer between them will lead to strong quenching and thus leads to lower fluorescence quantum yield. Therefore, plasmonic substrates providing optimal field enhancement are of interest when designing fluorescence biosensors. Plasmon-enhanced fluorescence biosensors can be divided into two types, based on SPs and LSPs enhancement. Metallic films such as Ag and Au are commonly used for SP enhanced fluorescence biosensor, while metallic nanoparticles, nanoholes, and other nanostructures are generally used for LSP enhanced fluorescence biosensors [71, 131].

Fluorescence biosensors utilize exogenous fluorophores to record and measure analyte binding events. They provide high sensitivity and specificity in the presence of interfering substances, but require additional preparation steps (labeling with the fluorophore), which may in certain situations increase the complexity of the biosensor, which may decrease its possibility to be used in PON applications.

### **Other techniques**

In addition to these techniques, other related optical techniques such as Surface Enhanced Infrared Absorption Spectroscopy (SEIRAS) and Tip Enhanced Raman Spectroscopy (TERS) are presented below. Furthermore, techniques aimed for ultrasensitive detection such as single molecule detection and chiral plasmonics are described as well.

**SEIRAS** utilizes the enhancement of the absorption of infrared light by the molecule when the molecule is adsorbed on nanostructured metal films [133]. The enhancement is attributed to the excitation of the localized surface plasmon resonance, the orientation of the vibrational dipole of the analyte, and the change of the polarizability of the analyte. But the main mechanism is usually

considered as the electromagnetic enhancement from the plasmon resonance excitation of the metallic film [134].

The most commonly used sensor configuration for SEIRAS measurement is known as metal underlayer configuration, where the metallic layer is under the sample but on the supporting substrate. With this arrangement, the analytes can be measured either in transmission configuration or attenuated total reflection (ATR) configuration. For transmission measurements [135], the thickness of the metal film is less than 10 nm, allowing for a large portion of the light to be transmitted, while for ATR configuration the thickness can be up to a few hundred nanometers.

As a surface sensitive technique, SEIRAS is commonly used for near-field monolayer analysis, especially for the functional and structural study of membrane proteins [134]. However, considering the rapid decrease of signal with the distance from the surface, the analyte has to be tethered extremely close to metal surface. Therefore, to improve the enhancement, molecules can be modified with high affinitive groups to metal surface such as thiol group or carboxyl group [134].

However, applications to the measurement of analytes in solutions are usually challenging due to the low infrared absorption of the analyte and the interference of the strong absorption band of water. Recently, plasmonic nanoantennas were designed and fabricated to address these problems by enhancing the absorption. For example, Naomi J. Halas et al. designed antennas consisting of bowtie-shaped nanostructure with a sub-3 nm gap, which confine the mid-IR radiation and yield a high enhancement factor theoretically up to  $10^7$  for the SEIRA signal [136]. Moreover, Hatice Altug's group has recently reviewed the concepts and the engineering of the plasmonic nanoantennas [137]. This group has also reported a platform for molecular barcoding with pixelated dielectric metasurfaces [138] and a sensor utilizing Au nanoantennas with near-field enhancement up to 1000 fold for the amide and methylene infrared bands, which allows for resolving the interaction of lipid membranes with different polypeptides in real time and distinguishing multiple analytes with high sensitivity [139]. These developments provide unique opportunities for fingerprinting of various molecules complementary to Raman spectroscopy.

SEIRAS offers lower enhancement factor compared to SERS, which makes it less competitive towards PON applications. It still offers high sensitivity, thus for some applications with moderate demand for sensitivity, it is still applicable.

**TERS:** TERS is a special approach in SERS where the enhancement happens only at the tip of plasmonic cantilever. The mechanism of TERS enhancement is similar to that observed in SERS and is due to localized electromagnetic field and chemical enhancement. The metallic nanotip is responsible for generating the electromagnetic field that is needed in Raman enhancement and allows simultaneously for high spatial resolution, while in other approaches such as SERS the plasmonic substrates with rough surface allows for field enhancement but no increased spatial resolution. The optical setup for TERS detection combines a typical micro-Raman system with a high-NA objective and an AFM controller to align the metallic nanotip on the sample surface within the laser focus [140]. As a sensitive spectroscopy technique at the nanometer scale, TERS allows for the identification and characterization of analytes such as biomolecules or bioparticles. For example, Deckert's group exploited this technique for the discrimination of two viruses at single particle level by collecting TERS spectra and then classifying them with chemometric methods [141]. Meanwhile, they also performed the identification of DNA [142], where TERS signal obtained with a silver tip and gold substrate can reach sub-nanometer resolution that enables the demonstration of the sequencing of single-stranded DNA molecules. This further indicates that TERS has the potential for high resolution Raman imaging of nanostructures and for the sequencing of other biopolymers of interest such as RNA and polypeptides. Lagugné-Labarthe et al. also utilized TERS to investigate DNA in different environments (such as free or in plasmid) and achieved a spatial resolution down to 8 nm [143]. In addition to the application to bioanalytes, they also explored the characterization of biominerals via TERS, such as the interactions of the phosphoprotein osteopontin (OPN) with calcium oxalate monohydrate (COM) crystals [144]. In this last application, TERS was uniquely able to help understand the competitive processes of COM growth and inhibition by OPN. Furthermore, TERS shows promising potential for the diagnosis of Alzheimer's disease by distinguishing the natural Ab1-42 fibrils (wild type) that are related to Alzheimer's disease from two other toxic mutants, i.e., L34T and oG37C [145]. Since the proportion of amino acids in these three peptides is similar, it is very critical to examine characteristic Raman amide I and amide III bands of which the intensities are different in these peptides.

Compared to SERS, the enhancement factor of TERS comparable but with a higher spatial resolution since it addresses the issue of optical diffraction limit of spatial resolution observed in

SERS [146],. While TERS provides the above-mentioned advantages vs SERS, it is complex, expansive, and complicated to use, and therefore not suitable for PON applications..

**Single molecule detection** has been achieved for SERS detection, enabling a more profound and fundamental understanding the interaction between the plasmonic surface and the analyte. Moreover, it allows for high sensitivity (low LOD), which is essential for the development of biosensors. Single molecule detection is possible when individual molecules are captured and detected in a confined volume, or when sparsely distributed molecules are detected in imaging mode. Fluorescence based techniques are often used due to the availability of strong signals (large quantum yield) in the presence of a dark background [147]. Single molecule SERS detection has also drawn a lot of attention during the past decades due to the high enhancement factor within the hot spots. Compared to single molecule fluorescence detection, single molecule SERS avoids the labeling with fluorophores or dyes. Meikun Fan et al. optimized the distribution of AgNPs aggregates evenly on glass surface, used as SERS substrate, and achieved nearly single molecule detection [148]. Another way to achieve (near) single molecule detection is to generate hot spots that capture a single molecule such that the signal from this molecule dominates the signal from neighboring molecules due to much stronger enhancement [149]. In addition, research has shown that SPR-based techniques show potential for single molecule detection by reducing the collection area using a smaller aperture [150]. The ability to image single molecules by SERS has been recently exploited for the development of biosensors. The main advantage comes from the fact that the LOD can theoretically become as low as one single molecule, as long as a calibration curve can be generated for quantification of the signal. In this case, plots of number of pixels that exhibit SERS signal (or alternatively the total intensity of those pixels) versus the concentration may provide the means for the quantification. However, elaborate sample preparation methods need to be used, as well as expensive and complicated detection schemes need to be applied to record the signal, which makes this technique unsuitable to PON applications.

**Chiral plasmonics.** Chirality refers to the asymmetry property of some biomolecules, such as some amino acids and carbohydrates, which are not superimposable with their mirror images and only exist in one handedness. This property can induce a phenomenon called circular dichroism (CD) that refers to different optical responses of the chiral structures to right- or left-handed circularly polarized light (RCP and LCP) [151]. Techniques based on this phenomenon have

emerged in recent years, such as CD spectroscopy, which measures the difference of the absorbance between left- and right-circularly polarized light. CD spectroscopy can be used for structural identification, chiral sensing, and medical diagnosis of biomarkers of interest [152]. However, the chiral optical response of natural molecules is typically weak, which makes it challenging for CD spectroscopy to become mainstream.

It has been shown that the CD spectroscopy signal can be enhanced when the chiral molecule of interest is in the vicinity with metallic nanoparticles due to near field enhancement and it is known as plasma induced chirality [152]. In addition, when the plasmonic nanoparticles are arranged in chiral geometries, strong plasmonic chirality is generated. There are already review articles discussing the fundamental and progress in chiral plasmonics [153, 154]. We would like to comment here that chiral plasmonic biosensing is now still in a development stage. Theoretical and experimental studies showing a more comprehensive understanding of this phenomenon are needed for designing chiral plasmonic biosensing systems with better reproducibility. Thus, while possible, it is likely too early to apply chiral plasmonics in PON applications.

## **2.5 Applications**

Plasmonic materials are applied in many different biosensing areas. Table 1 shows a brief summary based on reported applications within the past 5 years. We review publications aimed at the characterization of substrates and (bio)materials, as well as applications to environment monitoring, diagnosis, and food safety. We highlight the analyte of interest, whether or not they were functionalized, detection methods that were used, the substrates used in these measurements, as well as the sensitivity, specificity, ease of fabrication, response and cost (if applicable).

### **2.5.1 Characterization of substrates and (bio)materials**

There are numerous studies dedicated to the characterization of plasmonic substrates and materials before these can be applied to any area of application. These studies provide a good indication about the performance for potential application and allows for further optimization for targeted real applications. Based on the specific area of application, the analytes include proteins, DNA, bacteria, viruses, and other biological particles such as exosomes [13, 155].

For different detection methods, certain test molecules are generally used for the characterization of plasmonic substrates. For example, 4-ATP and Rhodamine 6G are normally used as probe

molecules for substrate characterization for SERS [61, 91]. With these test molecules, the performance of the substrates can be characterized either by sensitivity (limit of detection), or by the enhancement factor. The performance of the substrates will be compared to normal Raman measurements to show the magnitude of surface enhancement due to the plasmonic nanostructures designed. On the other hand, to characterize an SPR system, which is highly sensitive to molecular interactions on the surface of the sensing substrate [111], researchers focus on the characterization of binding events such as antigen-antibody interactions, IgG examinations, or other types of specific molecular interaction [116].

The development of substrates should consider both the analytes as well as the detection methods. For larger molecules, such as proteins, the development of biosensors needs to take into account the ability to capture the analytes into the vicinity of the active part of substrates for higher sensitivity [156]. For SPR-based methods, by selecting better materials, such as Au or Ag, adjusting the thickness of sensing film, coating with other materials or incorporating nanoparticles to combine LSPR, higher sensitivity can be obtained [104, 157]. As for LSPR-based detection, such as SERS, as discussed before, in addition to the materials used, the fabrication of different shapes of nanoparticles, or nanostructures should be focused to achieve higher EF or higher sensitivity by generating hot spots [80]

### **2.5.2 Environment monitoring**

The importance of monitoring the environment is evident with the increasingly serious problems related to the pollution of water and air. The development of biosensors can facilitate the detection of pollutants in the environment in a direct and reliable manner. The biosensors used for environmental monitoring are mostly focused on pesticides that are used for crops or fruits, heavy metals in water that cannot be degraded, pathogens such as bacteria, and other chemicals that are potentially toxic or dangerous such as explosives [64, 92, 158]. For the detection of these pollutants in real life, it is crucial to develop biosensors that can achieve rapid measurement of samples, and easy accessibility for some situation such as low resources environments [5, 89, 115].

To improve the performance of the substrates for plasmonic biosensing, it is necessary to bring pollutants as close as possible to the surface of the plasmonic active parts. One way to achieve this is by functionalizing the substrates with specific recognition elements or by designing structures

to allow for the easy binding of analytes [159]. On the other way, considering the chemical structures of analytes of interest, plasmonic materials with higher affinity to analytes should be considered. For example, AuNPs show high affinity to dithiolcarbamate pesticides and SERS biosensors based on AuNPs have been reported for their detection [160].

### **2.5.3 Diagnosis for human health**

Monitoring health at the point of need is one of the most significant problem in our world, as it can lead to early diagnosis, help understand disease progression, and provide data that can be used to develop an optimal treatment scenario. Plasmonic biosensors are good candidates for these applications as they have the ability to detect analytes of interest such as biomarkers related to diseases[11]. By quantifying the biomarkers, specific health-related information can be obtained. Many biomarkers (antibodies, proteins, nucleic acids, and enzymes etc.) are the potential analytes to be monitored for the diagnosis of diseases, such as Alzheimer's, diabetes, and cancer [60, 86, 161, 162]. In addition, they can also be used for drug screening [163].

To capture these analytes from biofluids, specific receptors such as antibodies, or ligands are immobilized on the sensing substrates to bring the analytes closer to the sensing surface [62]. In addition, tags or probes are also introduced for the purpose of improved detection. Therefore, the substrates should be designed to allow functionalization and tuning of these receptor elements [132]. Consequently, the surface of the substrates designed for plasmonic biosensors need to consider the surface chemistry as well as the surface area to allow the immobilization of the receptors and stable binding of the analytes [164, 165]. Moreover, since the concentration of biomarkers is important for clinical determination, plasmonic biosensors used for diagnosis require high accuracy over the desired concentration range [166]. Meanwhile, the need of diagnosis and disease progression monitoring in low resource environments, at home, in remote locations, in disaster areas, or for astronauts in space, drives the development of portable substrates or devices based on plasmonic biosensors.

### **2.5.4 Food safety**

Monitoring the food quality is of global concern since food safety plays an important role in our daily life. The addition of high level of contaminants or adulterants in food could pose severe problems for our health, especially for infants. For example, high levels of heavy metals, plastic,

or food additives can lead to severe health problems [167]. In the application to food safety, plasmonic biosensors are generally used to detect chemical and microbial contaminants, such as the food colorants, food additives, or bacteria [168, 169]. Similar to environmental monitoring, plasmonic biosensors designed for food safety also require high sensitivity, simple preparation, and rapid detection [115, 170].

For the detection of chemical components such as small analytes, the substrates can be engineered for specific binding of these analytes [65]. However, for large analytes, such as proteins, or bacteria, the sensitivity of detection is typically lower [171] and functionalization of substrates with specific antibodies or aptamers may be needed [172].

### **2.5.5 PON applications**

To summarize, there are many factors to consider for the development and evaluation of plasmonic biosensors towards point-of-need applications (Table 2.2). We mainly reviewed the potential improvement for plasmonic biosensors from the point of view of materials, the design of nanostructures, the functionalization of the substrates, and finally the detection methods. For these sections, the emphasis is focused on how the performance of the plasmonic biosensors are affected by the properties of substrates.

When designing PON biosensors, it is important to address not only parameters related to cost, size, and stability, but also sensitivity, specificity and low limit of detection towards the analyte of interest for that particular applications. For this, significant effort is needed towards the design and preparation of the substrates in terms of the materials, composition, the shape, the size, and the structure [173, 174]. Particularly when there are other molecules that shares similar molecular properties as the test molecule (analyte), it is necessary to optimize the system accordingly, thus, the biosensing system can be specific towards the desired analytes.

The requirements regarding the sensitivity, specificity, and LOD are different when dealing with environment monitoring and food safety samples compared to PON applications in health diagnosis. The analytes of interest in environment monitoring or food safety are typically small molecules such as toxic chemicals [169], pesticides [170] and heavy metals [64], which can be detected with LSPR-based techniques. In food safety or medical diagnosis, however, bacteria, proteins [36], nucleic acids [162], or vesicles are often targeted as biomarkers of interest besides

small biological molecules. The detection of analytes with larger size or mass makes it more difficult for plasmonic biosensing since it demands immediate vicinity with substrate surface. Moreover, it is also more challenging to develop a biosensor for medical diagnosis due to the increased complexity of the sample and high variability of biomarkers for a specific disease. As a result, more careful functionalization of the substrate to immobilize target analytes needs to be taken into consideration for higher specificity in PON application. In addition, the reproducibility of detection with SERS is still relatively low, yielding to poor reliability for these applications. Better substrates are required in this case, and new developments in various labs indicate improved spot-to-spot reproducibility for certain substrates such as nanobowl arrays [82] gold nanofingers [63], or nanoposts [175], among others.

It is also worth noticing that when it comes to PON applications, the development of plasmonic biosensors should consider other factors beyond sensitivity and specificity, such as the complexity of substrate fabrication and the preparation of analytes, the cost, and the response time [176]. For PON applications, it is critical to balance the high cost, and/or the complexity of fabrication or preparation of the substrates. Since the sensitivity/LOD criteria varies in different areas, it is possible to compromise their quality when it is not highly necessary for either lower fabrication cost or less tedious preparation work.

For example, the synthesis of nanoparticles, as one of the simplest plasmonic structure, has been explored and improved for more than a hundred years [177], can be easily performed by a variety of methods. On the other hand, it is believed that the combination of the plasmonic materials such as the noble metal with hybrid nanostructures can enhance the SERS signal since more hot spots can be generated. However, the complexity of the fabrication of such nanostructures is also increased, thus it is important to balance the trade-off between the ease-of-fabrication and the design optimization of the nanostructured substrate. Making use of natural substances with unique structures is a promising approach to address this problem. For instance, Zhengyi Lu et al. developed an inexpensive SERS substrate by depositing AgNPs and graphene oxide (GO) on (a) *Mytilus coruscus* (M.c) shell offering several types of micro/nano-structures [93]. Other natural materials, such as (b) the dragonfly wing [94] and (c) cicada wing [178], combined with different metals and structures, are more explored. The utilization of the natural materials that can be readily obtained not only improves the ease-of-fabrication but also reduces the cost.

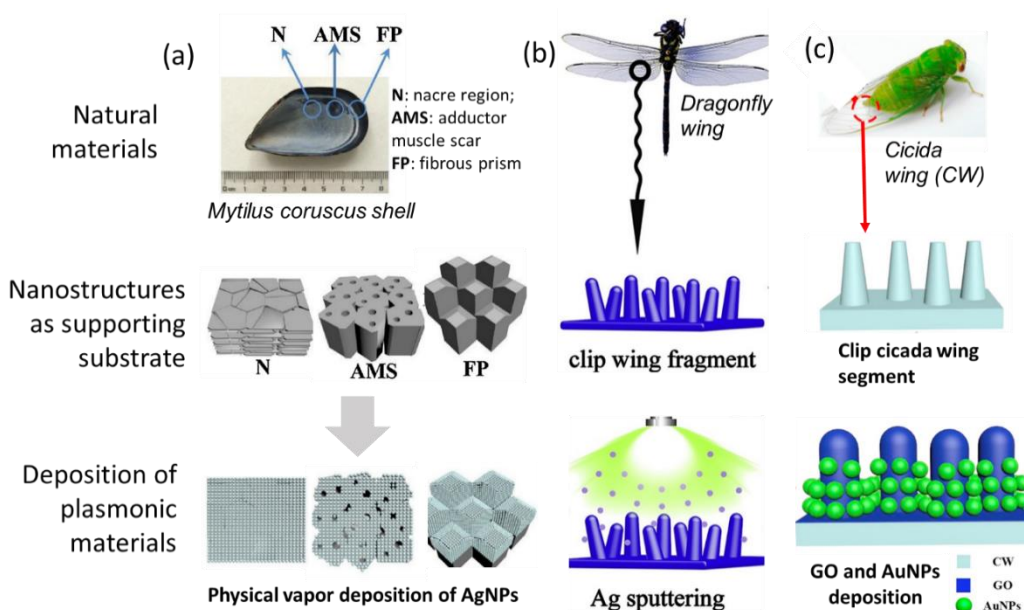


**Figure 2.5. Representative examples of utilizing natural materials as supporting substrate:** (a) AgNPs deposited on *Mytilus coruscus* (M.c) shell; (b) AgNPs sputtered on dragonfly wing; (c) Graphene oxide (GO) and AuNPs deposited on cicada wing. Figure 2.5a and b are adapted from reference [93] and [94] with permission under Copyright Clearance Center, Inc, Copyright (2019). Figure 5c is adapted from reference [178] with permission from Elsevier B.V., Copyright (2018).

Another important factor for PON applications is the duration of the measurement, which is mainly determined by the detection methods. In general, the measurement of the plasmonic biosensors based on SPR/LSPR is time effective, which is determined by the incident exposure and collection time. The recording time of the SERS spectra ranges from seconds to minutes, which fulfills the demand of rapid measurement for PON applications.

The ultimate goal in studying the plasmonic biosensors that can be used for PON applications is for the development of portable devices/platforms that can be easily operated with high sensitivity and specificity, and rapid readout. Currently, there are already several SERS substrates commercially available. Most of them use gold or silver as SERS active materials, mostly AgNPs, AuNPs (RAM-SERS-AU/RAM-SERS-AG (Ocean Optics), Q-SERS<sup>TM</sup> G1(Nanova Inc.)), or the combination of both (SERSitive). They are engineered on a supporting substrate such as glass or nanostructured Si wafer by various methods such as electrodeposition (SERSitive). The required

volume for the analyte is typically very small (micro liter level). These substrates have been used for the identification of various molecules of interest such as melamine and TNT, with a low LOD. However, several of the biosensor parameters described in **Table 2.1**, such as the sensitivity, specificity, and reproducibility, need to be further improved for successful applications in medical diagnosis.

Overall, the development of plasmonic biosensors fulfills basic requirement towards some specific PON applications regarding the sensitivity, fabrication cost, response time, etc. Even though there are still many challenges to be overcome for wider implementation, they show promising potential for future applications towards PON applications.

**Table 2.2.** Summary of applications of plasmonic biosensors. Applications that are close to PON situations are highlighted in bold.

Application	Analyte	Functionalization	Detection	Substrate/material	Sensitivity	Specificity	Response time	Ease of fabrication	Cost	Ref.
Characterization of substrates and (bio)materials	R6G and graphene for test	None	SERS	AgNPs arrays prepared by magnetic sputtering and thermal annealing process on silicon wafers		Non-applicable	Not reported	High temperature (500 °C) required for thermal annealing process	Low	[61]
	R6G	None	SERS	Paper with different porosities decorated with Ag nanostars	11.4±0.2 pg	Non-applicable	min	Simple (chemical reduction + wax ink printing on paper)	Low	[91]
	<i>Escherichia coli O157:H7</i>	Au nanorods functionalized with 4-ATP and ATT and antibodies	SERS	Nano-DEP microfluidic device. Bio-conjugated AuNPs as SERS probes. DEP force to trap cells.	10 colony-forming unit /mL	High specificity from non target strains	Sec	Long time (19 h stirring during synthesis of AuNRs)	Low	[155]
	Low molecular weight molecule (glycerol)	None	SPR	Hyperbolic metamaterials: 16 alternating thin films of gold and aluminium dioxide (Al <sub>2</sub> O <sub>3</sub> )	Ultra low molecular mass of 266 Da	Non-applicable	Not reported	e-beam lithography; photoresist coating	Low	[104]
	Recombinant protein A/G and goat anti-mouse IgG	None	Mid-IR spectroscopy	Graphene nanoribbon arrays		Chemical bond specificity	Not reported	Chemical vapor deposition to grow Graphene	Medium	[36]
	Thrombin	Thiol-modified thrombin aptamer was attached onto AuNPs/Fe <sub>3</sub> O <sub>4</sub>	LSPR/absorption	AuNPs loaded on magnetic Fe <sub>3</sub> O <sub>4</sub> nanoparticles	200 pM	High selectivity of thrombin aptamer	Not reported	Simple	Low	[156]
	The proposed meta surface architecture provides a unique platform to selectively detect aromatic ring structure biomolecules	None	SPR	Graphene-coated Au film	1 × 10 <sup>-18</sup> M 1 × 10 <sup>-18</sup> M 10 <sup>-18</sup> M	Non-applicable	Not reported	High temperature (1000 °C); chemical vapor deposition.	Medium	[157]
Environment monitoring	Explosives: such as PA and NTO	None	SERS	3D biomimetic superhydrophobic Ag micro/nano-pillar array surface, which is deposited on different types of Si arrays	R6G 10 <sup>-15</sup> mol/L; PA 10 <sup>-12</sup> mol/L; NTO 10 <sup>-13</sup> mol/L.	Non-applicable	Not reported	electrodeposition of Ag sheets may require long time (7 h)	Low	[158]
	Heavy metal ions	Diethylenetriaminepentaacetic acid-grafting to bind with heavy metal ions	SERS	Gold structure with DTPA to bind to heavy metal ions	10 <sup>-14</sup> M	Selective metal ions detection	Tens of seconds	Long time drying(24 h); laser irradiation for patterning	Low	[159]
	TNT explosive	PABT(Raman signal) modification	SERS	AgNPs modified by PABT decorating silicon wafer	~ 1 pM	High selectivity for TNT	Tens of seconds	Simple	Low	[89]
	<b>Mercury ion Hg<sup>2+</sup> in water</b>	<b>Assembling oligonucleotide probes</b>	<b>SERS</b>	<b>Silver nanorod array by OAD technique. Oligonucleotide probes are assembled through Ag-S covalent bond.</b>	<b>0.16 pM</b>	<b>High selectivity</b>	<b>Second</b>	<b>Simple</b>	<b>Low</b>	<b>[64]</b>

	Bromate in water	R6G used as a reference sample with or without bromate	SERS	Ag film made by electrostatic immobilization of AgNPs on glass slide	0.01 µg/L	Non-applicable	Tens of seconds	Simple (but long time 24h dipping)	Low	[92]
Diagnosis for human health	Neuron-Specific Enolase (NSE,protein)	Detection antibody-SERS probe conjugation	SERS-LFA	Au nanostar @Raman reporter@ silica (coating with 4-MBA (Raman reporter) and TEOS, then conjugated with detection antibody)		NSE detected in clinical blood plasma	Not reported	Simple	Low	[62]
	<b>MicroRNA</b>	<b>Hybridization between complementary probes</b>	<b>LSPR</b>	<b>Gold nanoprisms attached to silanized glass</b>	<b>~10<sup>-15</sup>M</b>	<b>High selectivity</b>	Not reported	<b>Simple but long time preparation</b>		<b>[16 2]</b>
	<b>Cytokines</b>	<b>Cytokine antibodies conjugation</b>	<b>LSPR/microfluidics</b>	<b>Au nanorods microarray</b>	<b>5 pg/mL</b>		Not reported	<b>Medium (multiple processes)</b>		<b>[16 6]</b>
	Human IgG-anti-human IgG recognition	Human IgG as a recognition element for anti-human IgG	LSPR-SERS	PDMS as substrate coated with Au film in nanocup shape (nanoplatfrom)	10 <sup>-14</sup> M of 4-MBA (4-mercaptobenzoic acid)	Specific for antigen-antibody binding	Tens of seconds	Simple	Low	[86]
	Cancer marker, Mucin-1	Hybridized aptamer	SERS	AuNPs on paper fibers	50 ng/mL	High selectivity	Not reported	Simple (but heating needs 5h)	Low	[60]
	Anticancer drug, DOX, assessment of DOX-dsDNA interaction (DNA damage)	None	SERS/EC	Magnetic Fe <sub>2</sub> Ni@Au nanoparticles on graphene oxide functionalized with double-stranded DNA (dsDNA)	8 µg/mL	High selectivity	Not reported	Auto clave long time (19 h)	Low	[16 3]
	Multiple label-free detection: cancer biomarkers, including AFP, CEA, and PSA	None	LSPR (scattering shift)	Immune-AuNPs immobilized on glass slide	91 fM, 94 fM and 10 fM for AFP, CEA and PSA	High selectivity	Not reported	Medium (long time stirring 10h, multiple processes)	Medium (promise ion for low cost)	[16 4]
PPI, related to DNA replication	Substrate immobilized with meso-tetra(4-carboxyphenyl)porphyrin	Fluorescence	AuNRs as core with a silica shell	820 × 10 <sup>-9</sup> M of PPI	High selectivity	Not reported	Simple but long time preparation (10 h during AuNR synthesis and 24 h for silica coating)	Low	[13 2]	
Food safety	<b>Melamine in milk</b>	<b>None</b>	<b>SERS</b>	<b>Silver dendrite</b>	<b>7.9 × 10<sup>-7</sup> M</b>	<b>Specific for melamine</b>	<b>Tens of seconds</b>	<b>Simple</b>	<b>Low</b>	<b>[16 9]</b>
	Melamine detection in animal feed	None	SERS	Ag nanorod array	0.9 µg/g feed	High selectivity	Tens of seconds	Simple (OAD)	Low	[65]
	Pesticide residues such as parathionmethyl, thiram, and chlorpyrifos	None	SERS	Colloidal AuNPs decorated commercial tapes	2.60 ng/cm <sup>2</sup> 0.24 ng/cm <sup>2</sup> 3.51 ng/cm <sup>2</sup>	Non-applicable	Tens of seconds	Simple	Low	[17 0]
	<b>Methylene-blue in fish</b>	<b>None</b>	<b>SERS</b>	<b>Ag nanoflowers sandwiched between PMMA and monolayer graphene</b>	<b>10<sup>-13</sup> M</b>	<b>Change with analyte in real sample</b>	Not reported	<b>Slow displacement reaction and etching process</b>	<b>Low</b>	<b>[16 8]</b>

\* Abbreviations in Table 1.

R6G: Rhodamine-6G  
4-ATP: 4-Aminothiophenol  
ATT: 3-Amino-1,2,4-triazole-5-thiol  
ATT: 3-Amino-1,2,4-triazole-5-thiol  
Nano-DEP: Nano-dielectrophoretic  
IgG: Immunoglobulin G  
PA: picric acid  
NTO: 3-nitro-1,2,4-triazol-5-one  
DTPA: Diethylenetriaminepentaacetic acid

PABT: Paminobenzenethiol  
OAD: oblique angle deposition  
LFA: lateral flow assay  
DOX: doxorubicin  
AFP:  $\alpha$ -fetoprotein  
CEA: carcinoembryonic antigen  
PSA: prostate specific antigen  
PPi: Pyrophosphate  
PMMA: polymethyl-methacrylate

## 2.6 Conclusions and outlook

The field of plasmonic biosensors has made great progress in recent years, which prompted many research groups to explore their potential in various fields and applications, such as environment monitoring, food safety, and diagnosis. However, taking these devices out of the lab into the field has been a difficult task, with only very few examples of use in real life applications, and in particular at the point of need. Due to their ability to absorb visible light and convert it into a heat signature, gold nanoparticles are currently used to improve the sensitivity of lateral flow assays. In order for plasmonic biosensors to expand their range of applications and become mainstream it is critical to improve their sensitivity, specificity, and reproducibility, as well as design and implement specifications that allow for their use in conditions typically found at the point of need. These include robustness, form factor, user interface, response time, and cost. The ability to connect to mobile devices for data transmission and analysis is also important.

There are many factors playing an important role in designing and fabricating plasmonic substrates. In the paper, we reviewed the fundamentals of plasmonics, the optical properties of substrates, and the detection methods that are used in the measurements of molecules of interest. Specifically, we describe material properties that allow optimization towards improved detection, the structures that allow for additional tuning of material properties, the functionalization and sample preparation, and the detection methods that can be used. Other factors include the limit of detection and the incorporation of LSPR devices into multiplexed platforms that are still challenging [179]. Improving the sample-to-sample reproducibility as well as reducing the sampling error is still difficult because of the limit in controlling the size, shape, and surface of the plasmonic nanostructures, especially for the Ag or Au nanoparticles [180].

We also reviewed in this article practical applications. Significant progress has been made, as highlighted in this review. However, most examples currently found in the literature include tests performed in the lab under controlled experimental conditions. They describe substrate manufacturing and functionalization, report improvements in detection schemes, and demonstrate their applicability to the detection of certain analytes. One drawback is the fact that in many of the examples shown, the samples are simulated and measured in the lab, and may not necessarily provide an accurate representation of the complex situations in the field. This makes, in general, the evaluation of the potential of these sensors difficult. In conclusion, while plasmonic biosensors

are not currently found in many PON applications, the increased quality of the data and exponential growth of the field demonstrates that such applications are not far away.

## 2.7 Author contributions

All authors made substantial intellectual contributions to the manuscript and approved it for publication.

## 2.8 Conflict of interest

The authors declare that the research was conducted in the absence of any commercial or financial relationships that could be construed as a potential conflict of interest.

## 2.9 Acknowledgements

This work was financially supported by the National Sciences and Engineering Research Council of Canada (NSERC), Discovery Grant RGPIN-2018-05675 (to S.W.-H.), and G247765 and G248584 (to S.M.). The authors also thank the Faculty of Engineering at McGill University. J.L. and M.J. acknowledge the McGill Engineering Doctoral Award (MEDA).

## 2.10 References

1. Chao, J., et al., *Nanostructure-based surface-enhanced Raman scattering biosensors for nucleic acids and proteins*. *Journal of Materials Chemistry B*, 2016. **4**(10): p. 1757-1769.
2. Zheng, J. and L. He, *Surface-Enhanced Raman Spectroscopy for the Chemical Analysis of Food*. *Comprehensive reviews in food science and food safety*, 2014. **13**(3): p. 317-328.
3. Mehrotra, P., *Biosensors and their applications—A review*. *Journal of oral biology and craniofacial research*, 2016. **6**(2): p. 153-159.
4. Justino, C.I., T.A. Rocha-Santos, and A.C. Duarte, *Review of analytical figures of merit of sensors and biosensors in clinical applications*. *TrAC Trends in Analytical Chemistry*, 2010. **29**(10): p. 1172-1183.
5. Justino, C.I., A.C. Duarte, and T.A. Rocha-Santos, *Recent progress in biosensors for environmental monitoring: A review*. *Sensors*, 2017. **17**(12): p. 2918.
6. Mejía-Salazar, J.R. and O.N. Oliveira, *Plasmonic Biosensing*. *Chemical Reviews*, 2018. **118**(20): p. 10617-10625.
7. Tang, L. and J. Li, *Plasmon-Based Colorimetric Nanosensors for Ultrasensitive Molecular Diagnostics*. *ACS Sensors*, 2017. **2**(7): p. 857-875.

8. Oliverio, M., et al., *Chemical Functionalization of Plasmonic Surface Biosensors: A Tutorial Review on Issues, Strategies, and Costs*. ACS Applied Materials & Interfaces, 2017. **9**(35): p. 29394-29411.
9. Hill, R.T., *Plasmonic biosensors*. Wiley Interdisciplinary Reviews: Nanomedicine and Nanobiotechnology, 2015. **7**(2): p. 152-168.
10. Langer, J., et al., *Present and Future of Surface-Enhanced Raman Scattering*. ACS Nano, 2019.
11. Soler, M., C.S. Huertas, and L.M. Lechuga, *Label-free plasmonic biosensors for point-of-care diagnostics: a review*. Expert Review of Molecular Diagnostics, 2019. **19**(1): p. 71-81.
12. Gupta, B.D., A. Pathak, and V. Semwal, *Carbon-Based Nanomaterials for Plasmonic Sensors: A Review*. Sensors (Basel, Switzerland), 2019. **19**(16): p. 3536.
13. Kahraman, M., et al., *Fundamentals and applications of SERS-based bioanalytical sensing*. Nanophotonics, 2017: p. 831.
14. Ozbay, E., *Plasmonics: merging photonics and electronics at nanoscale dimensions*. science, 2006. **311**(5758): p. 189-193.
15. Stewart, M.E., et al., *Nanostructured plasmonic sensors*. Chemical reviews, 2008. **108**(2): p. 494-521.
16. Born, M. and E. Wolf, *Principles of Optics, Cambridge Univ*. Principles of Optics (Sixth Edition), 1999.
17. Maier, S.A., *Plasmonics: fundamentals and applications*. 2007: Springer Science & Business Media.
18. Giannini, V., et al., *Plasmonic Nanoantennas: Fundamentals and Their Use in Controlling the Radiative Properties of Nanoemitters*. Chemical Reviews, 2011. **111**(6): p. 3888-3912.
19. Barnes, W.L., A. Dereux, and T.W. Ebbesen, *Surface plasmon subwavelength optics*. Nature, 2003. **424**(6950): p. 824-30.
20. Willets, K.A. and R.P. Van Duyne, *Localized Surface Plasmon Resonance Spectroscopy and Sensing*. Annual Review of Physical Chemistry, 2007. **58**(1): p. 267-297.
21. Jain, P.K. and M.A. El-Sayed, *Plasmonic coupling in noble metal nanostructures*. Chemical Physics Letters, 2010. **487**(4-6): p. 153-164.
22. Cuevas, M., *Spontaneous emission in plasmonic graphene subwavelength wires of arbitrary sections*. Journal of Quantitative Spectroscopy and Radiative Transfer, 2018. **206**: p. 157-162.
23. Brolo, A.G., *Plasmonics for future biosensors*. Nature Photonics, 2012. **6**(11): p. 709.
24. Petryayeva, E. and U.J. Krull, *Localized surface plasmon resonance: nanostructures, bioassays and biosensing—a review*. Analytica chimica acta, 2011. **706**(1): p. 8-24.

25. Hentschel, M., et al., *Transition from Isolated to Collective Modes in Plasmonic Oligomers*. Nano Letters, 2010. **10**(7): p. 2721-2726.
26. Rechberger, W., et al., *Optical properties of two interacting gold nanoparticles*. Optics Communications, 2003. **220**(1): p. 137-141.
27. Su, K.H., et al., *Interparticle Coupling Effects on Plasmon Resonances of Nanogold Particles*. Nano Letters, 2003. **3**(8): p. 1087-1090.
28. Murray, W.A. and W.L. Barnes, *Plasmonic materials*. Advanced materials, 2007. **19**(22): p. 3771-3782.
29. Pelton, M., J. Aizpurua, and G. Bryant, *Metal-nanoparticle plasmonics*. Laser Photonics Reviews, 2008. **2**(3): p. 136-159.
30. Lal, S., S. Link, and N.J. Halas, *Nano-optics from sensing to waveguiding*. Nature photonics, 2007. **1**(11): p. 641.
31. Koppens, F.H., D.E. Chang, and F.J. García de Abajo, *Graphene plasmonics: a platform for strong light-matter interactions*. Nano letters, 2011. **11**(8): p. 3370-3377.
32. Goykhman, I., et al., *On-chip integrated, silicon-graphene plasmonic Schottky photodetector with high responsivity and avalanche photogain*. Nano letters, 2016. **16**(5): p. 3005-3013.
33. Phare, C.T., et al., *Graphene electro-optic modulator with 30 GHz bandwidth*. Nature Photonics, 2015. **9**(8): p. 511.
34. Xiao, S., et al., *Graphene-plasmon polaritons: From fundamental properties to potential applications*. Frontiers of Physics, 2016. **11**(2): p. 117801.
35. Thongrattanasiri, S., A. Manjavacas, and F.J. García de Abajo, *Quantum Finite-Size Effects in Graphene Plasmons*. ACS Nano, 2012. **6**(2): p. 1766-1775.
36. Rodrigo, D., et al., *Mid-infrared plasmonic biosensing with graphene*. Science, 2015. **349**(6244): p. 165-168.
37. Liu, M., et al., *A graphene-based broadband optical modulator*. Nature, 2011. **474**(7349): p. 64.
38. Nair, R.R., et al., *Fine Structure Constant Defines Visual Transparency of Graphene*. Science, 2008. **320**(5881): p. 1308.
39. Xu, H., et al., *Effect of Graphene Fermi Level on the Raman Scattering Intensity of Molecules on Graphene*. ACS Nano, 2011. **5**(7): p. 5338-5344.
40. Jiang, T., et al., *Gate-tunable third-order nonlinear optical response of massless Dirac fermions in graphene*. Nat. Photonics, 2018. **12**: p. 430-436.
41. Garcia de Abajo, F.J., *Graphene plasmonics: challenges and opportunities*. Acs Photonics, 2014. **1**(3): p. 135-152.

42. Grigorenko, A., M. Polini, and K. Novoselov, *Graphene plasmonics*. Nature photonics, 2012. **6**(11): p. 749.
43. Low, T. and P. Avouris, *Graphene plasmonics for terahertz to mid-infrared applications*. ACS Nano, 2014. **8**(2): p. 1086-1101.
44. Thongrattanasiri, S., A. Manjavacas, and F.J. García de Abajo, *Quantum finite-size effects in graphene plasmons*. ACS Nano, 2012. **6**(2): p. 1766-1775.
45. Jiang, D., et al., *One-pot hydrothermal route to fabricate nitrogen doped graphene/Ag-TiO<sub>2</sub>: Efficient charge separation, and high-performance “on-off-on” switch system based photoelectrochemical biosensing*. Biosensors Bioelectronics, 2016. **83**: p. 149-155.
46. Peiris, S., J. McMurtrie, and H.-Y. Zhu, *Metal nanoparticle photocatalysts: emerging processes for green organic synthesis*. Catalysis Science Technology, 2016. **6**(2): p. 320-338.
47. Knight, M.W., et al., *Aluminum for plasmonics*. ACS nano, 2013. **8**(1): p. 834-840.
48. Estevez, M.-C., et al., *Trends and challenges of refractometric nanoplasmonic biosensors: A review*. Analytica chimica acta, 2014. **806**: p. 55-73.
49. Špačková, B., et al., *Optical Biosensors Based on Plasmonic Nanostructures: A Review*. Proceedings of the IEEE, 2016. **104**(12): p. 2380-2408.
50. Güney, D.Ö., T. Koschny, and C.M. Soukoulis, *Reducing ohmic losses in metamaterials by geometric tailoring*. Physical Review B, 2009. **80**(12): p. 125129.
51. Gjerding, M.N., M. Pandey, and K.S. Thygesen, *Band structure engineered layered metals for low-loss plasmonics*. Nature communications, 2017. **8**: p. 15133.
52. Boltasseva, A. and H.A. Atwater, *Low-loss plasmonic metamaterials*. Science, 2011. **331**(6015): p. 290-291.
53. Khurgin, J.B. and G. Sun, *In search of the elusive lossless metal*. Applied Physics Letters, 2010. **96**(18): p. 181102.
54. West, P.R., et al., *Searching for better plasmonic materials*. Laser & Photonics Reviews, 2010. **4**(6): p. 795-808.
55. Naik, G.V., V.M. Shalae, and A. Boltasseva, *Alternative plasmonic materials: beyond gold and silver*. Advanced Materials, 2013. **25**(24): p. 3264-3294.
56. Okamoto, K., *Tuning of the surface plasmon resonance in the UV-IR range for wider applications*, in *Frontiers of Plasmon Enhanced Spectroscopy Volume 2*. 2016, ACS Publications. p. 247-259.
57. Robb, G., *Graphene plasmonics: Ultra-Tunable graphene light source*. Nature Photonics, 2016. **10**(1): p. 3.
58. Jablan, M., H. Buljan, and M. Soljačić, *Plasmonics in graphene at infrared frequencies*. Physical review B, 2009. **80**(24): p. 245435.

59. Langer, J., S.M. Novikov, and L.M. Liz-Marzán, *Sensing using plasmonic nanostructures and nanoparticles*. Nanotechnology, 2015. **26**(32): p. 322001.
60. Hu, S.-W., et al., *A paper-based SERS test strip for quantitative detection of Mucin-1 in whole blood*. Talanta, 2018. **179**: p. 9-14.
61. Bai, Y., et al., *Highly reproducible and uniform SERS substrates based on Ag nanoparticles with optimized size and gap*. Photonics and Nanostructures - Fundamentals and Applications, 2017. **23**: p. 58-63.
62. Gao, X., et al., *Based Surface-Enhanced Raman Scattering Lateral Flow Strip for Detection of Neuron-Specific Enolase in Blood Plasma*. Analytical Chemistry, 2017. **89**(18): p. 10104-10110.
63. Kim, A., S.J. Barcelo, and Z. Li, *SERS-based pesticide detection by using nanofinger sensors*. Nanotechnology, 2014. **26**(1): p. 015502.
64. Song, C., et al., *Ultrasensitive silver nanorods array SERS sensor for mercury ions*. Biosensors and Bioelectronics, 2017. **87**: p. 59-65.
65. Cheng, J., et al., *Highly sensitive detection of melamine using a one-step sample treatment combined with a portable Ag nanostructure array SERS sensor*. PloS one, 2016. **11**(4): p. e0154402.
66. Song, C., et al., *An ultrasensitive SERS sensor for simultaneous detection of multiple cancer-related miRNAs*. Nanoscale, 2016. **8**(39): p. 17365-17373.
67. Zhang, Z., et al., *Iodine-mediated etching of gold nanorods for plasmonic sensing of dissolved oxygen and salt iodine*. Analyst, 2016. **141**(10): p. 2955-2961.
68. Zhang, Z., et al., *Iodine-Mediated Etching of Gold Nanorods for Plasmonic ELISA Based on Colorimetric Detection of Alkaline Phosphatase*. ACS Applied Materials & Interfaces, 2015. **7**(50): p. 27639-27645.
69. Chen, H., et al., *Gold nanorods and their plasmonic properties*. Chemical Society Reviews, 2013. **42**(7): p. 2679-2724.
70. Bedford, E.E., et al., *Spiky gold shells on magnetic particles for DNA biosensors*. Talanta, 2018. **182**: p. 259-266.
71. Cui, X., et al., *Enhanced fluorescence microscopic imaging by plasmonic nanostructures: from a 1D grating to a 2D nanohole array*. Advanced Functional Materials, 2010. **20**(6): p. 945-950.
72. Joseph, D., et al., *Synthesis of AuAg@ Ag core@ shell hollow cubic nanostructures as SERS substrates for attomolar chemical sensing*. Sensors Actuators B: Chemical, 2019. **281**: p. 471-477.
73. Khlebtsov, N.G. and L.A. Dykman, *Optical properties and biomedical applications of plasmonic nanoparticles*. Journal of Quantitative Spectroscopy and Radiative Transfer, 2010. **111**(1): p. 1-35.

74. Avella-Oliver, M., et al., *Label-free SERS analysis of proteins and exosomes with large-scale substrates from recordable compact disks*. *Sensors and Actuators B: Chemical*, 2017. **252**: p. 657-662.
75. Kabiri, S., et al., *Graphene-diatom silica aerogels for efficient removal of mercury ions from water*. *ACS applied materials & interfaces*, 2015. **7**(22): p. 11815-11823.
76. Kim, J., S.-J. Park, and D.-H. Min, *Emerging Approaches for Graphene Oxide Biosensor*. *Analytical chemistry*, 2016. **89**(1): p. 232-248.
77. Zhao, Y., et al., *Plasmonic-enhanced Raman scattering of graphene on growth substrates and its application in SERS*. *Nanoscale*, 2014. **6**(22): p. 13754-13760.
78. Peng, F., et al., *Silicon nanomaterials platform for bioimaging, biosensing, and cancer therapy*. *Accounts of chemical research*, 2014. **47**(2): p. 612-623.
79. Wei, H. and H. Xu, *Hot spots in different metal nanostructures for plasmon-enhanced Raman spectroscopy*. *Nanoscale*, 2013. **5**(22): p. 10794-10805.
80. Li, S., et al., *Surface enhanced Raman scattering substrate with high-density hotspots fabricated by depositing Ag film on TiO<sub>2</sub>-catalyzed Ag nanoparticles*. *Journal of Alloys and Compounds*, 2016. **689**: p. 439-445.
81. Chanda, D., et al., *Coupling of plasmonic and optical cavity modes in quasi-three-dimensional plasmonic crystals*. *Nature communications*, 2011. **2**: p. 479.
82. Kahraman, M., et al., *Fabrication and characterization of flexible and tunable plasmonic nanostructures*. *Scientific reports*, 2013. **3**: p. 3396.
83. Kahraman, M. and S. Wachsmann-Hogiu, *Label-free and direct protein detection on 3D plasmonic nanovoid structures using surface-enhanced Raman scattering*. *Analytica chimica acta*, 2015. **856**: p. 74-81.
84. Ngo, H.T., et al., *Multiplex detection of disease biomarkers using SERS molecular sentinel-on-chip*. *Analytical and bioanalytical chemistry*, 2014. **406**(14): p. 3335-3344.
85. Štolcová, L., et al., *Gold film over very small (107 nm) spheres as efficient substrate for sensitive and reproducible surface-enhanced Raman scattering (SERS) detection of biologically important molecules*. *Journal of Raman Spectroscopy*, 2018. **49**(3): p. 499-505.
86. Focsan, M., et al., *Flexible and Tunable 3D Gold Nanocups Platform as Plasmonic Biosensor for Specific Dual LSPR-SERS Immuno-Detection*. *Scientific Reports*, 2017. **7**(1): p. 14240.
87. Lee, C., et al., *Thickness of a metallic film, in addition to its roughness, plays a significant role in SERS activity*. *Scientific reports*, 2015. **5**: p. 11644.
88. Lee, C., et al., *3D plasmonic nanobowl platform for the study of exosomes in solution*. *Nanoscale*, 2015. **7**(20): p. 9290-9297.

89. Chen, N., et al., *Portable and Reliable Surface-Enhanced Raman Scattering Silicon Chip for Signal-On Detection of Trace Trinitrotoluene Explosive in Real Systems*. Analytical chemistry, 2017. **89**(9): p. 5072-5078.
90. Berger, A.G., S.M. Restaino, and I.M. White, *Vertical-flow paper SERS system for therapeutic drug monitoring of flucytosine in serum*. Analytica chimica acta, 2017. **949**: p. 59-66.
91. Oliveira, M.J., et al., *Office paper decorated with silver nanostars-an alternative cost effective platform for trace analyte detection by SERS*. Scientific Reports, 2017. **7**(1): p. 2480.
92. Kulakovich, O., et al., *Nanoplasmonic Raman detection of bromate in water*. Optics express, 2016. **24**(2): p. A174-A179.
93. Lu, Z., et al., *A novel natural surface-enhanced Raman spectroscopy (SERS) substrate based on graphene oxide-Ag nanoparticles-Mytilus coruscus hybrid system*. Sensors and Actuators B: Chemical, 2018. **261**: p. 1-10.
94. Wang, Y., et al., *High-performance flexible surface-enhanced Raman scattering substrates fabricated by depositing Ag nanoislands on the dragonfly wing*. Applied Surface Science, 2018. **436**: p. 391-397.
95. Chamuah, N., et al., *A naturally occurring diatom frustule as a SERS substrate for the detection and quantification of chemicals*. Journal of Physics D: Applied Physics, 2017. **50**(17): p. 175103.
96. Kong, X., et al., *Detecting explosive molecules from nanoliter solution: A new paradigm of SERS sensing on hydrophilic photonic crystal biosilica*. Biosensors and Bioelectronics, 2017. **88**: p. 63-70.
97. Yang, J., et al., *Ultra-sensitive immunoassay biosensors using hybrid plasmonic-biosilica nanostructured materials*. Journal of biophotonics, 2015. **8**(8): p. 659-667.
98. Lin, M., et al., *"Elastic" property of mesoporous silica shell: for dynamic surface enhanced Raman scattering ability monitoring of growing noble metal nanostructures via a simplified spatially confined growth method*. ACS applied materials&interfaces, 2015. **7**(14): p. 7516-7525.
99. Xue, L., et al., *Advanced SERS Sensor Based on Capillarity-Assisted Preconcentration through Gold Nanoparticle-Decorated Porous Nanorods*. small, 2017. **13**(22): p. 1603947.
100. Liu, W., et al., *Strong Exciton-Plasmon Coupling in MoS<sub>2</sub> Coupled with Plasmonic Lattice*. Nano Letters, 2016. **16**(2): p. 1262-1269.
101. Korkmaz, A., et al., *Inexpensive and Flexible SERS Substrates on Adhesive Tape Based on Biosilica Plasmonic Nanocomposites*. ACS Applied Nano Materials, 2018. **1**(9): p. 5316-5326.
102. Biswas, A., et al., *Advances in top-down and bottom-up surface nanofabrication: Techniques, applications & future prospects*. Advances in Colloid and Interface Science, 2012. **170**(1): p. 2-27.

103. Jensen, T.R., et al., *Nanosphere Lithography: Tunable Localized Surface Plasmon Resonance Spectra of Silver Nanoparticles*. The Journal of Physical Chemistry B, 2000. **104**(45): p. 10549-10556.
104. Sreekanth, K.V., et al., *Extreme sensitivity biosensing platform based on hyperbolic metamaterials*. Nature Materials, 2016. **15**(6): p. 621.
105. Lee, J., K. Takemura, and E.J.S. Park, *Plasmonic nanomaterial-based optical biosensing platforms for virus detection*. Sensors (Basel), 2017. **17**(10): p. 2332.
106. Soelberg, S.D., et al., *Surface Plasmon Resonance (SPR) Detection Using Antibody-Linked Magnetic Nanoparticles for Analyte Capture, Purification, Concentration and Signal Amplification*. Analytical chemistry, 2009. **81**(6): p. 2357-2363.
107. Yaseen, T., H. Pu, and D.-W. Sun, *Functionalization techniques for improving SERS substrates and their applications in food safety evaluation: A review of recent research trends*. Trends in Food Science & Technology, 2018. **72**: p. 162-174.
108. Pang, S., T.P. Labuza, and L. He, *Development of a single aptamer-based surface enhanced Raman scattering method for rapid detection of multiple pesticides*. Analyst, 2014. **139**(8): p. 1895-1901.
109. Mello, L.D. and L.T. Kubota, *Review of the use of biosensors as analytical tools in the food and drink industries*. Food chemistry, 2002. **77**(2): p. 237-256.
110. Damborský, P., J. Švitel, and J. Katrlík, *Optical biosensors*. Essays in biochemistry, 2016. **60**(1): p. 91-100.
111. Nguyen, H.H., et al., *Surface plasmon resonance: a versatile technique for biosensor applications*. Sensors, 2015. **15**(5): p. 10481-10510.
112. Campbell, C.T. and G. Kim, *SPR microscopy and its applications to high-throughput analyses of biomolecular binding events and their kinetics*. Biomaterials, 2007. **28**(15): p. 2380-2392.
113. Damborska, D., et al., *Nanomaterial-based biosensors for detection of prostate specific antigen*. Microchimica Acta, 2017. **184**(9): p. 3049-3067.
114. Tang, Y., X. Zeng, and J. Liang, *Surface plasmon resonance: an introduction to a surface spectroscopy technique*. Journal of chemical education, 2010. **87**(7): p. 742-746.
115. Homola, J., *Present and future of surface plasmon resonance biosensors*. Analytical and bioanalytical chemistry, 2003. **377**(3): p. 528-539.
116. Homola, J., S.S. Yee, and G. Gauglitz, *Surface plasmon resonance sensors*. Sensors Actuators B: Chemical, 1999. **54**(1-2): p. 3-15.
117. Zeng, S., et al., *Graphene–MoS<sub>2</sub> hybrid nanostructures enhanced surface plasmon resonance biosensors*. Sensors Actuators B: Chemical, 2015. **207**: p. 801-810.

118. Ouyang, Q., et al., *Sensitivity Enhancement of Transition Metal Dichalcogenides/Silicon Nanostructure-based Surface Plasmon Resonance Biosensor*. Scientific Reports, 2016. **6**: p. 28190.
119. Hutter, E. and J.H. Fendler, *Exploitation of localized surface plasmon resonance*. Advanced materials, 2004. **16**(19): p. 1685-1706.
120. Jatschka, J., et al., *Propagating and localized surface plasmon resonance sensing—A critical comparison based on measurements and theory*. Sensing and bio-sensing research, 2016. **7**: p. 62-70.
121. Svedendahl, M., R. Verre, and M. Käll, *Refractometric biosensing based on optical phase flips in sparse and short-range-ordered nanoplasmonic layers*. Light: Science & Applications, 2014. **3**: p. e220.
122. Borisov, S.M. and O.S. Wolfbeis, *Optical biosensors*. Chemical reviews, 2008. **108**(2): p. 423-461.
123. Fleischmann, M., P.J. Hendra, and A.J. McQuillan, *Raman spectra of pyridine adsorbed at a silver electrode*. Chemical Physics Letters, 1974. **26**(2): p. 163-166.
124. Wang, Y., B. Yan, and L. Chen, *SERS Tags: Novel Optical Nanoprobes for Bioanalysis*. Chemical Reviews, 2013. **113**(3): p. 1391-1428.
125. Gersten, J. and A. Nitzan, *Electromagnetic theory of enhanced Raman scattering by molecules adsorbed on rough surfaces*. The Journal of Chemical Physics, 1980. **73**(7): p. 3023-3037.
126. Stiles, P.L., et al., *Surface-Enhanced Raman Spectroscopy*. Annual Review of Analytical Chemistry, 2008. **1**(1): p. 601-626.
127. Bantz, K.C., et al., *Recent progress in SERS biosensing*. Physical Chemistry Chemical Physics, 2011. **13**(24): p. 11551-11567.
128. García, I., et al., *Plasmonic Detection of Carbohydrate-Mediated Biological Events*. Advanced Optical Materials, 2018. **6**(23): p. 1800680.
129. Zhang, Z., et al., *Plasmonic colorimetric sensors based on etching and growth of noble metal nanoparticles: Strategies and applications*. Biosensors and Bioelectronics, 2018. **114**: p. 52-65.
130. De Acha, N., et al., *Luminescence-based optical sensors fabricated by means of the layer-by-layer nano-assembly technique*. Sensors (Basel), 2017. **17**(12): p. 2826.
131. Bauch, M., et al., *Plasmon-enhanced fluorescence biosensors: a review*. Plasmonics, 2014. **9**(4): p. 781-799.
132. Wang, L., et al., *Plasmon-Enhanced Fluorescence-Based Core-Shell Gold Nanorods as a Near-IR Fluorescent Turn-On Sensor for the Highly Sensitive Detection of Pyrophosphate in Aqueous Solution*. Advanced Functional Materials, 2015. **25**(45): p. 7017-7027.

133. Osawa, M. and M. Ikeda, *Surface-enhanced infrared absorption of p-nitrobenzoic acid deposited on silver island films: contributions of electromagnetic and chemical mechanisms*. The Journal of Physical Chemistry, 1991. **95**(24): p. 9914-9919.
134. Ataka, K., S.T. Stripp, and J. Heberle, *Surface-enhanced infrared absorption spectroscopy (SEIRAS) to probe monolayers of membrane proteins*. Biochimica et Biophysica Acta (BBA) - Biomembranes, 2013. **1828**(10): p. 2283-2293.
135. Ataka, K. and J. Heberle, *Biochemical applications of surface-enhanced infrared absorption spectroscopy*. Analytical and bioanalytical chemistry, 2007. **388**(1): p. 47-54.
136. Dong, L., et al., *Nanogapped Au Antennas for Ultrasensitive Surface-Enhanced Infrared Absorption Spectroscopy*. Nano Letters, 2017. **17**(9): p. 5768-5774.
137. Adato, R., S. Aksu, and H. Altug, *Engineering mid-infrared nanoantennas for surface enhanced infrared absorption spectroscopy*. Materials Today, 2015. **18**(8): p. 436-446.
138. Tittl, A., et al., *Imaging-based molecular barcoding with pixelated dielectric metasurfaces*. Science, 2018. **360**(6393): p. 1105.
139. Rodrigo, D., et al., *Resolving molecule-specific information in dynamic lipid membrane processes with multi-resonant infrared metasurfaces*. Nature Communications, 2018. **9**(1): p. 2160.
140. Verma, P., *Tip-Enhanced Raman Spectroscopy: Technique and Recent Advances*. Chemical Reviews, 2017. **117**(9): p. 6447-6466.
141. Olschewski, K., et al., *A manual and an automatic TERS based virus discrimination*. Nanoscale, 2015. **7**(10): p. 4545-4552.
142. He, Z., et al., *Tip-Enhanced Raman Imaging of Single-Stranded DNA with Single Base Resolution*. Journal of the American Chemical Society, 2019. **141**(2): p. 753-757.
143. Pashaei, F., et al., *Tip-enhanced Raman spectroscopy: plasmid-free vs. plasmid-embedded DNA*. Analyst, 2016. **141**(11): p. 3251-3258.
144. Kazemi-Zanjani, N., et al., *Label-Free Mapping of Osteopontin Adsorption to Calcium Oxalate Monohydrate Crystals by Tip-Enhanced Raman Spectroscopy*. Journal of the American Chemical Society, 2012. **134**(41): p. 17076-17082.
145. Bonhommeau, S., et al., *Tip-Enhanced Raman Spectroscopy to Distinguish Toxic Oligomers from A $\beta$ 1-42 Fibrils at the Nanometer Scale*. Angewandte Chemie International Edition, 2017. **56**(7): p. 1771-1774.
146. Shao, F. and R. Zenobi, *Tip-enhanced Raman spectroscopy: principles, practice, and applications to nanospectroscopic imaging of 2D materials*. Analytical and Bioanalytical Chemistry, 2019. **411**(1): p. 37-61.

147. Walt, D.R., *Optical Methods for Single Molecule Detection and Analysis*. Analytical Chemistry, 2013. **85**(3): p. 1258-1263.
148. Fan, M. and A.G. Brolo, *Silver nanoparticles self assembly as SERS substrates with near single molecule detection limit*. Physical Chemistry Chemical Physics, 2009. **11**(34): p. 7381-7389.
149. Kneipp, J., H. Kneipp, and K. Kneipp, *SERS—a single-molecule and nanoscale tool for bioanalytics*. Chemical Society Reviews, 2008. **37**(5): p. 1052-1060.
150. Kvasnička, P., et al., *Toward single-molecule detection with sensors based on propagating surface plasmons*. Optics Letters, 2012. **37**(2): p. 163-165.
151. Hentschel, M., et al., *Chiral plasmonics*. Science Advances, 2017. **3**(5): p. e1602735.
152. Urban, M.J., et al., *Chiral Plasmonic Nanostructures Enabled by Bottom-Up Approaches*. Annual Review of Physical Chemistry, 2019. **70**(1): p. 275-299.
153. Valev, V.K., et al., *Chirality and Chiroptical Effects in Plasmonic Nanostructures: Fundamentals, Recent Progress, and Outlook*. Advanced Materials, 2013. **25**(18): p. 2517-2534.
154. Collins, J.T., et al., *Chirality and Chiroptical Effects in Metal Nanostructures: Fundamentals and Current Trends*. Advanced Optical Materials, 2018. **6**(2): p. 1701345.
155. Wang, C., et al., *Detection of extremely low concentration waterborne pathogen using a multiplexing self-referencing SERS microfluidic biosensor*. Journal of biological engineering, 2017. **11**(1): p. 9.
156. Yan, J., et al., *Enzyme-guided plasmonic biosensor based on dual-functional nanohybrid for sensitive detection of thrombin*. Biosensors and Bioelectronics, 2015. **70**: p. 404-410.
157. Zeng, S., et al., *Graphene–gold metasurface architectures for ultrasensitive plasmonic biosensing*. Advanced Materials, 2015. **27**(40): p. 6163-6169.
158. He, X., et al., *Ultrasensitive detection of explosives via hydrophobic condensation effect on biomimetic SERS platforms*. Journal of Materials Chemistry C, 2017. **5**(47): p. 12384-12392.
159. Guselnikova, O., et al., *Pretreatment-free selective and reproducible SERS-based detection of heavy metal ions on DTPA functionalized plasmonic platform*. Sensors and Actuators B: Chemical, 2017. **253**: p. 830-838.
160. Wei, H., S.M.H. Abtahi, and P.J. Vikesland, *Plasmonic colorimetric and SERS sensors for environmental analysis*. Environmental Science: Nano, 2015. **2**(2): p. 120-135.
161. Masson, J.-F., *Surface Plasmon Resonance Clinical Biosensors for Medical Diagnostics*. ACS Sensors, 2017. **2**(1): p. 16-30.
162. Joshi, G.K., et al., *Highly Specific Plasmonic Biosensors for Ultrasensitive MicroRNA Detection in Plasma from Pancreatic Cancer Patients*. Nano Letters, 2014. **14**(12): p. 6955-6963.

163. Ilkhani, H., et al., *Nanostructured SERS-electrochemical biosensors for testing of anticancer drug interactions with DNA*. Biosensors and Bioelectronics, 2016. **80**: p. 257-264.
164. Lee, J.U., A.H. Nguyen, and S.J. Sim, *A nanoplasmonic biosensor for label-free multiplex detection of cancer biomarkers*. Biosensors and Bioelectronics, 2015. **74**: p. 341-346.
165. El-Sayed, I.H., X. Huang, and M.A. El-Sayed, *Surface Plasmon Resonance Scattering and Absorption of anti-EGFR Antibody Conjugated Gold Nanoparticles in Cancer Diagnostics: Applications in Oral Cancer*. Nano Letters, 2005. **5**(5): p. 829-834.
166. Chen, P., et al., *Multiplex serum cytokine immunoassay using nanoplasmonic biosensor microarrays*. ACS nano, 2015. **9**(4): p. 4173-4181.
167. Chan, E.Y.Y., S.M. Griffiths, and C.W. Chan, *Public-health risks of melamine in milk products*. The Lancet, 2008. **372**(9648): p. 1444-1445.
168. Qiu, H., et al., *Reliable molecular trace-detection based on flexible SERS substrate of graphene/Ag-nanoflowers/PMMA*. Sensors Actuators B: Chemical, 2017. **249**: p. 439-450.
169. Li, X., et al., *Rapid detection of melamine in milk using immunological separation and surface enhanced raman spectroscopy*. Journal of food science, 2015. **80**(6): p. C1196-C1201.
170. Chen, J., et al., *Flexible and Adhesive Surface Enhance Raman Scattering Active Tape for Rapid Detection of Pesticide Residues in Fruits and Vegetables*. Analytical Chemistry, 2016. **88**(4): p. 2149-2155.
171. Xie, X., H. Pu, and D.-W. Sun, *Recent advances in nanofabrication techniques for SERS substrates and their applications in food safety analysis*. Critical reviews in food science and nutrition, 2018. **58**(16): p. 2800-2813.
172. Najafi, R., et al., *Development of a rapid capture-cum-detection method for Escherichia coli O157 from apple juice comprising nano-immunomagnetic separation in tandem with surface enhanced Raman scattering*. International Journal of Food Microbiology, 2014. **189**: p. 89-97.
173. Chen, X. and L. Jensen, *Understanding the shape effect on the plasmonic response of small ligand coated nanoparticles*. Journal of Optics, 2016. **18**(7): p. 074009.
174. El-Brolossy, T.A., et al., *Shape and size dependence of the surface plasmon resonance of gold nanoparticles studied by Photoacoustic technique*. The European Physical Journal Special Topics, 2008. **153**(1): p. 361-364.
175. Caitlin S., D., et al., *Bacterial detection and differentiation via direct volatile organic compound sensing with surface enhanced Raman spectroscopy*. 2017.
176. Soares, R.R.G., et al., *Advances, challenges and opportunities for point-of-need screening of mycotoxins in foods and feeds*. Analyst, 2018. **143**(5): p. 1015-1035.

177. Boken, J., et al., *Plasmonic nanoparticles and their analytical applications: A review*. Applied Spectroscopy Reviews, 2017. **52**(9): p. 774-820.
178. Shi, G., et al., *A flexible and stable surface-enhanced Raman scattering (SERS) substrate based on Au nanoparticles/Graphene oxide/Cicada wing array*. Optics Communications, 2018. **412**: p. 28-36.
179. Unser, S., et al., *Localized surface plasmon resonance biosensing: current challenges and approaches*. Sensors, 2015. **15**(7): p. 15684-15716.
180. Sun, J., Y. Xianyu, and X. Jiang, *Point-of-care biochemical assays using gold nanoparticle-implemented microfluidics*. Chemical Society Reviews, 2014. **43**(17): p. 6239-6253.

### **Chapter III: An AgNP-deposited commercial electrochemistry test strip as a platform for urea detection**

In the previous chapter, the development of sensors for PON applications are discussed from fundamental properties of materials to substrate functionalization for improved detection. Profound discussions on the design considerations that need to be taken into account for the development of sensors for PON applications are presented in detail. These considerations include different sensor parameters, such as size, response time, and cost. In addition, other parameters such as complexity of the fabrication are also important for the design. Therefore, in order to develop a sensor that balances the trade-off between the ease-of-fabrication and the sensing performance such as sensitivity, a low cost sensing platform for urea detection is proposed here. The sensing platform is built from a commercial glucose test strip, onto which AgNPs are electrochemically deposited to achieve better electrical conductivity and catalytic reactivity. The test strip can be obtained at low cost and the modification of AgNPs on the test strip can be achieved easily. Its sensing performance such as sensitivity and stability are explored with urea, which is an important biomarker for kidney or liver related diseases and also a potential additive for disqualified dairy products. The developed test strip shows catalytic activity for urea detection. A linear detection range of 1-8 mM is obtained and the limit of detection is calculated to be 0.14 mM. The results indicate that this fabricated substrate has the potential for PON applications to diagnostics and food safety.

This chapter is based on my second publication as a first author [2]. The details of the publication are as following:

**Juanjuan Liu**, Roozbeh Siavash Moakhar, Ayyappasamy Sudalaiyadum Perumal, Horia Roman, Sara Mahshid & Sebastian Wachsmann-Hogiu (2020). *An AgNP-deposited commercial electrochemistry test strip as a platform for urea detection*. Scientific Reports 10 (1): 9527. <https://doi.org/10.1038/s41598-020-66422-x>

The contributions of each author are as below:

JL, RSM, and SWH conceived the experiments, JL conducted the experiments, JL and RSM analyzed the results. JL wrote the main manuscript with input from all the authors. All authors made substantial intellectual contributions to the manuscript. SWH supervised the whole project.

Specifically, I fabricated the AgNP-coated test strips by using electrodeposition of AgNPs on a commercial test strip, and characterized the morphology by SEM, along with EDS. After the fabrication and characterization of the test strip, I performed CV to confirm the electroactivity of this substrate. For the application, I conducted a series of CV measurements to explore the catalytic activity for urea detection, the limit of detection, and other sensing performance such as the reproducibility, reusability, stability, as well as selectivity. I also detected urea in real samples including plasma and milk to evaluate its potential for practical applications for medical diagnosis and food safety.

# An AgNP-deposited commercial electrochemistry test strip as a platform for urea detection

Juanjuan Liu<sup>1</sup>, Roozbeh Siavash Moakhar<sup>1</sup>, Ayyappasamy Sudalaiyadum Perumal<sup>1</sup>, Horia Nicolae Roman<sup>1</sup>, Sara Mahshid<sup>1</sup>, Sebastian Wachsmann-Hogiu<sup>1,\*</sup>

<sup>1</sup>Department of Bioengineering, McGill University, Montreal, Quebec, H3A 0C3, Canada

**\*Correspondence:**

[Sebastian.wachsmannhogiu@mcgill.ca](mailto:Sebastian.wachsmannhogiu@mcgill.ca)

## 3.1 Abstract

We developed an inexpensive, portable platform for urea detection via electrochemistry by depositing silver nanoparticles (AgNPs) on a commercial glucose test strip. We modified this strip by first removing the enzymes from the surface, followed by electrodeposition of AgNPs on one channel (working electrode). The morphology of the modified test strip was characterized by Scanning Electron Microscopy (SEM), and its electrochemical performance was evaluated via Cyclic Voltammetry (CV) and Electrochemical Impedance Spectroscopy (EIS). We evaluated the performance of the device for urea detection via measurements of the dependency of peak currents vs the analyte concentration and from the relationship between the peak current and the square root of the scan rates. The observed linear range is 1-8 mM (corresponding to the physiological range of urea concentration in human blood), and the limit of detection (LOD) is 0.14 mM. The selectivity, reproducibility, reusability, and storage stability of the modified test strips are also reported. Additional tests were performed to validate the ability to measure urea in the presence of confounding factors such as spiked plasma and milk. The results demonstrate the potential of this simple and portable EC platform to be used in applications such as medical diagnosis and food safety.

**Keywords:** urea, electrochemical detection, silver nanoparticles, portable test strip, point of need applications

### 3.2 Introduction

Urea is an important biomarker for medical diagnosis [1], which is a product of the urea cycle to lower the toxic level induced by high concentration of nitrogen compound by converting ammonium ions into urea, and will be eventually eliminated by the kidney as urine [2]. As a result, the concentration of urea in serum can be used for disease diagnosis related to kidney and liver function [3]. In addition, the concentration of urea in food products such as milk is crucial for food safety [4]. For example, there have been reports of milk adulteration by urea into diluted milk to preserve the thickness and viscosity [5]. Therefore, accurate measurements of urea adulteration is important for health and food safety.

Biosensors convert the biological or chemical information into detectable signals with applications in medical diagnostics, food safety and environmental monitoring [6]. Based on different detection methods, there are various types of biosensors that have been developed for urea detection based on optical [7, 8], thermal [9], piezoelectric [10], or magnetic measurements [11, 12]. In addition, EC biosensors, have attracted a lot of attention in urea detection recently, due to their simplicity and low limit of detection [13].

EC biosensors directly convert the reaction of biological/chemical molecules to electrical response, providing a straightforward way to detect the target of interest [14, 15]. A change in electrical current or potential is measured due to the reaction related to the analytes occurring on the electrode. In the case of voltammetry, the analyte is detected by measuring the corresponding current obtained by applying a varying potential between the working and reference electrodes. There are many different techniques based on the input modes of potential. Among them, CV is one of the most widely used [16]. For CV, potential is scanned between two fixed potential at a constant rate. Researches have been reported for biological detection via CV [17, 18].

Most biosensors for urea detection via electrochemical methods rely on enzymes such as urease to catalyze urea hydrolysis [19, 20]. For example, urea can indirectly be detected by measuring the change in indicators such as photoluminescence (PL) intensity of quantum dots that are sensitive to the pH change induced by the reaction of urea or by measuring the change in the product under the catalysis of urease [3, 21, 22]. Au based sensors for urea detection have been explored mostly as enzymatic sensors, including Au electrode modified with other materials or electrodes such as ITO glass modified with AuNP modification. However, the utilization of an enzyme brings more

complexity such as the immobilization of the enzyme which reduces its stability [23]. To address these issues, more non-enzymatic biosensors are being developed and have shown potential for urea detection [24-26]. More research examples on urea biosensors fabricated with nano-materials are discussed by Pundir et al in a recent review article [27].

Metallic nanoparticles draw significant attention in this field due to their chemical and physical properties compared to their bulk counterparts. When used in combination with EC electrodes, they exhibit several advantages such as high conductivity due to faster electron transfer, catalytic activity, and capturing affinity towards specific biomolecules [28]. These properties greatly facilitate the reaction of the analytes happening on metallic nanoparticles-modified electrode and increase the detection signal.

Ag-based biosensors have also been explored recently due to their good catalytic activity. Silver as a metal is not stable and it can be easily oxidized [29]. However, the oxidized compound of silver such as  $\text{Ag}(\text{OH})_2$  acts as a catalyst that enables the hydrolysis of urea [23]. Ag coated zeolitic volcanic tuff and ZnO nanorod structures have been reported for non-enzymatic Ag-biosensors operating in the range of  $\mu\text{M}$  to  $\text{mM}$  LOD [29]. Recently, a LOD in the range of  $\text{nM}$  (4.7 $\text{nM}$ ) has been reported using Ag-coated carbon nanotubes [23].

There are many test strips for glucose detection commercially available made of plastic or paper substrates on which metallic layers (electrodes) are deposited for EC functionality [30]. Accu-chek aviva is one of them which is characterized by small physical dimensions, low cost, high accuracy and short measurement time for blood glucose estimation. The strip is composed of patterned AuPd electrodes (channels) deposited on a plastic substrate. In this article, we report the modification of this glucose EC strip with AgNPs for the detection of urea.

This work is aiming for a platform that is flexible, portable, and inexpensive for the detection of urea via electrochemistry. For this purpose, it is important to choose materials that are highly conductive and catalytically active. As mentioned above, there are already commercial strips available for glucose detection via EC. Naturally, to decrease the cost for materials, the use of commercial strips with good conductivity and low cost is a reasonable option. Moreover, since AgNPs have been shown to exhibit catalytic reactivity towards urea detection [23, 29], we built a novel device that uses AgNPs on an inexpensive and readily available EC test strip. Therefore, in this article, the development and characterization of this novel EC substrate based on a commercial

glucose test strip, on which AgNPs were deposited, were reported. All biochemical components like enzymes on the surface of the electrode were first removed to make sure that the channels are only coated with Au and Pd as conductive materials. The morphology of the substrate and the distribution of AgNPs were characterized by SEM and optical microscopy. Further, urea was used as a test molecule in our set-up due to the demand for accurate measurements in biomedical applications where urea levels are important. Furthermore, we tested our device at mM concentrations, since this is the normal physiological range of urea in blood.

The sensing system uses three different channels on the commercial strip, which were selected as the 3-electrode system and connected to a potentiostat. The utilization of the whole strip makes this sensor a portable and simple platform that avoids the use of complex EC cells typically seen in a regular 3-electrode system.

### 3.3 Results and discussion

The representation of the steps followed for the preparation of the sensor and sample is presented in **Figure 3.1**. To build the system, we first removed all the components such as the enzymes for glucose test with ethanol and then distilled water (**Figure 3.1(i)**). The removal is evaluated visually by observing the disappearance of the yellow color associated with the enzyme. It is followed by the electrodeposition of AgNPs on the working electrode in the sensing area by applying a potential at -0.6 V for 30 s (**Figure 3.1(ii)**) between the working and reference electrodes in the presence of AgNO<sub>3</sub> and KNO<sub>3</sub>. The samples were then drop-cast onto the sensing area (**Figure 3.1(iii)**) for measurements and performance characterization. (**Figure 3.1(iv)**).

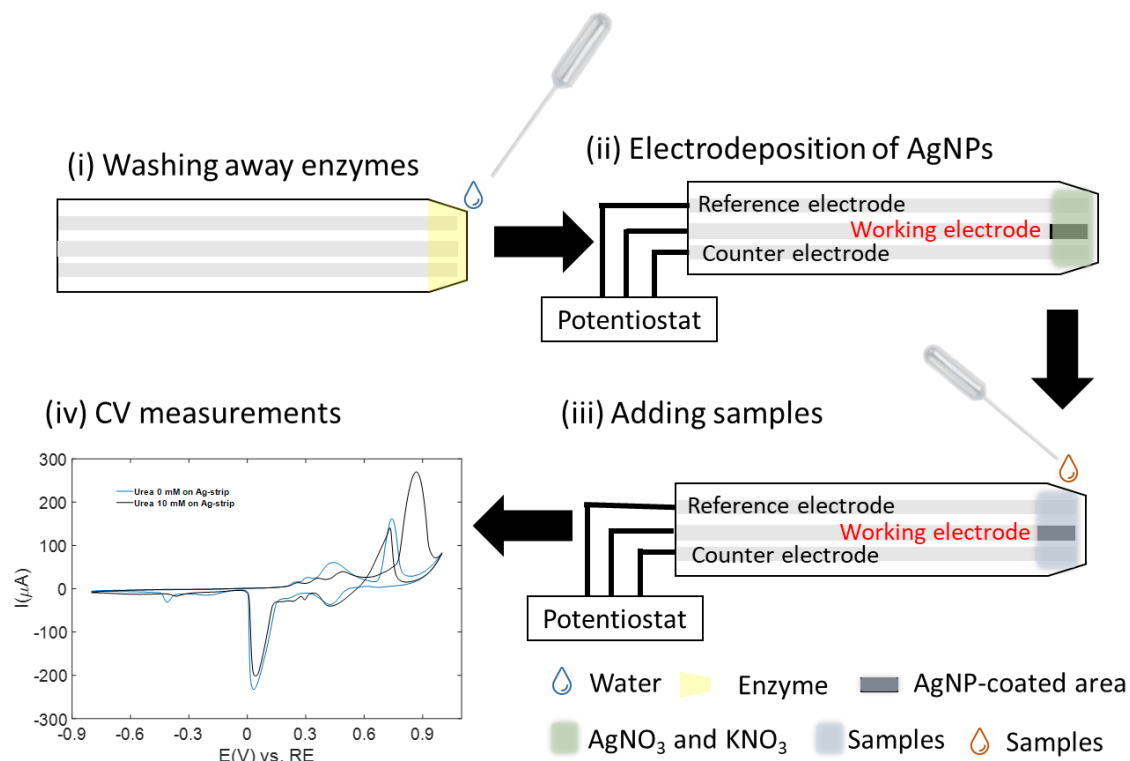


**Figure 3.1. Schematic representation of the workflow.** (i) preparation of the test strip before modification (by removing the enzyme layer). (ii) electrodeposition of AgNPs directly on the test strip by applying a potential at  $-0.6$  V for 30 s between the working and reference electrodes in presence of  $\text{AgNO}_3$  and  $\text{KNO}_3$ . (iii) drop casting of the sample on the sensing area of the test strip for detection. (iv) EC measurements.

### 3.3.1 Choice of Materials

For this work, we chose a substrate that is easy to fabricate, consisting of AgNPs and a commercial glucose test strip. To achieve good performance of the biosensor substrate for EC detection, the conductivity and catalytic activity of the electrode are important. The glucose test strip we used here is composed of a plastic substrate deposited with Au and Pd bimetallic channels. Compared to the commonly used electrodes such as Au, glassy carbon electrode (GCE), and screen-printed electrodes (SPE), this substrate is inexpensive and easy to obtain. Moreover, it consists of several channels that can work as a typical 3-electrode electrochemical system, which confers portability to this complex EC system.

However, urea cannot be detected by the test strip alone without any modification. As a result, in addition to the test strip, other material(s) that provide catalytic activity the test strip for urea detection is (are) necessary. Research has shown that Ag after oxidation can catalyze the hydrolysis

of urea. In addition, nanoparticles provide a larger surface area compared to bulk materials. Therefore, AgNPs are selected to functionalize the substrate for urea detection and for simplicity are grown in situ via electrodeposition.

### 3.3.2 Fabrication and characterizations of AgNP-coated electrode

To prepare the AgNP-coated test strip, the commercial Au strip was peeled off (**Figure 3.2A (i)**) and AgNPs were then coated on the surface of this electrode by electrodeposition. After the electrodeposition of AgNPs on the electrode, a dark layer on the surface is observed due to the formation of AgNPs (**Figure 3.2A (ii)**). To further confirm the deposition and observe the morphology of AgNPs, microscopy images and SEM images of both bare electrode (test strip) and AgNPs-coated electrode were recorded (**Figure 3.2B (i) vs. (ii)**). The result showed that the bare electrode is relatively flat. The deposited AgNPs add distinct features to the electrode and are relatively uniform sized at 30 – 100 nm. Several conditions of electrodeposition regarding the constant potential and time applied were adjusted to get better deposition of AgNPs. A potential of -0.6 V for 30 s was finally decided to be used due to a better uniformity of the nanoparticle layer.

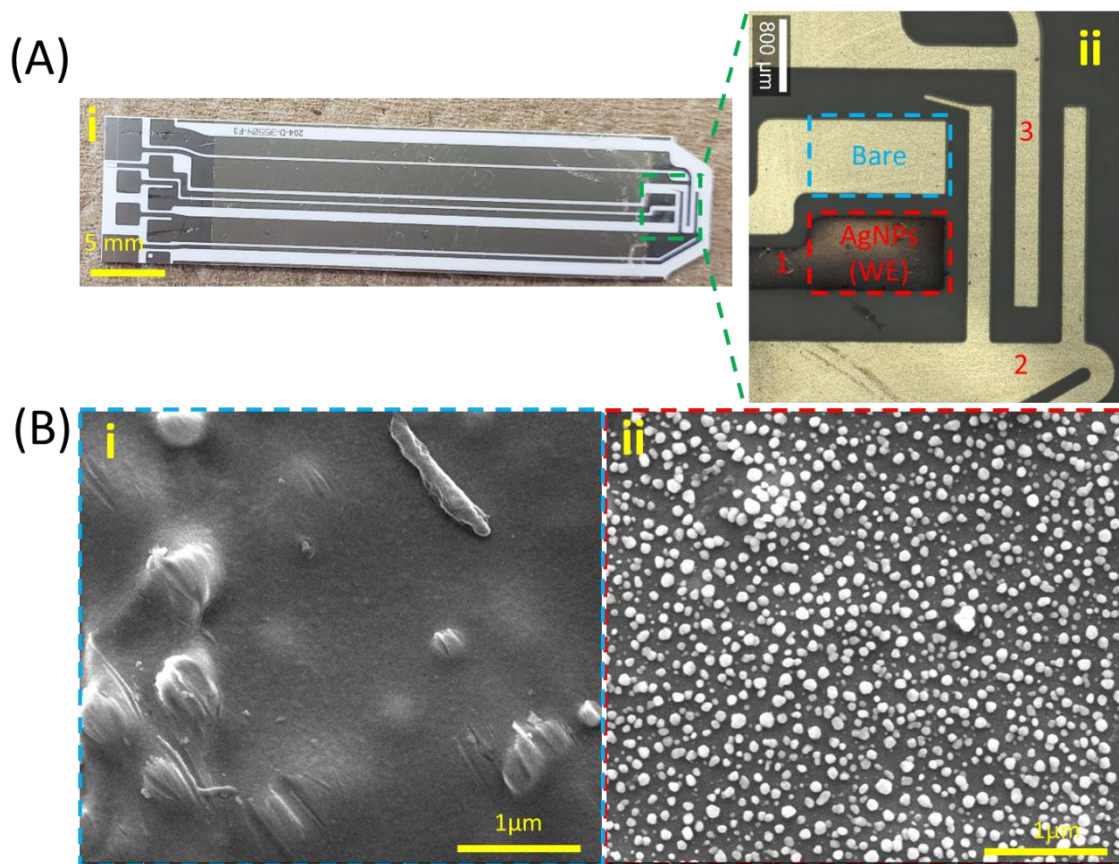


**Figure 3.2** The fabrication and characterization of the test strip. (A) the photo (i) and optical imaging (ii) of commercial glucose test strip before (i) and after (ii) electrodeposition of AgNPs (inset: 1-working electrode; 2-counter electrode; 3-reference electrode); (B) SEM images of bare test strip (i) and AgNP-coated test strip (ii).

To further confirm the deposition of AgNPs on the surface, EDS was conducted on AgNP-coated electrodes (**Figure 3.3**). The results showed that the bare electrode is composed of both Au and Pd. Ag was also detected on the substrate after the deposition (**Figure 3.3A**). The distribution of each elemental composition was also demonstrated with EDS mapping that confirms the successful coating of AgNPs (**Figure 3.3B**).

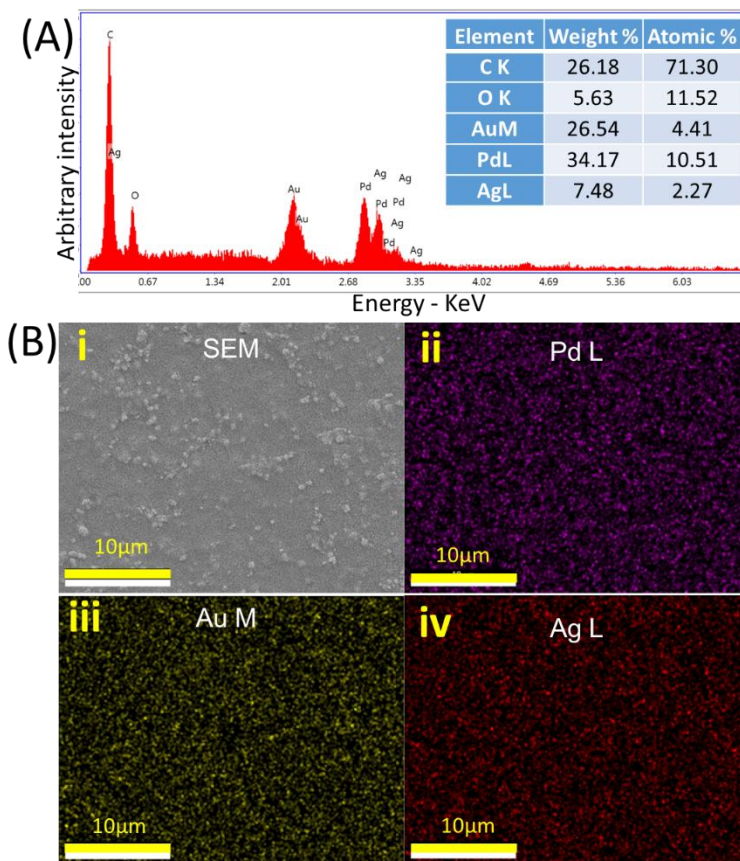


**Figure 3.3. EDS characterization of the test strip.** (A) EDS spectrum and (B) EDS mapping of the AgNP-coated commercial glucose test strip.

### 3.3.3 Electrochemical evaluation of the electrode

Ferricyanide ( $K_3Fe(CN)_6$ ) is a typical test molecule used to characterize electrochemical performance of an electrode. To confirm the electroactivity of the electrodes before and after the modification with AgNPs, 5 mM potassium ferricyanide in 0.1 M KCl was added. AgNP-coated electrode showed similar oxidation and reduction peaks of ferricyanide and ferrocyanide conversion, with slightly higher peak current and peak potential, indicating a comparable electrochemical reactivity and conductivity of the modified electrode (**Figure 3.4A**). It is important to note that, compared to the bare electrode, the modified electrode with AgNPs exhibited an extra peak during forward scanning, in addition to the oxidation peak from ferricyanide. This is due to the fact that Ag can be easily oxidized. In addition, EIS was performed to characterize the change in impedance of the electrode upon the deposition of AgNPs (**Figure**

**3.4B**), which was indicated by the resistance of charge transfer  $R_{CT}$ . The results show that after the deposition of AgNPs, the impedance increases by one magnitude (from  $10^6$  Ohm for bare strip to  $10^7$  Ohm for AgNP-coated test strip). This is likely due to the fact that the AgNPs deposited on the electrode are not continuously distributed (as shown in **Figure 3.2B (ii)**). Another possible reason is that the formation of the oxidation layer of Ag such as AgO and Ag<sub>2</sub>O decreases the electrical conductivity of the strip, which may result in a higher impedance [31].

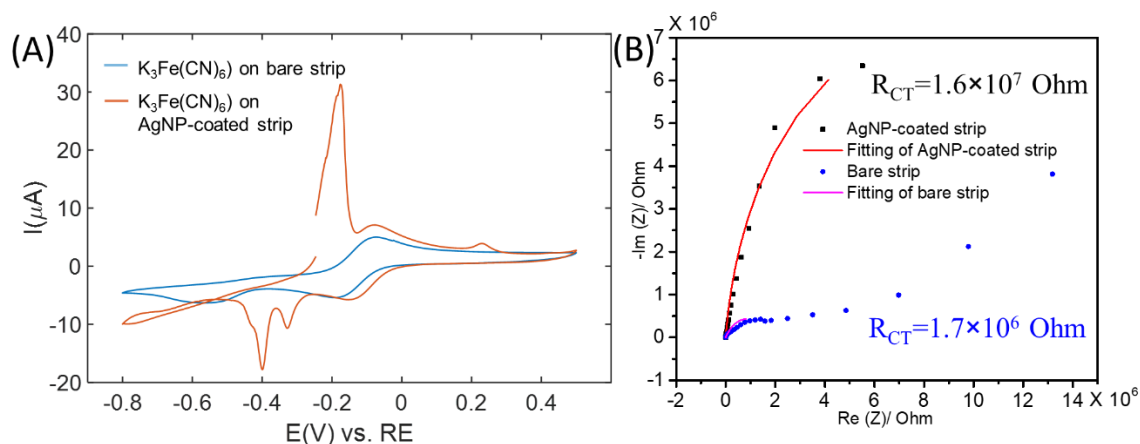


**Figure 3.4. EC evaluation of the AgNP-coated test strip.** (A) Electrochemical evaluation with  $K_3Fe(CN)_6$  and (B) EIS of bare and AgNP-coated glucose test strip. Electrolyte: 0.1 M KCl for  $K_3Fe(CN)_6$  (5 mM), and 0.1 M NaOH for EIS; scan rate for CV: 20 mV/s.

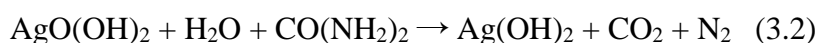
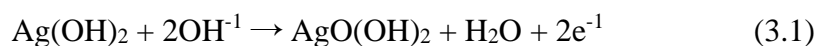
### 3.3.4 Urea detection

The electrodes are then characterized for their catalytic activity as related to the detection of urea. CV and EIS were performed on the AgNP coated strip electrode in 0.1M NaOH in the absence and presence of urea (**Figure 3.5A and B**). The effective area of the electrode considered as working electrode is  $\sim 2.5 \text{ mm}^2$  (**Figure 3.2A (ii)**). It is demonstrated that for same range of applied potential (-0.8 V – 1 V), the current response in the absence and presence of urea are quite different (**Figure 3.5A and B**). The change in the impedance of the electrolyte (solution impedance  $R_s$ ) after adding urea is presented in **Figure 3.5B**. It shows that the addition of urea results in a decrease of the impedance of the electrolyte, which corresponds to the increase in the current observed in the CV curves. In addition, it has been reported and mentioned that the electrodeposition of AgNPs provides high selectivity towards urea hydrolysis [23, 29]. Thus it is necessary to make sure that Au and Pd on the original substrates are not interfering the detection of urea. To confirm that,

control experiments to test the performance of the bare strip for urea detection were conducted, as well as to confirm the catalytic function of AgNPs. CV responses were also recorded on bare test strip in the absence and presence of urea. Since there are no peaks related to urea hydrolysis in these curves, we can conclude that the bare strip is not able to detect urea without the catalytic contribution from AgNPs.

In the presence of urea, the AgNP-coated electrode, shows multiple peaks on the forward scanning. This is due to the oxidation of AgNPs on the surface, which leads to the formation of different layers on the surface of the electrode during the forward scanning, such as, Ag<sub>2</sub>O, AgO, and Ag(OH)<sub>2</sub> (**Figure 3.5A**) [29, 32]. On the reverse scanning, a peak near 0.7 V appears, due to the oxidation of urea under the catalysis of Ag(OH)<sub>2</sub>, (also observed in other reports) [23], shown in **Figure 3.5A**. This peak demonstrates that the AgNP-coated electrode has catalytic activity for the detection of urea in alkaline electrolytes due to the formation of Ag(OH)<sub>2</sub>. The peak observed in forward scanning near 0.85 V corresponds to the reaction of the catalyst Ag(OH)<sub>2</sub>, while the peak near 0.7 V on the reverse scanning corresponds to the hydrolysis of urea under the catalysis of Ag(OH)<sub>2</sub> (equations 3.1-3.2). The overall electrocatalytic urea oxidation reaction catalyzed by the oxidation product of Ag can be summarized in equations 3.1-3.4. As a result, the electrodeposition of AgNPs on the electrode improves the ability to detect urea due to higher catalytic reactivity.

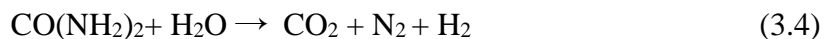
Oxidation:



Reduction:



Overall:



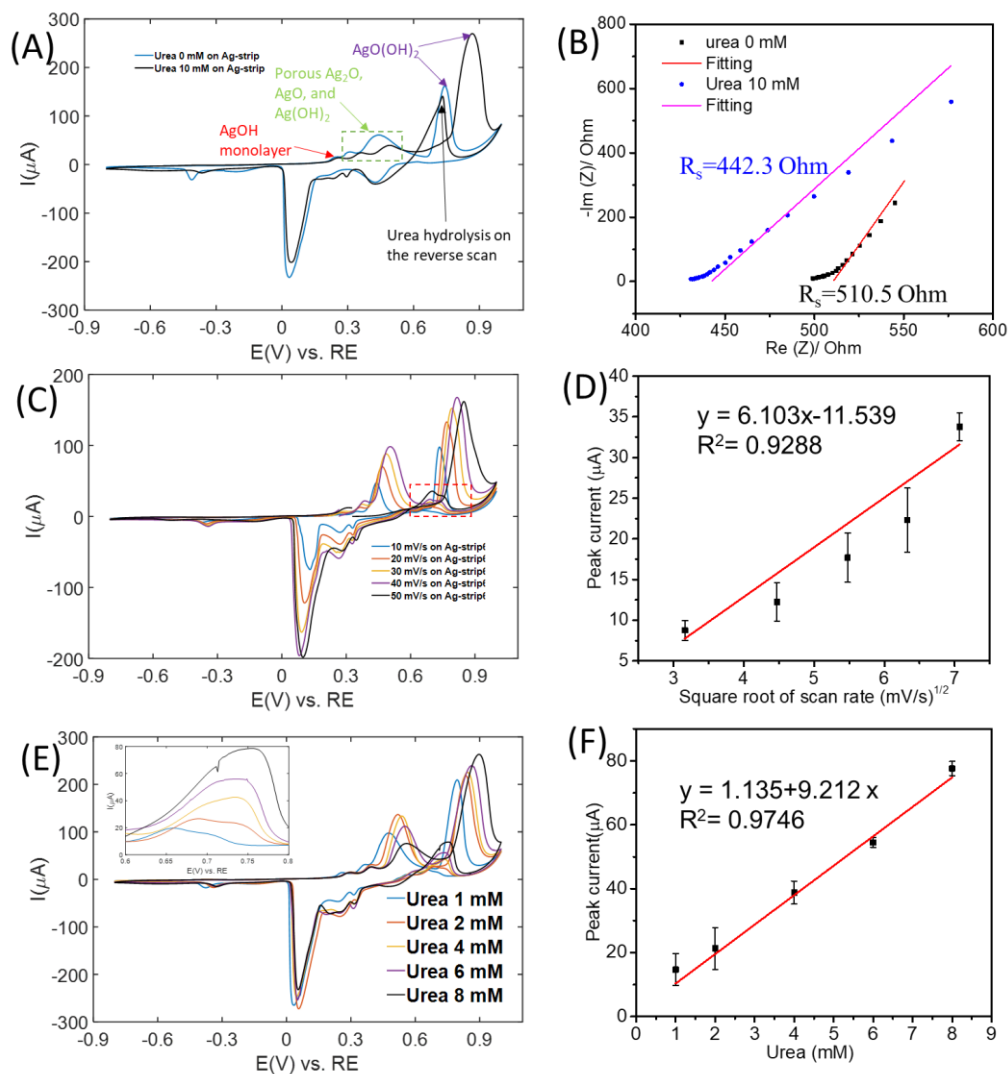


**Figure 3.5. Sensing performance of the AgNP-coated test strip for urea detection.** (A) CV response and (B) EIS of AgNP-coated glucose test strip in the absence and presence of urea; (C) CV response of AgNP-coated glucose test strip in the presence of urea at different scan rates (10-50 mV/s), and (D) corresponding calibration plot of peak current vs. square root of scan rates. (E) CV response of AgNP-coated glucose test strip in the presence of urea at different concentrations (1-8 mM) and (F) corresponding calibration plot of peak current vs. urea concentration.

After morphological, elemental, and electrochemical characterization of the electrode, we investigated its sensing performance by measuring the dependence of redox peaks on the square root of scan rates and the concentration of urea. The normal range of urea in blood is 2.5~7.5 mM [12]. Therefore, in our measurements we used concentrations of urea in the range of 1-8 mM, such that it better mimics the concentrations in real blood samples.

The effects of scan rates on the peak potential and the peak current were studied by measuring CV curves at scan rates ranging from 50 mV/s to 10 mV/s with the modified electrode in 0.1 M NaOH containing 2 mM urea (**Figure 3.5C-D**). A linear relation between the peak current and the square root of the scan rate was observed (**Figure 3.5D**), with a correlation coefficient 0.9288, indicating that the redox process is diffusion-controlled. Based on the Randles-Sevcik equation [33], the diffusion coefficient of urea is then calculated to be  $2.5 \times 10^{-3} \text{ cm}^2/\text{s}$ .

To further evaluate the sensitivity of the modified electrode, the current dependence of the urea oxidation peak on the concentration was investigated (**Figure 3.5E-F**) by recording the CV response at a series of concentrations. A linear relationship between the concentration and the peak current was observed with a correlation coefficient 0.9746. The resulting LOD is 0.1419 mM and is comparable with value reported in the literature for measurements with other EC sensors (**Table 3.1**), while at the same time we utilize a simpler sensor that was built by modifying inexpensive commercial glucose EC strips.

Type	Materials and morphology	Technique	LOD	Sensitivity	Linear detection range	Ref.
Enzymatic	Self-assembled monolayer of dihydroxythiophenol modified gold electrode with urease	LSV	0.2 mM	-	0.2-5 mM	[34]
	Amine functionalized hyperbranched AuNP modified ITO glass electrode modified with urease	CV	10 $\mu\text{M}$	7.48 nA/mM	10 $\mu\text{M}$ -35 mM	[35]
	Polyaniline-Nafion/Au/ceramic composite	CV	0.5 $\mu\text{M}$	3.162 $\text{mAmM}^{-1}\text{cm}^{-2}$	10 $\mu\text{M}$ -100 $\mu\text{M}$	[22]
	Glassy carbon electrode was electrochemically modified with	CV, DPV, CA	67 $\mu\text{M}$	-	1.0-25.0 mM	[36]

	Fe <sub>3</sub> O <sub>4</sub> /MWCNT/PANI-Nafion nanocomposite film with bacterial enzyme					
	Urease-immobilized graphene nanoplatelets and graphitized nanodiamonds.	Direct current voltage (IV)	83.3 $\mu$ M	48.1 $\mu$ AmM <sup>-1</sup> cm <sup>-2</sup>	-	[37]
Non-enzymatic	Gold Electrodes Modified with Peptide Self-Assemblies 4-mercaptopyridine (MCP) and L,L-diphenylalanine micro/nanostructures (FF-MNSs) (Benzene rings and amide groups interacts with NH <sub>4</sub> <sup>+</sup> )	CV	0.17 mM	2.83 $\mu$ AmM <sup>-1</sup> cm <sup>-2</sup>	0.1-1 mM	[38]
	AgNP-decorated nitrogen doped single wall carbon nanotubes	CV	4.7 nM	141 $\mu$ AmM <sup>-1</sup> cm <sup>-2</sup>	66 nM – 20.6 mM	[23]
	Graphite composite electrode based on natural zeolitic volcanic tuff modified with silver	SWV	50 $\mu$ M	0.058 mA/mM	0.2-1.4 mM	[29]
	Sputtered Ag on zinc oxide (ZnO) nanorod-structures grown on a carbon paper substrate	CA	13.98 $\mu$ M	0.1622 $\mu$ A $\mu$ M <sup>-1</sup> cm <sup>-2</sup>	26.3 – 450 $\mu$ M	[39]
	Glassy carbon modified with nickel sulfide/graphene oxide	CV, DPV	3.79 $\mu$ M	-	10–50 $\mu$ M	[40]
	Au electrode deposited with Ni	CV	33.5 $\mu$ M	52.20 $\mu$ AmM <sup>-1</sup> cm <sup>-2</sup>	-	[41]

	NiO nanosheet	CA	2 $\mu\text{M}$	3.4 A/(M $\text{cm}^2$ )	4.4 $\mu\text{M}$ - 181.6 $\mu\text{M}$	[42]
Our work, non-enzymatic	AgNP-deposited commercial gold electrode	CV	141.9 $\mu\text{M}$	9.212 $\mu\text{A}/\text{mM}$	1 – 8 mM	

**Table 3.1.** Comparison of electrochemical electrodes reported in the literature for urea detection

### 3.3.5 Reproducibility, reusability, stability, and selectivity of the EC strip

The reproducibility of different strips and the reusability regarding multiple cycles with one strip were investigated via CV responses (3 consecutive cycles for reproducibility) with different strips and different cycles. For reproducibility evaluation, 5 strips here were tested in 10 mM urea solution in NaOH electrolyte (**Figure 3.6A**). The relative standard deviation (RSD) of the peak current for these 5 different strips was 7.33% after 3 consecutive cycles, which indicates that the detection of urea using different electrodes/strips is reproducible.

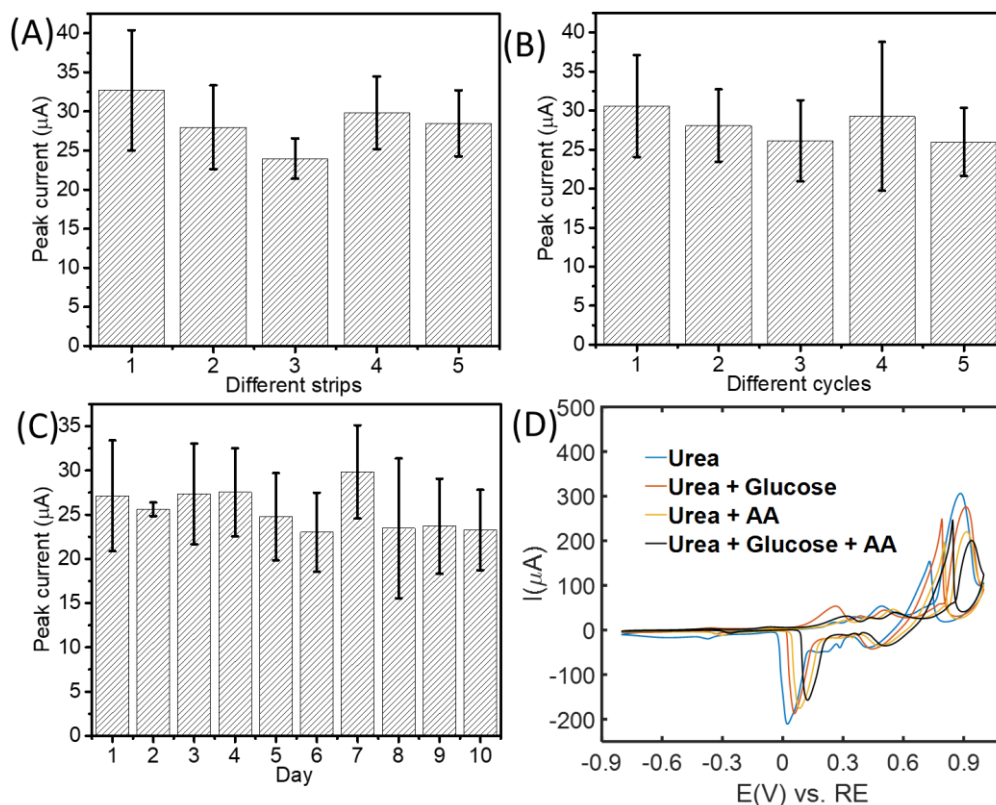


**Figure 3.6.** CV response of AgNP-coated glucose test strips in the presence of urea. (A) with different strips, (B) different cycles with the same strip, (C) with strips stored for different times, and (D) with interference of other substances glucose and AA. Electrolyte: 0.1 M NaOH; Scan rate: 50 mV/s.

The reusability of the AgNP-coated strip was also investigated by performing multiple cycles on the same electrode consistently ( $n=4$ ) (**Figure 3.6B**) in 2 mM urea solution in NaOH electrolyte. The result showed that the oxidation peak changes over time. However, since the test strips we fabricated here are inexpensive (<\$2 / strip), they are disposable, and their reusability might not be a concern.

The stability of the strips for storage was tested for 10 days to evaluate the shelf lifetime. AgNP-coated strips were prepared via electrodeposition of AgNPs on the first day. They were then stored under vacuum to prevent the oxidation of Ag. 2~3 strips were used for urea detection every day for 10 days in a row to see if the strips after 10 days storage can still function for urea detection via EC. On the other hand, because the oxidation of Ag is necessary prior to the oxidation of urea, for practical purposes it should be acceptable that the test strips are stored in air (rather than under vacuum). The peak currents of urea oxidation were recorded and plotted versus time (different

days) (**Figure 3.6C**). The results indicate that after 10 days, the fabricated strip is still functional to urea detection even the variability appears. This result shows that our strips have potential for commercialization.

Since glucose is a common component in human blood and ascorbic acid (AA) plays a vital role in metabolic processes, the selectivity of AgNP-coated strip electrode in the presence of AA and glucose was evaluated by performing CV in urea in the presence of these two analytes. As shown in **Figure 3.6D**, in the presence of urea, after the addition of glucose and/or AA, the oxidation peak of urea was shifted, and the peak current also changed. However, there were no other peaks corresponding to the interference of the additional analytes. This indicates that urea can still be detected on the AgNP-coated strip in the presence of glucose and AA.

### 3.3.6 Urea detection in reconstituted plasma solution and in milk samples

To investigate the potential of the substrate for applications in medical diagnosis and food safety, the modified test strips were used for the detection of urea in urea-spiked solutions of plasma and milk. Different concentrations of plasma and milk samples were prepared. CV responses were collected (Figure S), and the recovery rates were calculated and presented in **Table 3.2**. Since we are aiming to achieve urea detection in samples that are close to the original concentration of the potential sample with less dilution and preparation, only two lowest dilutions (highest detectable ratios) were shown here (1:10 and 1:5).

To perform urea determination in treated milk sample, CV responses and the peak currents corresponding to urea oxidation for different concentrations of milk samples in NaOH electrolyte (100 mM) were collected. Based on the calibration plot, the detected concentration of urea was calculated and compared to the actual spiked concentration. The recovery rates were then calculated. The results show that to detect urea with a higher recovery rate in real milk sample, it is important to dilute the milk sample to a proper ratio. In this set-up, we observed that urea detection is more accurate for a higher dilution of milk sample in NaOH electrolyte.

In addition, the detection of urea in plasma sample was performed following a similar procedure as described for the detection in milk. CV responses and peak currents were collected with different concentrations of plasma sample in electrolyte buffer. Compared to the detection of urea in milk

sample, the detection of urea with similar sample dilution ratio is less accurate due to the interference from the more complicated components in plasma. As a result, our AgNP-decorated electrode is more suitable for urea detection in milk samples. However, it is also important to note that our results in plasma and milk samples indicate that the platform will need to be further improved before it can be used in practical applications. This can be achieved by improvements to the sample preparation method that can lead to a better recovery rate and optimization of the catalytic material for improved sensitivity and reproducibility.

<b>Ratio of milk in NaOH electrolyte (n=5)</b>	<b>1:10</b>	<b>1:5</b>
Urea added (mM)	10	10
Total found (mM)	8.937581	3.14036
RSD %	13.9	14.0
Recovery %	89.38	31.40
<b>Ratio of plasma in NaOH electrolyte(n=5)</b>	<b>1:10</b>	<b>1:5</b>
Urea added (mM)	10	10
Total found (mM)	3.108446	1.201476
RSD %	26.4	26.86
Recovery %	31.1	12.0

**Table 3.2.** Detection of urea in milk and plasma sample

### 3.4 Conclusions

Urea detection is important for diagnosis and food safety applications. Significant research, both related to methods and materials, is dedicated towards the development of biosensors that can provide valuable data for these applications. In this work, a flexible electrochemical sensor device for urea detection was developed by decorating the working electrode of a commercial glucose

test strip with AgNPs. This provides an inexpensive and portable platform that leverages existing technology and describes improvements for the specific use case described here. The commercial strip was first modified by removing the enzyme layer and then by electrodepositing AgNPs on the surface of the working electrode. The uniform deposition of AgNPs improves the surface area and leads to better performance for electrochemical measurements. Furthermore, the presence of AgNPs on the surface of the working electrode and the interaction with the electrolyte acts as a catalyst in the hydrolysis of urea and allows for its detection. The sensing performance of the strip was studied by CV measurements. The linear dependence of the peak current on the square root of scan rates indicates a diffusion-controlled electrochemical process. On the other hand, the linear detection range between 1-8 mM shows the potential of this platform for real application in diagnosis. Moreover, the reproducibility, reusability, storage stability, and selectivity of this substrate were evaluated to validate its potential for practical applications. The platform was also used for urea detection in samples that mimic real environments such as plasma and milk. Although more improvements are still needed to be further used in for urea detection in real samples, the results still show promising potential of the substrate for urea detection within the physiological concentration range in human blood as well as in milk for possible contamination. It is also worth noticing that more improvements in reproducibility and selectivity need to be made in order to make this platform useful for point of need applications.

### 3.5 Materials and methods

**Materials:** Silver nitrite, potassium nitrate, sodium hydroxide, plasma and urea were purchased from Sigma-Aldrich. They were used as received without any treatment. The commercial glucose test strip (Accu-chek aviva glucose test strip) was purchased from a local pharmacy. Milk was purchased from a local shop.

**Preparation of AgNP-coated test strip:** The enzyme coating the original strip (which is used for glucose measurement) was chemically removed by washing with ethanol and distilled water, and the plastic coverage on the electrode end was physically peeled off. Next, an AgNPs coating was created by electrodeposition as described in [43]. Briefly, it was conducted with a typical 3-electrode system in an EC cell with a reference electrode, a counter electrode and a working electrode. The EC set-up was built directly on the whole test strip with three channels selected as

the three electrodes (working electrode, counter electrode, and reference electrode) (**Figure 3.2A**). For the fabrication of AgNP-coated test strip, electrodeposition was performed. Briefly, 30  $\mu\text{L}$  of a mixed solution including silver nitrate ( $\text{AgNO}_3$ ) and potassium nitrate ( $\text{KNO}_3$ ) was dropped on the tip of the strip substrate. A constant potential  $-0.6\text{ V}$  (vs. reference electrode) was applied for 30 s. This value was confirmed by exploring the reduction potential via CV in  $\text{AgNO}_3$ . It could be observed that after the electrodeposition a darker layer of AgNPs was formed on the surface of the test strip (**Figure 3.2A (ii)**).

**Scanning electron microscopy (SEM):** SEM images of the electrode with/without the deposition AgNPs were obtained using a Carl Zeiss SEM instrument at high vacuum with the acceleration voltage of 5 kV equipped with Quanta 450 FE-SEM that can be used to obtain Energy Dispersive Spectroscopy (EDS) mapping. These images provide information regarding the morphology of the surface condition of the test strip electrode and the deposition status of the AgNPs.

**Electrochemical measurement:** All the EC measurements are performed with a single-channel Potentiostat (BioLogic Science Instrument, SP-150, France) controlled by the EC-lab software installed on a PC. The EC system was set up by connecting the three electrodes to a Potentiostat device. The electrolyte used for urea detection was NaOH (0.1 M, 30  $\mu\text{l}$  in the whole strip system). To avoid fluctuations in the signal, the second or third cycles (if not specified) of CV curves after stabilization of the first scan were recorded as the reaction occurred at the working electrode. The currents were examined and shown as the voltammograms. The limit of the detection was then calculated by the following relation:  $\text{LOD} = 3\text{SD}/\text{S}$ , where LOD is the limit of detection, SD is the standard deviation of blank measurement when there is no urea, and S is the slope of the linear equation.

**Urea detection in milk:** To remove the excess fat and proteins from the purchased milk, it was pretreated by mixing 5 ml of milk with 10 ml acetonitrile. The mixture was then centrifuged at 10,000 rpm for 3 min. After centrifugation, the supernatant was collected as the ready milk sample for urea detection. The electrolyte NaOH at 0.1 M was prepared with the milk sample at different ratios, e.g., treated milk sample was diluted different times in the electrolyte. 10 mM of urea was then prepared in milk sample diluted in NaOH (1:100, 1:50, 1:10, 1:5, 1:1). For each concentration of milk sample, 5 measurements on different substrates were collected.

**Urea detection in plasma:** The plasma was firstly 10 times diluted in phosphate buffered solution (1X, pH 7.4) before using it. Similar to the preparation of milk sample, the diluted plasma was then diluted with NaOH electrolyte at different ratios/concentrations (1:100, 1:50, 1:10, 1:5, and 1:1). 10 mM of urea was then prepared in these samples. 5 measurements were collected with different strips for each condition.

### **3.6 Author contributions**

J.L., R.M., and S.W.-H. conceived the experiments, J.L. conducted the experiments, J.L. and R.M. analyzed the results. J.L. wrote the main manuscript with input from all the authors. All authors made substantial intellectual contributions to the manuscript and approved it for publication.

### **3.7 Conflict of interest**

The authors declare that the research was conducted in the absence of any commercial or financial relationships that could be construed as a potential conflict of interest.

### **3.8 Acknowledgements**

This work was financially supported by the National Sciences and Engineering Research Council of Canada (NSERC), Discovery Grant RGPIN-2018-05675 (to S.W.-H.), and G247765 and G248584 (to S.M.). The authors also thank the Faculty of Engineering at McGill University. J.L. acknowledge the McGill Engineering Doctoral Award (MEDA).

### 3.9 References

- 1 Hao, W., Das, G. & Yoon, H. H. Fabrication of an amperometric urea biosensor using urease and metal catalysts immobilized by a polyion complex. *Journal of Electroanalytical Chemistry* **747**, 143-148, doi:<https://doi.org/10.1016/j.jelechem.2015.03.015> (2015).
- 2 Wu, G. & Morris, S. M., Jr. Arginine metabolism: nitric oxide and beyond. *Biochem J* **336** ( Pt 1), 1-17, doi:10.1042/bj3360001 (1998).
- 3 Huang, C.-P., Li, Y.-K. & Chen, T.-M. A highly sensitive system for urea detection by using CdSe/ZnS core-shell quantum dots. *Biosensors and Bioelectronics* **22**, 1835-1838, doi:<https://doi.org/10.1016/j.bios.2006.09.003> (2007).
- 4 Ezhilan, M. *et al.* Design and development of electrochemical biosensor for the simultaneous detection of melamine and urea in adulterated milk samples. *Sensors and Actuators B: Chemical* **238**, 1283-1292, doi:<https://doi.org/10.1016/j.snb.2016.09.100> (2017).
- 5 Handford, C. E., Campbell, K. & Elliott, C. T. Impacts of Milk Fraud on Food Safety and Nutrition with Special Emphasis on Developing Countries. *Comprehensive Reviews in Food Science and Food Safety* **15**, 130-142, doi:10.1111/1541-4337.12181 (2016).
- 6 Liu, J., Jalali, M., Mahshid, S. & Wachsmann-Hogiu, S. Are plasmonic optical biosensors ready for use in point-of-need applications? *Analyst* **145**, 364-384, doi:10.1039/C9AN02149C (2020).
- 7 Tsai, H.-c. & Doong, R.-a. Simultaneous determination of pH, urea, acetylcholine and heavy metals using array-based enzymatic optical biosensor. *Biosensors and Bioelectronics* **20**, 1796-1804, doi:<https://doi.org/10.1016/j.bios.2004.07.008> (2005).
- 8 Kahraman, M., Mullen Emma, R., Korkmaz, A. & Wachsmann-Hogiu, S. in *Nanophotonics* Vol. 6 831 (2017).
- 9 Bjarnason, B., Johansson, P. & Johansson, G. A novel thermal biosensor: evaluation for determination of urea in serum. *Analytica Chimica Acta* **372**, 341-348, doi:[https://doi.org/10.1016/S0003-2670\(98\)00383-3](https://doi.org/10.1016/S0003-2670(98)00383-3) (1998).
- 10 Yang, Z. & Zhang, C. Single-enzyme nanoparticles based urea biosensor. *Sensors and Actuators B: Chemical* **188**, 313-317, doi:<https://doi.org/10.1016/j.snb.2013.07.004> (2013).
- 11 Chemla, Y. R. *et al.* Ultrasensitive magnetic biosensor for homogeneous immunoassay. *Proceedings of the National Academy of Sciences* **97**, 14268, doi:10.1073/pnas.97.26.14268 (2000).
- 12 Dhawan, G., Sumana, G. & Malhotra, B. D. Recent developments in urea biosensors. *Biochemical Engineering Journal* **44**, 42-52, doi:<https://doi.org/10.1016/j.bej.2008.07.004> (2009).
- 13 Mahshid, S. S. *et al.* Template-based electrodeposition of Pt/Ni nanowires and its catalytic activity towards glucose oxidation. *Electrochimica Acta* **58**, 551-555, doi:<https://doi.org/10.1016/j.electacta.2011.09.083> (2011).

- 14 Sanati, A. *et al.* A review on recent advancements in electrochemical biosensing using carbonaceous nanomaterials. *Microchimica Acta* **186**, 773, doi:10.1007/s00604-019-3854-2 (2019).
- 15 Grieshaber, D., MacKenzie, R., Vörös, J. & Reimhult, E. Electrochemical Biosensors - Sensor Principles and Architectures. *Sensors (Basel)* **8**, 1400-1458, doi:10.3390/s80314000 (2008).
- 16 del Caño, R. *et al.* Hemoglobin becomes electroactive upon interaction with surface-protected Au nanoparticles. *Talanta* **176**, 667-673, doi:<https://doi.org/10.1016/j.talanta.2017.08.090> (2018).
- 17 Zhu, H. *et al.* Effects of cyclic voltammetric scan rates, scan time, temperatures and carbon addition on sulphation of Pb disc electrodes in aqueous H<sub>2</sub>SO<sub>4</sub>. *Materials Technology* **35**, 135-140, doi:10.1080/10667857.2015.1133157 (2020).
- 18 Iida, Y., Suganuma, Y., Matsumoto, K. & Satoh, I. Novel Determination System for Urea in Alcoholic Beverages by Using an FIA System with an Acid Urease Column. *Analytical Sciences* **22**, 173-176, doi:10.2116/analsci.22.173 (2006).
- 19 Yang, J.-K., Ha, K.-S., Baek, H.-S., Lee, S.-S. & Seo, M.-L. Amperometric determination of urea using enzyme-modified carbon paste electrode. *Bulletin of the Korean Chemical Society* **25**, 1499-1502, doi:<https://doi.org/10.5012/bkcs.2004.25.10.1499> (2004).
- 20 Kim, K. *et al.* Fabrication of a Urea Biosensor for Real-Time Dynamic Fluid Measurement. *Sensors (Basel)* **18**, 2607, doi:10.3390/s18082607 (2018).
- 21 Song, Y. *et al.* pH-Switchable Electrochemical Sensing Platform based on Chitosan-Reduced Graphene Oxide/Concanavalin A Layer for Assay of Glucose and Urea. *Analytical Chemistry* **86**, 1980-1987, doi:10.1021/ac402742m (2014).
- 22 Luo, Y.-C. & Do, J.-S. Urea biosensor based on PANi(urease)-Nafion®/Au composite electrode. *Biosensors and Bioelectronics* **20**, 15-23, doi:<https://doi.org/10.1016/j.bios.2003.11.028> (2004).
- 23 Kumar, T. H. V. & Sundramoorthy, A. K. Non-Enzymatic Electrochemical Detection of Urea on Silver Nanoparticles Anchored Nitrogen-Doped Single-Walled Carbon Nanotube Modified Electrode. *Journal of The Electrochemical Society* **165**, B3006-B3016, doi:10.1149/2.0021808jes (2018).
- 24 Amin, S. *et al.* A practical non-enzymatic urea sensor based on NiCo<sub>2</sub>O<sub>4</sub> nanoneedles. *RSC Advances* **9**, 14443-14451, doi:10.1039/C9RA00909D (2019).
- 25 Guo, F., Ye, K., Cheng, K., Wang, G. & Cao, D. Preparation of nickel nanowire arrays electrode for urea electro-oxidation in alkaline medium. *Journal of Power Sources* **278**, 562-568, doi:<https://doi.org/10.1016/j.jpowsour.2014.12.125> (2015).
- 26 Dutta, D., Chandra, S., Swain, A. K. & Bahadur, D. SnO<sub>2</sub> Quantum Dots-Reduced Graphene Oxide Composite for Enzyme-Free Ultrasensitive Electrochemical Detection of Urea. *Analytical Chemistry* **86**, 5914-5921, doi:10.1021/ac5007365 (2014).

- 27 Pundir, C. S., Jakhar, S. & Narwal, V. Determination of urea with special emphasis on biosensors: A review. *Biosensors and Bioelectronics* **123**, 36-50, doi:<https://doi.org/10.1016/j.bios.2018.09.067> (2019).
- 28 Luo, X., Morrin, A., Killard, A. J. & Smyth, M. R. Application of Nanoparticles in Electrochemical Sensors and Biosensors. *Electroanalysis* **18**, 319-326, doi:10.1002/elan.200503415 (2006).
- 29 Manea, F. *et al.* Voltammetric Detection of Urea on an Ag-Modified Zeolite-Expanded Graphite-Epoxy Composite Electrode. *Sensors* **8**, doi:10.3390/s8095806 (2008).
- 30 Heller, A. & Feldman, B. Electrochemical Glucose Sensors and Their Applications in Diabetes Management. *Chemical Reviews* **108**, 2482-2505, doi:10.1021/cr068069y (2008).
- 31 Friend, J. A. & Gutmann, F. *Electrochemistry: Proceedings of the First Australian Conference on Held in Sydney, 13—15th February and Hobart, 18—20th February 1963.* (Elsevier, 2013).
- 32 Jovic, B. & Jovic, V. Electrochemical formation and characterization of Ag<sub>2</sub>O. *Journal of the Serbian Chemical Society* **69**, 153-166 (2004).
- 33 Tammam, R. H. & Saleh, M. M. On the electrocatalytic urea oxidation on nickel oxide nanoparticles modified glassy carbon electrode. *Journal of Electroanalytical Chemistry* **794**, 189-196, doi:<https://doi.org/10.1016/j.jelechem.2017.04.023> (2017).
- 34 Mizutani, F., Yabuki, S. & Sato, Y. Voltammetric enzyme sensor for urea using mercaptohydroquinone-modified gold electrode as the base transducer. *Biosensors and Bioelectronics* **12**, 321-328, doi:[https://doi.org/10.1016/S0956-5663\(96\)00073-5](https://doi.org/10.1016/S0956-5663(96)00073-5) (1997).
- 35 Tiwari, A., Aryal, S., Pilla, S. & Gong, S. An amperometric urea biosensor based on covalently immobilized urease on an electrode made of hyperbranched polyester functionalized gold nanoparticles. *Talanta* **78**, 1401-1407, doi:<https://doi.org/10.1016/j.talanta.2009.02.038> (2009).
- 36 Singh, A. K., Singh, M. & Verma, N. Electrochemical preparation of Fe<sub>3</sub>O<sub>4</sub>/MWCNT-polyaniline nanocomposite film for development of urea biosensor and its application in milk sample. *Journal of Food Measurement and Characterization* **14**, 163-175, doi:10.1007/s11694-019-00278-2 (2020).
- 37 Kumar, V. *et al.* Graphene nanoplatelet/graphitized nanodiamond-based nanocomposite for mediator-free electrochemical sensing of urea. *Food Chemistry* **303**, 125375, doi:<https://doi.org/10.1016/j.foodchem.2019.125375> (2020).
- 38 Bianchi, R. C., da Silva, E. R., Dall'Antonia, L. H., Ferreira, F. F. & Alves, W. A. A Nonenzymatic Biosensor Based on Gold Electrodes Modified with Peptide Self-Assemblies for Detecting Ammonia and Urea Oxidation. *Langmuir* **30**, 11464-11473, doi:10.1021/la502315m (2014).
- 39 Yoon, J. *et al.* Communication—Highly Sensitive Ag/ZnO Nanorods Composite Electrode for Non-Enzymatic Urea Detection. *Journal of The Electrochemical Society* **164**, B558-B560, doi:10.1149/2.1341712jes (2017).

- 40 Sunil Kumar Naik, T. S., Saravanan, S., Sri Saravana, K. N., Pratiush, U. & Ramamurthy, P. C. A non-enzymatic urea sensor based on the nickel sulfide / graphene oxide modified glassy carbon electrode. *Materials Chemistry and Physics* **245**, 122798, doi:<https://doi.org/10.1016/j.matchemphys.2020.122798> (2020).
- 41 Irzalinda, A. D., Gunlazuardi, J. & Wibowo, R. Development of a non-enzymatic urea sensor based on a Ni/Au electrode. *Journal of Physics: Conference Series* **1442**, 012054, doi:10.1088/1742-6596/1442/1/012054 (2020).
- 42 Qin, Y., Chen, F., Halder, A. & Zhang, M. Free-Standing NiO Nanosheets as Non-Enzymatic Electrochemical Sensors. *ChemistrySelect* **5**, 2424-2429, doi:10.1002/slct.201904511 (2020).
- 43 Roushani, M. & Shahdost-fard, F. A glassy carbon electrode with electrodeposited silver nanoparticles for aptamer based voltammetric determination of trinitrotoluene using riboflavin as a redox probe. *Microchimica Acta* **185**, 558, doi:10.1007/s00604-018-3098-6 (2018).

## Chapter IV: Multimodal Electrochemical and SERS platform for chlorfenapyr detection

In the previous chapter, we demonstrate the fabrication and characterization of the AgNP-deposited test strip, as well as its application to the analytical detection of urea. The materials used to build the AgNP-deposited test strip are inexpensive, and the fabrication is simple. These features make this substrate suitable for PON applications. On the other side, urea is an important by-product of metabolism and can be used for the diagnosis of diseases related to kidney or liver. The AgNP-deposited test strip for urea detection has been shown to work in a linear range within the physiological concentration range of urea, which makes it ideal for monitoring health condition. To further explore this substrate for other application, as well as its multifunctional ability, the substrate we developed previously is then adapted for chlorfenapyr detection via both EC and SERS. Chlorfenapyr is a pesticide commonly used for plants such as vegetables and the its residues on vegetables may cause severe problems to human health. Therefore, analytical identification of chlorfenapyr in food is of significance. However, the current techniques for chlorfenapyr detection suffer from either high cost or complicated sample preparation. Therefore, to address these issues, the inexpensive AgNP-deposited test strip fabricated previously is adapted for chlorfenapyr detection in this chapter. Since it is the first time to detect chlorfenapyr via EC, SERS is also used to achieve characteristic determination by identifying a unique chemical bond of chlorfenapyr. EC, in turn, provides analytical measurements to quantify the concentration. The results show that the AgNP-deposited strip has the ability for multimodal detection. It also opens up the way for cost effective applications at PON in food industry.

This chapter is based on my third publication as a first author [3]. The details of the publication are as following:

**Juanjuan Liu**, Roozbeh Siavash Moakhar, Sara Mahshid, Fartash Vasefi, Sebastian Wachsmann-Hogiu, *Multimodal Electrochemical and SERS platform for chlorfenapyr detection*, Applied Surface Science, 2021, <https://doi.org/10.1016/j.apsusc.2021.150617>

The contributions of each author are as below.

JL, RSM, and SWH designed the experiments. JL performed the experiments and collected data. JL and RSM conducted data analysis. FV provided the samples. JL wrote the manuscript with substantial contributions from all authors.

Specifically, I fabricated the AgNP-deposited test strip and then adapted it for the multimodal detection of chlorfenapyr. I performed CV measurements and demonstrated its ability for chlorfenapyr detection via EC as well as SERS measurements. I collected SERS spectra of chlorfenapyr on the fabricated substrate and confirmed the characteristic peak of chlorfenapyr by comparing with other control samples. I evaluated the reproducibility and the selectivity towards other pesticides. Further, I performed CV measurements for chlorfenapyr and confirmed the ability of this substrate to provide quantitative results. Finally, I demonstrated the potential of this substrate for real life applications by conducting real sample analysis of chlorfenapyr with chives.

# Multimodal Electrochemical and SERS platform for chlorfenapyr detection

Juanjuan Liu <sup>1</sup>, Roozbeh Siavash Moakhar <sup>1</sup>, Sara Mahshid <sup>1</sup>, Fartash Vasefi <sup>2</sup>, Sebastian Wachsmann-Hogiu <sup>1,\*</sup>

<sup>1</sup> Department of Bioengineering, McGill University, Montreal, Quebec, Canada

<sup>2</sup> SafetySpect Inc., Los Angeles, California, USA

\* Corresponding author: [sebastian.wachsmannhogiu@mcgill.ca](mailto:sebastian.wachsmannhogiu@mcgill.ca)

## 4.1 Abstract

Multimodal sensors combining different detection methodologies on a single platform can provide complementary information for the detection of analytes. Here we developed a novel inexpensive metallic substrate that can be used for dual functional sensing via ElectroChemistry (EC) and Surface Enhanced Raman Spectroscopy (SERS). We demonstrated the utility of this platform for the detection of chlorfenapyr, which is an agricultural insecticide and a toxin that disrupts respiratory pathways and proton gradients in mitochondria. Our platform is based on a commercial bimetallic glucose test strip modified with silver nanoparticles. The performance of EC and SERS was evaluated via test probes potassium ferricyanide ( $(\text{K}_3\text{Fe}(\text{CN})_6)$ ) and 4-Aminothiophenol, respectively. The substrate was used as a working electrode for chlorfenapyr detection via EC and SERS. SERS allows the identification of chlorfenapyr by its characteristic peak near  $2230\text{ cm}^{-1}$ , with a Limit of Detection (LOD) of 7 ppm. EC allows for quantitative measurement of the analyte within the concentration range of 20-50 ppm. The EC LOD of 4.2 ppm meets residue tolerance limit in chive, according to the US Code of Federal Regulations. This platform may open up avenues towards cost-effective and portable detection of other analytes.

**Key words:** multimodal, SERS, EC, AgNPs, nanofabrication, pesticide

## 4.2 Introduction

The development of multimodal sensors is playing an important role in different applications [1-3]. Compared to single modality sensors, multimodal approaches offer multiple transducers on one platform, thus combine the advantages of multiple modalities, such as higher sensitivity and specificity. It is also advantageous to provide complementary information via multimodal

detection [4]. In addition, it is particularly beneficial for the analytes that are difficult to detect in certain applications. Among different multimodal sensors, the combination of Surface Enhanced Raman Spectroscopy (SERS) and Electrochemistry (EC) is receiving more and more attention owing to their unique merits.

SERS and EC are two commonly used detection methods that offer high sensitivity and specificity. The combination of SERS and EC have been explored in the past for several applications, as noted in these references [5, 6]. Based on the specific applications and use cases, the pursuit of the combination of SERS and EC followed two main paths. The first approach aims to amplify the SERS signal of chemical or biological species of interest by applying a voltage onto the working electrode of an electrochemical cell [7]. The other direction commonly followed is the combination of SERS and EC, where dual detection via SERS and EC is pursued into a multimodal sensor which can provide complementary information about the analyte of interest [8]. In this manuscript we pursue the second direction, where we identify the analyte via SERS and quantitatively analyze it via EC.

SERS is a promising technique for sensing as it can significantly enhance Raman signals by utilizing plasmonic nanoparticles and nanostructures [9, 10]. The dominant mechanism responsible for SERS enhancement is considered to be electromagnetic enhancement [11], where the Raman scattered photons are significantly enhanced by the electromagnetic fields generated by Surface Plasmons (SPs) and Localized Surface Plasmons (LSPs) at the surface of the plasmonic substrates. SERS allows for highly sensitive structural detection of low-concentration analytes through the amplification of electromagnetic fields generated by the excitation of LSPs [12]. As a result, SERS shows great potential in sensing due to its high sensitivity, and the ability to measure unique spectra that are specific to the analyte of interest [13]. Metallic nanoparticles such as AgNPs or gold nanoparticles (AuNPs) serve as an attractive option for SERS substrates. They can enhance the local electric field, allowing for highly sensitive structural detection of low-concentration analytes, which thus overcomes the low sensitivity drawback of normal Raman spectroscopy [11, 12, 14]. Therefore, inexpensive materials and fabrication methods have a wide application in the development of SERS technique [15-17].

On the other side, EC emerges as a powerful tool that implements advanced electrode systems with the ability to measure the redox potentials of the analytes of interest. EC sensors directly

convert the reaction of biological/chemical molecules to electrical, providing a straightforward approach of detecting the target of interest [18]. One of the most commonly used EC techniques is Cyclic Voltammetry (CV), which applies a triangular voltage at a constant scan rate to the working electrode and then measures current vs. voltage. It is an analytical approach that offers quantitative information of the target analyte by analyzing the peak potential/current in CV responses. Different materials are reported to fabricate working electrodes for EC sensors, including metallic materials such as Au [19] and Ag [20, 21], as well as carbon materials such as graphene [22]. Metallic nanoparticles such as AgNPs have several advantages working as EC electrodes: (a) high conductivity due to faster electron transfer; (b) catalytic activity; and (c) immobilization for some biomolecules [23].

As mentioned above, SERS relies on the utilization of plasmonic substrates such as metallic nanostructure or nanoparticles that provide localized electromagnetic fields [14], while EC detection is performed on electrically conductive electrodes where an electric potential or current is applied to activate a redox reaction at the surface of the electrode, where the analyte is adsorbed [24].

Therefore, the development of substrates such as metallic nanoparticles with optical and electrical properties that allow for both EC and SERS sensing is significant. Recently, research has been focused on the development of dual functional substrates for SERS and EC sensing, such as Au nanostructured microarrays using polystyrene beads [8], Ag nanowires on coffee filter [25], and Au coated silicon nanowires [26]. In addition, for both SERS and EC detections, metallic nanoparticles also offer good biocompatibility, high surface-to-volume ratio, and unusual electrical and optical properties compared to the traditional bulk materials. Thus, in this work, AgNPs and gold are combined to fabricate the substrate for SERS and EC.

Chlorfenapyr, a broad-spectrum insecticide, has the appearance of a white/tan crystalline powder [27, 28]. It is commercially used to protect crops such as cotton, vegetables, and fruits from insects [29, 30]. Its main mechanism of action on the invasive species is by disrupting their ability to produce ATP which interferes with oxidative phosphorylation at the mitochondria and eventually leads to apoptosis. However, when humans are exposed to chlorfenapyr, it can cause significant medical problems that could lead to death in severe cases upon oral digestion [31], vapor exposure [32], and dermal exposure [33]. According to world health organization (WHO), the IPCS hazard classification of chlorfenapyr is moderately hazardous. Moreover, according to Regulation No.

1272/2008/EC, its EU classification is toxic and harmful. In addition, the residues of chlorfenapyr can cause pollution in the environment, and research shows that it can be dangerous to aquatic organisms [34].

Currently, standard methods for chlorfenapyr detection are based on high-performance liquid chromatography (HPLC) [30, 35] and gas chromatography–mass spectrometry (GC-MS) [36]. These methods offer high sensitivity and low limit of detection ranging from 0.5 ~ 1.05 ng/ml and mostly are measuring water samples. However, chromatography based techniques require expensive reagents and are time-consuming. The alternative is the development of (bio)sensors that reach similar performance but have lower costs and are easier to implement, and can be specifically engineered for a particular use case. There are only few articles describing these types of sensors. Shiro Miyake et al. reported a linear detection range of 2.5 -25 ng/mL via SPR [37] with a recovery rate of 90 – 112% in tomato samples, where an immunosensor is utilized with immobilized antibodies. In addition, a commercial enzyme-linked immunosorbent assay (ELISA) kit that utilizes monoclonal antibody has also been reported for chlorfenapyr detection in fruit samples [38]. A detection range from 0.05 to 1.5 ppm is reported and compared with GC-MS. Though these methods are low-cost compared to chromatography-based techniques, the requirement for monoclonal antibodies introduces a certain complexity for the assay. Moreover, additional incubation time is required for ELISA tests, which makes it time-consuming. Another reported technique for chlorfenapyr detection is via SERS on polyvinyl alcohol and cellulose film coated with silver nanoparticles [39], for which the reported limit of detection for chlorfenapyr is 1 ppm (1000 ng/mL). Compared to traditional techniques such as HPLC, the limit of detection via SERS is worse, but it benefits from simple sample preparation and operation, and fast measurement. However, in the reported work [39], no quantitative analysis is provided. On the other hand, to our knowledge, there are no reports describing chlorfenapyr detection via EC yet. Therefore, in this article we combine SERS, as a method to obtain molecular fingerprints, with EC that provides analytical capability for quantitative measurements of the concentration of chlorfenapyr in the concentration range typically found in food samples. These techniques therefore complement each other to allow for accurate detection of the analyte.

In this work, a sensing platform developed on a commercial metallic test strip that is composed of gold (Au) and palladium (Pd) with electrodeposition of AgNPs will be applied to the detection of the chlorfenapyr (**Figure 4.1**). The analyte of interest will be detected with our sensing system via

EC and SERS techniques. The sensing performance including the sensitivity and LOD will be studied. In addition, we prepared and tested a working electrode by drop casting AgNPs, which is a simpler and more cost-effective preparation procedure. The performance of this electrode is compared with that of the electrochemically-deposited electrode both in terms of EC and SERS characteristics.

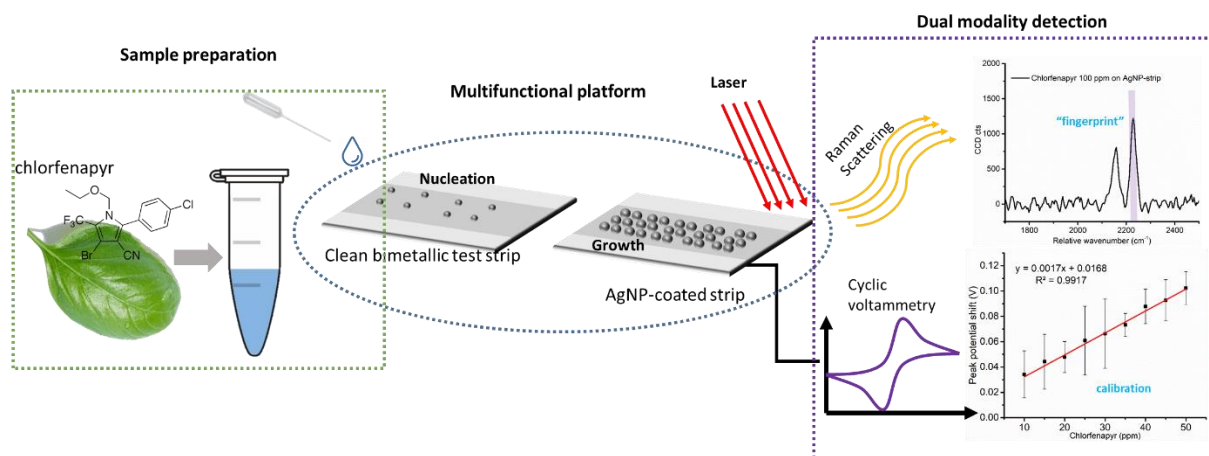


**Figure 4.1. Schematic representation of the dual detection of chlorfenapyr via EC and SERS on AgNP-coated test strips prepared by electrodeposition:** sample preparation of chlorfenapyr (left), fabrication of dual functional sensing platform based on bimetallic test strip, including the nucleation and growth of AgNPs during electrodeposition (middle), and dual detection of chlorfenapyr via SERS (identification) and EC (calibration).

### 4.3 Materials and methods

**Materials:** Silver nitrite, potassium nitrate, sodium citrate, potassium ferricyanide ( $K_3Fe(CN)_6$ ), Dimethyl sulfoxide (DMSO), and 4-ATP were purchased from Sigma-Aldrich. Chlorfenapyr was purchased from Toronto Research Chemicals Inc. (Toronto, Canada, Catalogue # C428500). They were used as received without any treatment. The commercial glucose test strips (Accu-chek aviva glucose test strip) were purchased from a local pharmacy.

**AgNP-strip prepared by electrodeposition:** The commercial glucose test strip was prepared following the procedure described in a previous report [17]. Briefly, to remove interferences from other substances on the surface before the deposition of AgNPs, the cover layer was physically removed with a blade, and then the enzyme for glucose oxidation was removed with ethanol and distilled water.

Electrodeposition was performed with a single-channel Potentiostat (BioLogic Science Instrument, SP-150, France) controlled by the EC-lab software installed on a PC. A typical 3-electrode system

was built directly on the test strip with three channels selected as the three electrodes (working electrode, counter electrode, and reference electrode). The electrolyte used for AgNPs deposition was a mixed solution including silver nitrate ( $\text{AgNO}_3$ , at a concentration of 10 mM) and potassium nitrate ( $\text{KNO}_3$ , at a concentration of 100 mM). 30  $\mu\text{L}$  of the mixed solution was dropped on the tip of the prepared test strip. Cyclic Voltammetry (CV) was performed prior to electrodeposition to confirm the critical potential that is needed to reduce  $\text{AgNO}_3$ . A constant voltage at -0.6V was applied for 30 seconds for electrodeposition of AgNPs. As expected, a dark layer on the surface of the working electrode was observed after the deposition of AgNPs.

**Synthesis of colloidal AgNPs:** colloidal silver nanoparticles used for drop casting were synthesized from silver nitrate based on the protocol reported by Lee and Meisel [35]. Briefly, 90 mg silver nitrite were dissolved in 500 mL water. The solution was then heated and stirred on hot plate at 300 °C with a speed of 300 rpm until it was boiled. Once boiled, 10 mL of 1% sodium citrate solution was added to the solution drop by drop. Colloidal AgNPs were then obtained after the solution was kept boiling for another 1h.

**AgNP-strip prepared by drop casting:** 1.0 mL of the colloidal AgNPs suspension was transferred to Eppendorf tubes, followed by centrifugation for 20 minutes at 8000 rpm. The supernatant in the tubes was then removed and discarded. The AgNPs remaining from all the Eppendorf tubes were collected into one tube and centrifuged again at 8000 rpm for 20 minutes to obtain a concentrated AgNP paste. The clean test strip was then coated with AgNPs by drop casting three layers of the concentrated AgNPs (2.5  $\mu\text{L}$  each layer) onto the surface using a micropipette. The test strip was left to dry completely in air between each deposition layer. Finally, to eliminate citrate on the surface of AgNPs, the coated test strip was immersed in 0.5 M KCl for 30 min and then washed with MilliQ water.

**SEM:** SEM images of AgNPs were obtained using a Carl Zeiss SEM instrument at high vacuum with an acceleration voltage of 10 kV to obtain information regarding the morphology of the nanobiocomposite strips and the aggregation status of the silver nanoparticles.

**Electrochemical measurement:** A single-channel Potentiostat (BioLogic Science Instrument, SP-150, France) was used to perform all the electrochemical measurements. It was connected to a computer with EC-lab software installed. A three-electrode system was set up with a reference electrode (Ag/AgCl), a counter electrode (Pt wire), and a working electrode (AgNP-coated test

strip or bare test strip that is cut from the whole test strip). Two cycles of CV were performed for all the measurements and the first cycle was analyzed. The limit of detection (LOD) was calculated by  $LOD = 3SD/S$ , where LOD is the limit of detection, SD is the standard deviation of blank measurement when there is no analyte, and S is the slope of the linear equation. For EC measurements of chlorfenapyr detection, chlorfenapyr samples at different concentrations were prepared by dissolving in DMSO and then mixed with the test probe potassium ferricyanide (5 mM) at a ratio of 1:1. In the absence of chlorfenapyr, DMSO was mixed directly with potassium ferricyanide under the same condition.

**Raman and SERS measurements:** SERS measurements were conducted on AgNP-coated test strips and Raman measurements were performed on the bare test strips without any deposition of AgNPs. Raman and SERS measurements were performed with a WITec Alpha300R Confocal Raman Microscope system equipped with a 633 nm laser (WITec, Germany) under laser power of approximately 1 mW at the sample. We are using a 10x magnification objective with a numerical aperture of 0.25, which yields a theoretical laser spot diameter of  $\sim 3 \mu\text{m}$ , corresponding to a power density at the sample of up to  $1.34 \times 10^7 \text{ mW/cm}^2$ . Chlorfenapyr prepared in DMSO was deposited by drop casting on the substrate and dried under vacuum. To achieve better signal, the deposition of samples was repeated several times after evaporation. For chlorfenapyr measurements via SERS, 3 spectra from different spots on the same substrate were recorded and averaged, and the standard deviation was obtained. In addition, the spectra were also smoothed by using Savitzky–Golay filters.

**Chlorfenapyr detection in vegetable samples:** the vegetable chive, was purchased from a local supermarket. They were first homogenized with a blender, followed by centrifugation. The supernatant was collected and used for the preparation of desired samples with a standard solution. The standard solution was prepared by mixing chlorfenapyr (in DMSO, 80 ppm), or DMSO (for control experiment), with potassium ferricyanide (1:1). Then, the standard solution was mixed with the pretreated supernatant of chive (1:1). The mixture was then used as the reconstituted vegetable sample with chlorfenapyr at a final concentration of 20 ppm.

## 4.4 Results and discussions

### 4.4.1 Fabrication and characterization of AgNP-coated test strip

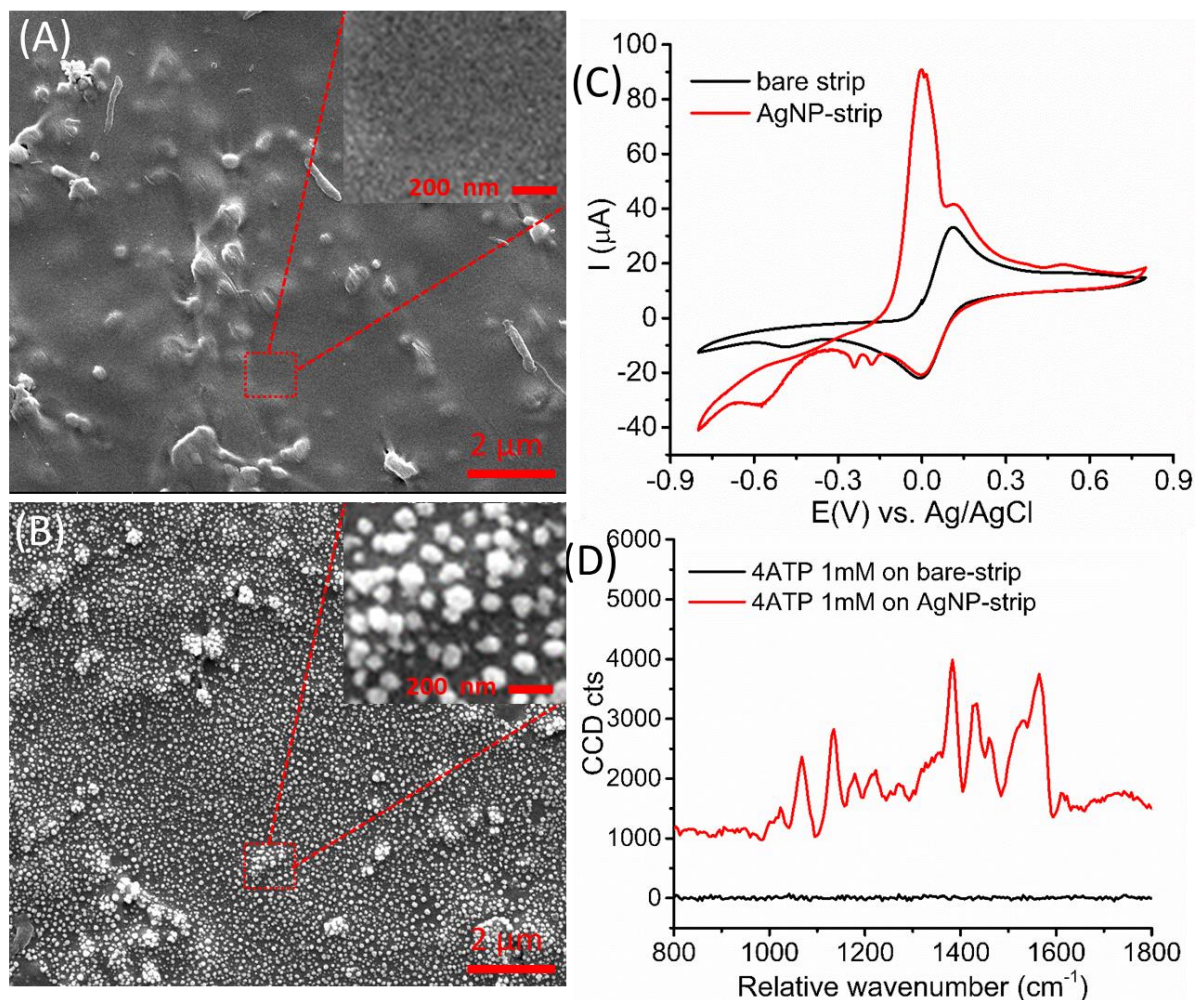


**Figure 4.2. Characterization of AgNP-strip via SEM and EC:** (A) SEM image of bare strip without AgNP deposition and (B) AgNP-strip after AgNP deposition, inset: enlarged image of the area indicated in red box. (C) CV curves of the bare strip and AgNP-strip in the response to potassium ferricyanide and (D) Raman spectra of the bare strip (black, 60s) and AgNP-strip in the presence of 4ATP (red, 10s).

The sensing platform was built on a commercial test strip as introduced before. Modifications with AgNPs were performed by electrodeposition. For this, an electrochemical 3-electrode system was formed on the test strip and then connected to a potentiostat. AgNPs were then grown directly on the substrate after applying a constant voltage of -0.6 V for 30 seconds. To observe the morphology of AgNPs electrodeposited on the surface of the test strip, SEM images were recorded (**Figure**

**4.2A-B**). The results show that most of the silver nanoparticles were successfully deposited with sizes ranging between 30 nm to 100 nm as compared to the unmodified test strip, of which the surface is relatively flat (**Figure 4.2A**).

#### 4.4.2 SERS performance

To study the performance of the substrates for SERS, 4-ATP, a typical test molecule used for SERS characterization, was prepared and then dropped on the AgNP-coated test strips. SERS spectra were then recorded from 4-ATP on the substrates. The experimental conditions (incident laser power, microscope objective) were the same for both SERS and Raman measurements. The results show that the signal from 4-ATP on AgNP-strips was significantly enhanced even at short integration time (**Figure 4.2D**). For Raman measurements, no signal from 4-ATP on the bare strip is observable when the same concentration and laser power are used. For the substrates coated with electrodeposited AgNPs, the signal from 4-ATP is strong and the peaks are well-defined. The results indicate that AgNPs deposited on the bare strip enhance the Raman signals significantly.

#### 4.4.3 EC performance

Potassium ferricyanide ( $\text{K}_3\text{Fe}(\text{CN})_6$ ) was used as a test molecule to evaluate the electroactivity of the AgNP-coated strip electrode prepared by electrodeposition. For this purpose, the supporting electrolyte for  $\text{K}_3\text{Fe}(\text{CN})_6$  of 5 mM was 0.1 M KCl. Meanwhile, the bare strip composed of Au and Pd was explored too as a control measurement. The results show that after modification with AgNPs, the strip electrode shows similar peaks corresponding to the redox reaction between ferricyanide ( $\text{Fe}(\text{CN})_6^{3-}$ ) and ferrocyanide ( $\text{Fe}(\text{CN})_6^{4-}$ ), regarding both peak potential and current (**Figure 4.2C**). In addition, the CV response of AgNP-coated test strip also shows additional peaks compared to the bare test strip. These peaks are caused by the oxidized AgNPs deposited on the strip surface.

#### 4.4.4 Chlorfenapyr detection via SERS

While there are no reports of chlorfenapyr detection via EC, there are so far very few reports of chlorfenapyr detection via SERS. To show the ability of the substrate fabricated here for chlorfenapyr detection via SERS, chlorfenapyr samples at different concentrations were placed on the AgNP-coated test strip. Previous research has shown that chlorfenapyr has a strong sharp peak

near  $1660\text{ cm}^{-1}$  corresponding to the C=C and C–N stretching bonds [39]. However, near this wavenumber range, we also observe additional interference peaks from the substrate, which makes it difficult to deconvolve the contribution from chlorfenapyr. On the other hand, another prominent Raman peak near  $2230\text{ cm}^{-1}$  can be used to distinctively identify chlorfenapyr [39], which has been reported to correspond to C≡N bond [41].

To demonstrate the ability of the electrodeposited AgNPs to exhibit SERS enhancement, a control experiment of chlorfenapyr detection on bare strip before the modification with AgNPs is conducted (**Figure 4.3A**). The results indicate that only in the presence of AgNPs chlorfenapyr can be detected, and the characteristic peak near  $2230\text{ cm}^{-1}$  can be observed. To exclude the interference of the background including the substrate and the solvent, which is DMSO, a background control measurement is also performed (**Figure 4.3B**) as well as the Raman measurement of chlorfenapyr powder on cover slip. The green band indicated in Figure 4B highlights the characteristic peak of chlorfenapyr for both SERS and Raman. In this region, there is no interference from the solvent, which simplifies the detection of chlorfenapyr via SERS on AgNP-coated strips.

More measurements with different concentrations of chlorfenapyr are then performed to estimate the limit of detection of this platform. As shown in **Figure 4.3C**, the characteristic peak near  $2230\text{ cm}^{-1}$  can still be detected when the concentration is 7 ppm and it is not detectable below 7 ppm (at 4 ppm), suggesting a 7 ppm limit of detection via SERS. The reproducibility is indicated using RSD as shown in the grey area. Moreover, a AgNP-coated strip prepared by drop casting is also explored for chlorfenapyr detection via SERS. As shown in **Figure 4.3D**, the characteristic peak near  $2230\text{ cm}^{-1}$  is still observed, indicating that chlorfenapyr is detectable via SERS on AgNP-coated strips prepared by both methods. In addition to the characteristic peak that corresponds to chlorfenapyr at  $2230\text{ cm}^{-1}$ , we observed another peak nearby at  $2155\text{ cm}^{-1}$ . This peak has also been observed from the substrate without any analytes, and it is therefore assigned to originate from the substrate.

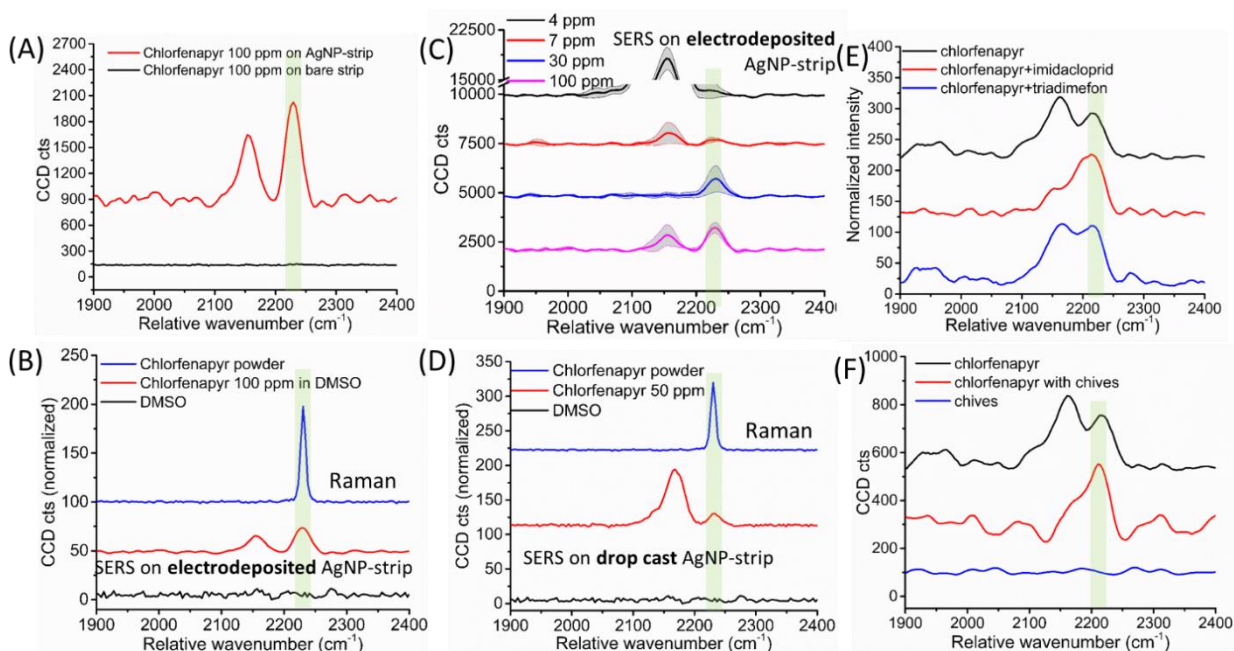


**Figure 4.3 Chlorfenapyr detection via SERS:** (A) Raman spectra of chlorfenapyr 100 ppm (3uLx3) on unmodified (bare strip, black) and modified (AgNP-strip, red) strips; integrations time: 300s. (B) SERS spectra of control sample (DMSO alone, black, 10s) and chlorfenapyr (in DMSO, red, 300s) on AgNP-strip and the Raman spectrum of chlorfenapyr powder on cover slip (blue, 60s). (C) SERS spectra of chlorfenapyr on AgNP-strip at different concentrations (in DMSO, 300s). (D) SERS spectra of control sample (DMSO alone, black, 10s) and chlorfenapyr (in DMSO, red, 10s) on AgNP-strip and the Raman spectrum of chlorfenapyr powder on cover slip (blue, 60s). (E) SERS spectra of chlorfenapyr (50 ppm) on AgNP-strip in the absence and presence of imidacloprid and triadimefon (2.5 ppm); integration time: 60s. (F) SERS spectra of chlorfenapyr in the absence and presence of chives on AgNP-strip; integration time: 60s.

The selectivity is then studied by using two different pesticides, imidacloprid and triadimefon as interference molecules since they have been reported to be used on chives and other plants [42]. 5 SERS spectra of chlorfenapyr are collected and averaged in the presence of imidacloprid and triadimefon (**Figure 4.3E**). Compared to SERS spectrum of chlorfenapyr alone, the characteristic peaks at 2230  $\text{cm}^{-1}$  are observed and not affected by the interference molecules. This result indicated good selectivity of the AgNP-strip for SERS measurements.

To explore the potential of the fabricated substrate for practical application, the ability for real sample analysis via SERS detection is evaluated. Chive is selected to prepare vegetable sample. Pretreated chive supernatant after centrifugation (14,000 rpm, 20 min) is spiked in 50 ppm chlorfenapyr solution at a ratio of 1:10 and dropped on the AgNP-coated strip for SERS detection. 3 spectra are collected and averaged. As shown in **Figure 4.3F**, the characteristic peak is still

observed in the presence of chives, indicating the ability of the substrate for real sample detection of chlorfenapyr via SERS.

Furthermore, the reproducibility of SERS measurements for chlorfenapyr detection is explored with respect to spot-to-spot and strip-to-strip variations. To evaluate the reproducibility of SERS measurements from different spots, SERS spectra at 10 different spots on the same AgNP-coated strip are recorded and analyzed. As shown in **Figure 4.4A**, the signal at the characteristic peak is highly stable and reproducible. To quantify spot-to-spot variability, the averaged SERS spectrum is calculated and presented with standard deviation (indicated in grey area, **Figure 4.4B**, **Figure 4.3C**). The RSD of intensity at the characteristic peak is calculated to be 17.6%, indicating good reproducibility of the substrate for SERS measurements. On the other side, to explore the reproducibility of SERS measurements for different strips, 8 AgNP-deposited strips are prepared and used to collect SERS spectra of chlorfenapyr. 10 spectra from different spots are collected and averaged for each strip. 8 averaged spectra are presented in **Figure 4.4C**. They are then averaged and presented with standard deviation (indicated in grey area, **Figure 4.4D**). The RSD of intensity at the characteristic peak is 30.3%.

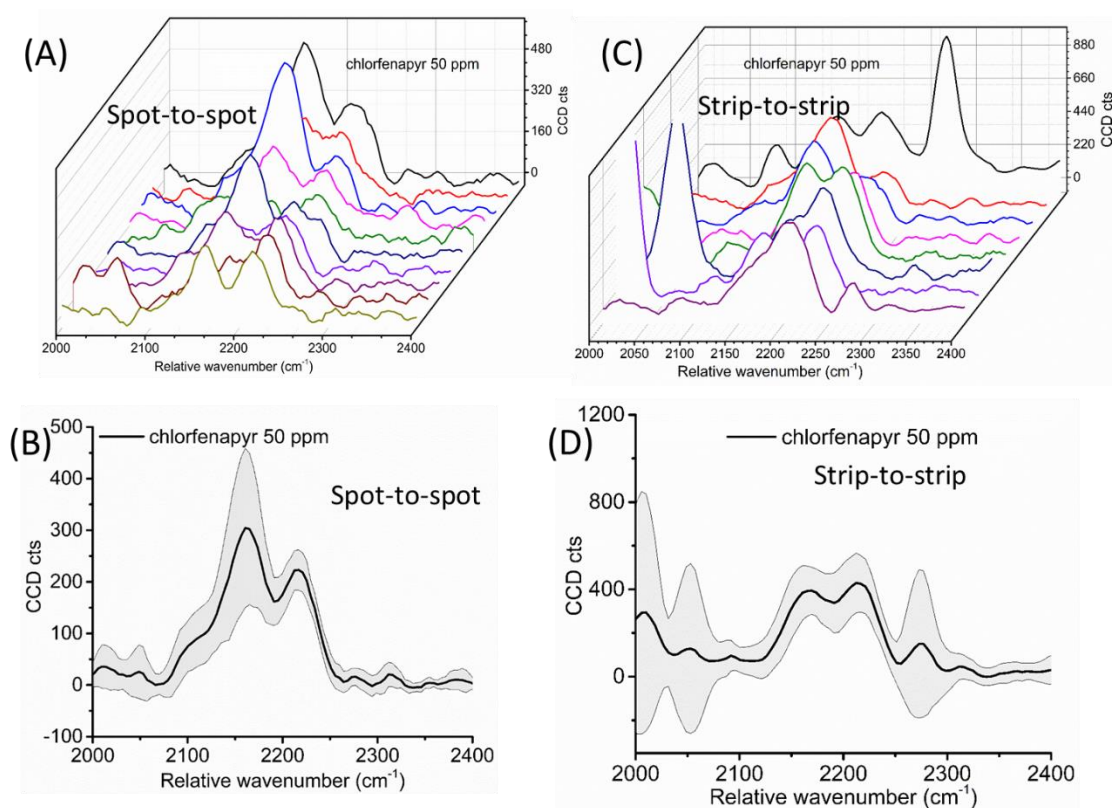


**Figure 4.4 Reproducibility of SERS measurements for chlorfenapyr on AgNP-coated strip:** (A) 10 SERS spectra of chlorfenapyr at 50 ppm from different spots on AgNP-strip; integrations time: 60s; (B) Averaged SERS spectra of 10 SERS spectra from different spots with standard deviation. (C) 8 averaged SERS spectra (of 10 spots) of chlorfenapyr at 50 ppm on different AgNP-strips; integration time: 60s; (D) Averaged SERS spectra of 8 SERS spectra from different strips with standard deviation.

#### 4.4.5 Chlorfenapyr detection via EC

So far, there are no reports on detection of chlorfenapyr using EC. In order to make this measurement possible, a commercial glucose test strip has been modified as described earlier. In addition, potassium ferricyanide was used as a probe, and was mixed with chlorfenapyr dissolved in DMSO. As shown in **Figure 4.5**, CV measurements of chlorfenapyr at different concentrations from 20-50 ppm in DMSO mixed with potassium ferricyanide are conducted on both bare strip electrode and AgNP-coated strip electrodes prepared by both electrodeposition and drop casting. A scanning range of potential from -0.8 V to 1 V is applied.

On the bare strip electrode without AgNPs, which served as a control experiment, the recorded currents are low and no well-defined peaks in the forward scanning range are observed (**Figure 4.5A**), indicating that the unmodified strip is not working for chlorfenapyr detection via CV. However, when the measurements are performed on AgNP-coated strips the results are very different. First, in the case the substrate was prepared via drop cast of AgNP on the strip, higher currents compared to the bare strip are observed, but no well-defined characteristic peaks (**Figure 4.5B**), which suggests that the drop cast AgNP-strip is not able to detect chlorfenapyr via EC. Second,

when the substrate was prepared via electrodeposition of AgNP on the working electrode, redox peaks are observed in CV curves (**Figure 4.5C**). Moreover, the oxidation peaks in the forward scanning in the presence of chlorfenapyr are shifted compared to peaks collected in the absence of chlorfenapyr. With the increase of chlorfenapyr concentration, the peak potential shifts towards lower potentials and the value of the shift is proportional to the concentration (**Figure 4.5D**). The possible explanation of this result is that chlorfenapyr is a relatively large molecule (MW: 407.61 g/mol), hence it hinders the diffusion of the probe molecule (ferricyanide) during the charging current-controlled regime at the interface of the electrode. As a result, the concentration of the test probe in the close vicinity of the electrode will be depleted earlier, but not enough test ions are supplemented since their movement towards the interface is hindered by the presence of

chlorfenapyr. The reaction reaches the diffusion-controlled regime faster, resulting in a shift of the peak potential towards smaller values.

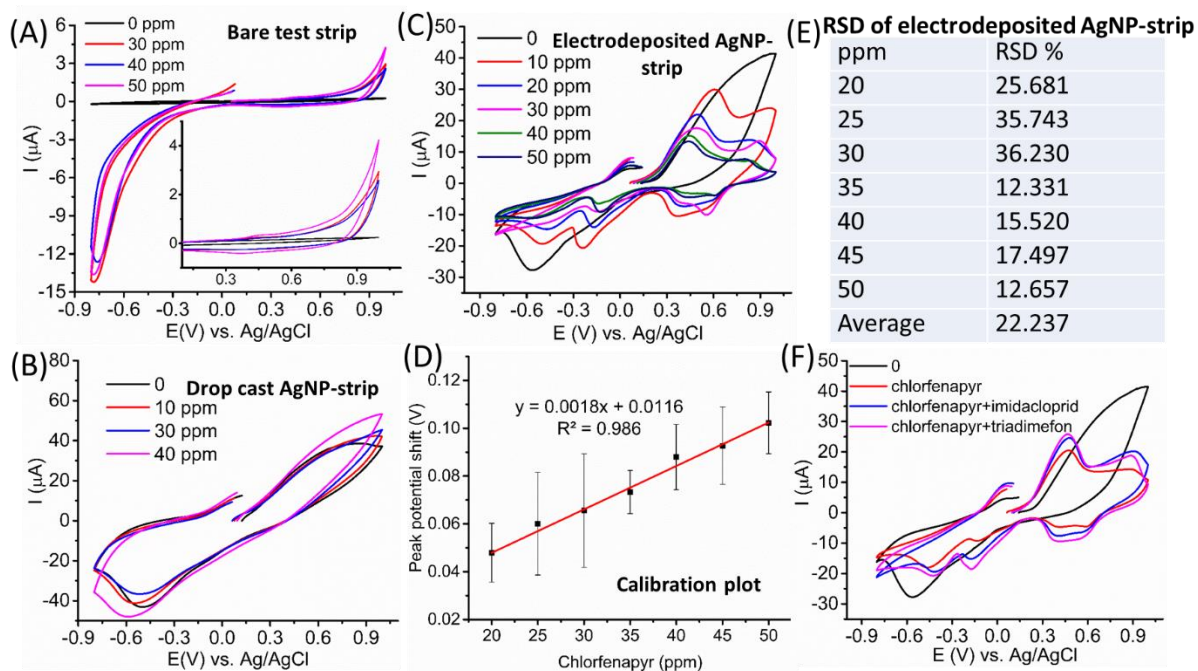


**Figure 4.5 Chlorfenapyr detection on AgNP-strip via EC:** (A) CV curves of chlorfenapyr on bare strips. (B) CV curves of the drop cast AgNP-strip in the absence and presence of chlorfenapyr at different concentrations. (C) CV curves of the electrodeposited AgNP-strip in the absence and presence of chlorfenapyr at different concentrations, scan rate: 50 mV/s. (D) the relation of the potential shift in the presence of chlorfenapyr compared to the blank measurement versus the concentration of chlorfenapyr detected on electrodeposited AgNP-strip. (E) Relative standard deviation of the peak potential shifts on different substrates ( $n=3\sim7$ ) for chlorfenapyr detection at different concentrations. (F) CV curves of the electrodeposited AgNP-strip in the absence and presence of chlorfenapyr, in the presence of imidacloprid and triadimefon with chlorfenapyr at 20 ppm.

Further, to explore the sensitivity and limit of detection (LOD) of the AgNP-coated substrate for chlorfenapyr detection, the peak potential shifts at different concentrations, relative to the solvent alone mixed with probe molecule, are analyzed. 3~7 substrates are used for the measurement of each concentration, the relationship between the peak potential shifts and the concentration as a calibration plot is obtained. The result (Figure 4.5D) shows good linearity and correlation coefficient (0.986), and the limit of detection (LOD) for chlorfenapyr detection via EC on the AgNP-coated strip is calculated to be 4.2 ppm. Compared to other techniques (Table 4.1), the linear detection range and the LOD are within a higher concentration range. However, they are

within acceptable ranges for specific use cases such as the detection of pesticide in vegetables for food quality control. Our platform and reported technique show advantages of simple sample preparation, rapid detection, and high sensitivity within demanded concentration range. In addition, the low cost and ease-of-fabrication makes the substrate a good candidate for point-of-need applications.

**Table 4.1 Chlorfenapyr detection using various techniques**

<b>technique</b>	<b>Linear detection range</b>	<b>LOD</b>	<b>Pre-preparation</b>	<b>Real sample analysis</b>	<b>Ref</b>
HPLC	$5 \times 10^{-4}$ - 0.4 ppm	$4 \times 10^{-4}$ ppm	Dispersive micro-solid phase extraction	Environmental water	[30]
HPLC	$2 \times 10^{-3}$ - 0.1 ppm	$1 \times 10^{-3}$ ppm	ionic liquid dispersive liquid-liquid microextraction	Environmental water	[35]
GC- $\mu$ ECD*	0.025 – 2 ppm	0.0015 mg/Kg	High temperature required	Leek	[43]
SPR	$2.5 \times 10^{-3}$ – 0.025 ppm	-	Anti-chlorfenapyr monoclonal antibody required	Tomato	[47]
ELISA	0.05 to 1.5 $\mu$ g/g	0.1 ng/g	Anti-chlorfenapyr monoclonal antibody required	Apple	[38]
SERS	-	1 ppm	-	-	[39]

EC-SERS	20 - 50ppm	4.2 ppm	-	Chive	Thi s wor k
---------	------------	---------	---	-------	----------------------

\*GC- $\mu$ ECD: Gas chromatography with microelectron-capture detection

Moreover, to evaluate the reproducibility of the substrates, the relative standard deviations for the measurements of chlorfenapyr on different substrates for each concentration are calculated to be between 12% and 36% (**Figure 4.5E**). The average is ~ 22%, which is close to the acceptable RSD value of 20% according to European Directorate General for Health and Food Safety (DG-SANTE) guidelines [44]. In addition, it is noticeable that with the increase of the concentration of chlorfenapyr, RSD is decreasing. When the detected concentration is above 30 ppm, the RSDs are below 20%, indicating that the results are more reliable. Considering the tolerance concentration of chlorfenapyr residues in vegetables, our proposed approach provides value for practical applications, since concentrations above the limit of tolerance concentration can be detected with high reliability.

Finally, to evaluate the selectivity of the substrate for chlorfenapyr detection, two different pesticides, imidacloprid and triadimefon, are used as interference molecules since they have been reported to be used on chives and other plants [45]. Chlorfenapyr at 20 ppm is detected in the presence of these two pesticides respectively and the peak potential shifts are then compared with the results obtained from chlorfenapyr detection in the absence of interference molecules under same experimental conditions. As shown in **Figure 4.5F**, though the currents are not exactly the same, the peak potential is not affected by the existence of the interference pesticides. The coefficients of variation are 2.20% (n=3) and 1.19% (n=3) for imidacloprid and triadimefon, respectively. The results indicate that the presence of other pesticides will not affect the measurements of the fabricated AgNP-coated test strip for the detection of chlorfenapyr.

#### 4.4.6 Chlorfenapyr detection in vegetable sample with chive solution

We demonstrated so far that chlorfenapyr can be detected via EC using the electrodeposited AgNP strip electrode. Next, we investigate the potential of the substrate for applications in food safety. Similarly to SERS detection, chive is used as a vegetable sample. According to the US Code of Federal Regulations (#180.513), the tolerance residue of chlorfenapyr in chives is 20 ppm. Hence, reconstituted sample containing the supernatant of chive and chlorfenapyr at 20 ppm, which is the tolerance concentration, was prepared and detected via EC, followed by the calculation of the recovery rate.

To achieve this, samples with a standard solution of chlorfenapyr/DMSO and potassium ferricyanide are prepared and mixed with the real vegetable solution of chive at a ratio of 1:1. The CV responses were collected and the shift of electrochemical potential in the presence of chlorfenapyr at 20 ppm were analyzed. The recovery rate was calculated and presented in **Table 4.2**. The result demonstrates a recovery rate of chlorfenapyr in chive of approximately 98%, which is acceptable.

**Table 4.2 chlorfenapyr detection in vegetable samples**

chlorfenapyr added in <b>chive</b> supernatant (ppm)	20
Total found (ppm)	19.58
RSD (n=6) %	30.5
Recovery %	97.9

#### 4.5 Conclusions

Chlorfenapyr is a pesticide that can be harmful when ingested and it is important to develop analytical technologies that allow for quantitative and sensitive detection via portable and low-cost approaches. Previously, it has been demonstrated that SERS can be used for its detection at concentrations as low as 1 ppm. However, SERS alone is not able to provide reliable quantitative measurements, and therefore combinations with other, more quantitative methods, such as EC, are needed. In this work, we designed and fabricated a sensing platform that is prepared by electrodepositing AgNPs on a commercial bimetallic test strip. The platform is portable, inexpensive and was demonstrated to work for the detection of chlorfenapyr via both SERS and

EC. The AgNP-deposited strip is first characterized by SEM and evaluated for its SERS and EC performance before being used for chlorfenapyr detection. Then, chlorfenapyr is detected via both EC and SERS on the electrodeposited AgNP-strip. For comparison, AgNP-strips fabricated by drop casting colloidal AgNPs were also explored for chlorfenapyr detection via both methods. To further evaluate the sensing performance of the electrodeposited AgNP-coated strip substrate, a reference substrate prepared by drop casting AgNPs on the test strip is also used to perform EC and SERS measurements for chlorfenapyr detection. While both substrates perform similarly for SERS (with LOD in the 7 ppm range), the drop cast AgNP-strip is not able to detect chlorfenapyr using EC. On the other hand, AgNP-coated strips prepared by electrodeposition exhibit good EC performance, with a LOD on the order of 4.2 ppm with a linear range from 20-50 ppm. It fulfills the demand for the detection of chlorfenapyr residue in vegetables such as chive, since its tolerance concentration for chlorfenapyr residue, according to the US Code of Federal Regulations, is within this linear detection range of the substrate. On the other side, the average RSD for EC measurements of chlorfenapyr detection is ~ 22%, which is close to 20% that is acceptable according to European Directorate General for Health and Food Safety (DG-SANTE) guidelines, indicating its reproducibility. Therefore, considering the purpose of dual function detection, AgNP-coated strips prepared by electrodeposition show better balance for both detection methods, which not only offer complementary and more reliable results but also a more promising potential for practical applications.

The combination of the two methods demonstrates the ability of the substrate working as a multifunctional biosensing platform for chlorfenapyr detection. The characteristic peak at 2230  $\text{cm}^{-1}$  that corresponds to  $\text{C} \equiv \text{N}$  group provides the unique ability to identify the analyte. Complementarily, EC is a more quantitative technique that offers analytical measurements for chlorfenapyr, but without the specificity provided by SERS. A combination of both allows us to uniquely identify the analyte (via SERS) and measure its concentration (via EC).

In conclusion, we report a new metallic substrate that uses EC-deposited AgNPs on a commercial modified glucose test strip to provide quantitative measurements of chlorfenapyr via both SERS and EC methodologies and could be used to test food contamination. While SERS measurements of chlorfenapyr have been reported previously, this is the first time that EC detection is reported. In addition, we demonstrate that a combination of EC and SERS can be used to improve the sensitivity and specificity of the measurement. Compared to the traditional methods typically used

in centralized laboratories, this multimodal sensor that uses SERS and EC has the potential to detect and quantitatively measure chlorfenapyr at the point-of-need, paving the way towards cost effective and precise quality control of this analyte in the food industry.

#### **4.6 Author contributions**

JL contributed to the design of the experiments, performed the experiments, data analysis, and wrote the manuscript. RSM contributed to the design of the experiments and data analysis. SM provided feedback on the experiments. FV contributed to the use case and provided the samples. SWH contributed to the design, data analysis, writing of the manuscript, and overall supervised and managed the project. All authors reviewed and provided feedback to the manuscript and approved it for publication.

#### **4.7 Conflict of interest**

The authors declare that the research was conducted in the absence of any commercial or financial relationships that could be construed as a potential conflict of interest.

#### **4.8 Acknowledgements**

This work was financially supported by the National Sciences and Engineering Research Council of Canada (NSERC), Discovery Grant RGPIN-2018-05675 (to S.W.-H.), and G247765 and G248584 (to S.M.). The authors also thank the Faculty of Engineering at McGill University. J.L. acknowledge the McGill Engineering Doctoral Award (MEDA).

## 4.9 References

1. Zong, X., R. Zhu, and X. Guo, *Nanostructured gold microelectrodes for SERS and EIS measurements by incorporating ZnO nanorod growth with electroplating*. Scientific Reports, 2015. **5**(1): p. 16454.
2. Ilkhani, H., et al., *Nanostructured SERS-electrochemical biosensors for testing of anticancer drug interactions with DNA*. Biosensors and Bioelectronics, 2016. **80**: p. 257-264.
3. Bailey, M.R., R.S. Martin, and Z.D. Schultz, *Role of Surface Adsorption in the Surface-Enhanced Raman Scattering and Electrochemical Detection of Neurotransmitters*. The Journal of Physical Chemistry C, 2016. **120**(37): p. 20624-20633.
4. Sanger, K., et al., *Large-Scale, Lithography-Free Production of Transparent Nanostructured Surface for Dual-Functional Electrochemical and SERS Sensing*. ACS Sensors, 2017. **2**(12): p. 1869-1875.
5. Jeanmaire, D.L. and R.P. Van Duyne, *Surface raman spectroelectrochemistry: Part I. Heterocyclic, aromatic, and aliphatic amines adsorbed on the anodized silver electrode*. Journal of Electroanalytical Chemistry and Interfacial Electrochemistry, 1977. **84**(1): p. 1-20.
6. Fleischmann, M., P.J. Hendra, and A.J. McQuillan, *Raman spectra of pyridine adsorbed at a silver electrode*. Chemical Physics Letters, 1974. **26**(2): p. 163-166.
7. Abdelsalam, M.E., et al., *Electrochemical SERS at a structured gold surface*. Electrochemistry Communications, 2005. **7**(7): p. 740-744.
8. Kayran, Y.U., D. Jambrec, and W. Schuhmann, *Nanostructured DNA Microarrays for Dual SERS and Electrochemical Read-out*. Electroanalysis, 2019. **31**(2): p. 267-272.
9. Zheng, J. and L. He, *Surface-Enhanced Raman Spectroscopy for the Chemical Analysis of Food*. Comprehensive reviews in food science and food safety, 2014. **13**(3): p. 317-328.
10. Bantz, K.C., et al., *Recent progress in SERS biosensing*. Physical Chemistry Chemical Physics, 2011. **13**(24): p. 11551-11567.
11. Kahraman, M., et al., *Fundamentals and applications of SERS-based bioanalytical sensing*. Nanophotonics, 2017. **6**(5): p. 831-852.
12. Sharma, B., et al., *SERS: materials, applications, and the future*. Materials today, 2012. **15**(1): p. 16-25.
13. Suarasan, S., et al., *Superhydrophobic bowl-like SERS substrates patterned from CMOS sensors for extracellular vesicle characterization*. Journal of Materials Chemistry B, 2020. **8**(38): p. 8845-8852.
14. Liu, J., et al., *Are plasmonic optical biosensors ready for use in point-of-need applications?* Analyst, 2020. **145**(2): p. 364-384.

15. Avella-Oliver, M., et al., *Label-free SERS analysis of proteins and exosomes with large-scale substrates from recordable compact disks*. Sensors and Actuators B: Chemical, 2017. **252**: p. 657-662.
16. Kahraman, M., et al., *Fabrication and characterization of flexible and tunable plasmonic nanostructures*. Scientific reports, 2013. **3**: p. 3396.
17. Korkmaz, A., et al., *Inexpensive and Flexible SERS Substrates on Adhesive Tape Based on Biosilica Plasmonic Nanocomposites*. ACS Applied Nano Materials, 2018. **1**(9): p. 5316-5326.
18. Grieshaber, D., et al., *Electrochemical biosensors-sensor principles and architectures*. Sensors, 2008. **8**(3): p. 1400-1458.
19. Jalali, M., et al., *Microscale reactor embedded with Graphene/hierarchical gold nanostructures for electrochemical sensing: application to the determination of dopamine*. Microchimica Acta, 2020. **187**(1): p. 90.
20. Chen, L., H. Xie, and J. Li, *Electrochemical glucose biosensor based on silver nanoparticles/multiwalled carbon nanotubes modified electrode*. Journal of Solid State Electrochemistry, 2012. **16**(10): p. 3323-3329.
21. Liu, J., et al., *An AgNP-deposited commercial electrochemistry test strip as a platform for urea detection*. Scientific Reports, 2020. **10**(1): p. 9527.
22. Siavash Moakhar, R., et al., *A Nanostructured Gold/Graphene Microfluidic Device for Direct and Plasmonic-Assisted Impedimetric Detection of Bacteria*. ACS Applied Materials & Interfaces, 2020. **12**(20): p. 23298-23310.
23. Luo, X., et al., *Application of nanoparticles in electrochemical sensors and biosensors*. Electroanalysis, 2006. **18**(4): p. 319-326.
24. Zoski, C.G., *Handbook of electrochemistry*. 2006: Elsevier.
25. Chen, Y.-C., et al., *Silver nanowires on coffee filter as dual-sensing functionality for efficient and low-cost SERS substrate and electrochemical detection*. Sensors and Actuators B: Chemical, 2017. **245**: p. 189-195.
26. Convertino, A., V. Mussi, and L. Maiolo, *Disordered array of Au covered Silicon nanowires for SERS biosensing combined with electrochemical detection*. Scientific Reports, 2016. **6**(1): p. 25099.
27. Mascarenhas, R.N. and D.J. Boethel, *Responses of Field-Collected Strains of Soybean Looper (Lepidoptera: Noctuidae) to Selected Insecticides Using an Artificial Diet Overlay Bioassay*. Journal of Economic Entomology, 1997. **90**(5): p. 1117-1124.
28. Cao, Y., et al., *Photocatalytic degradation of chlorfenapyr in aqueous suspension of TiO<sub>2</sub>*. Journal of Molecular Catalysis A: Chemical, 2005. **233**(1): p. 61-66.

29. Raghavendra, K., et al., *Chlorfenapyr: a new insecticide with novel mode of action can control pyrethroid resistant malaria vectors*. Malaria journal, 2011. **10**: p. 16-16.
30. Peng, B., et al., *Dispersive micro-solid phase extraction based on self-assembling, ionic liquid-coated magnetic particles for the determination of clofentezine and chlorfenapyr in environmental water samples*. Analyst, 2013. **138**(22): p. 6834-6843.
31. Kang, C., et al., *A patient fatality following the ingestion of a small amount of chlorfenapyr*. 2014. **7**(3): p. 239-241.
32. Hoshiko, M., et al., *[Case report of acute death on the 7th day due to exposure to the vapor of the insecticide chlorfenapyr]*. Chudoku kenkyu : Chudoku Kenkyukai jun kikanshi = The Japanese journal of toxicology, 2007. **20**(2): p. 131-136.
33. Han, S.-K., et al., *A fatal case of chlorfenapyr poisoning following dermal exposure*. Hong Kong Journal of Emergency Medicine, 2018. **26**(6): p. 375-378.
34. Wu, Y. and Z. Zhou, *Application of liquid-phase microextraction and gas chromatography to the determination of chlorfenapyr in water samples*. Microchimica Acta, 2008. **162**(1): p. 161-165.
35. Liu, Y., et al., *Determination of four heterocyclic insecticides by ionic liquid dispersive liquid-liquid microextraction in water samples*. Journal of Chromatography A, 2009. **1216**(6): p. 885-891.
36. Mamun, M.I.R., et al., *Development and validation of a multiresidue method for determination of 82 pesticides in water using GC*. Journal of Separation Science, 2009. **32**(4): p. 559-574.
37. Miyake, S., et al., *Simultaneous Detection of Six Different Types of Pesticides by an Immunosensor Based on Surface Plasmon Resonance*. Anal Sci, 2020. **36**(3): p. 335-340.
38. Watanabe, E., et al., *Evaluation of a commercial immunoassay for the detection of chlorfenapyr in agricultural samples by comparison with gas chromatography and mass spectrometric detection*. Journal of Chromatography A, 2005. **1074**(1): p. 145-153.
39. Nguyen Thi, H., et al., *Fabrication process and characterization of AgNPs/PVA/cellulose as a SERS platform for in-situ detection of residual pesticides in fruit*. Materials Research Express, 2020. **7**(3): p. 035019.
40. Lee, P.C. and D. Meisel, *Adsorption and surface-enhanced Raman of dyes on silver and gold sols*. The Journal of Physical Chemistry, 1982. **86**(17): p. 3391-3395.
41. Mojica, E.-R.E., et al., *Solvent Sensitivity of the  $-C\equiv N$  Group: A Raman Spectroscopic Study*, in *Raman Spectroscopy in the Undergraduate Curriculum*. 2018, American Chemical Society. p. 181-197.
42. Yan, X., G. Zhao, and R. Han, *Integrated Management of Chive Gnats (*Bradysia odoriphaga* Yang & Zhang) in Chives Using Entomopathogenic Nematodes and Low-Toxicity Insecticides*. Insects, 2019. **10**(6).

43. Rahman, M.M., et al., *Determination of chlorfenapyr in leek grown under greenhouse conditions with GC- $\mu$ ECD and confirmation by mass spectrometry*. Biomedical Chromatography, 2012. **26**(2): p. 172-177.
44. Nguyen, T.T., et al., *Fate of Residual Pesticides in Fruit and Vegetable Waste (FVW) Processing*. Foods, 2020. **9**(10).

## Chapter V: Discussion

Sensors are powerful tools for medical diagnosis and food safety, both of which play important roles in human health. Particularly, the development of sensors at PON is attracting more and more attention since it enables the use of sensing devices in real life applications. However, it is still a challenge to develop sensors for PON applications, especially considering that many factors need to be considered for the design and implementation of the sensors. Therefore, to address these problems, in this thesis, a novel analytical biosensor is proposed and fabricated for PON applications. The developed sensing platform is explored for different applications with different analytes. Further, to evaluate its potential for the use in practical applications, detection of analytes in real samples are also performed.

As discussed in previous chapters, apart from the sensing performance that are used to justify the sensors, design parameters such as cost and ease-of-fabrication are crucial for the development of PON sensors as well. Moreover, the detection methods also play vital roles since their working mechanism and configuration directly determine if the sensitivity or specificity are achievable and if the experimental setup is suitable for PON applications. Therefore, in this chapter, these problems are discussed following the order of the development of the sensor. It is started with the fabrication of the sensing substrate. Specifically, the optimization of the biosensing platform is discussed, including the selection of the materials, the exploration of the parameters used for electrodeposition, and the evaluation of EC and SERS performance. Then, the detection methods used here, i.e., EC and SERS, are discussed. In the end, the applications to different analytes detection using this platform are also discussed and compared for justification.

### 5.1 Optimization of the biosensing platform

In **chapter II**, the importance of multiple design considerations for the development of PON sensors. Ease-of-fabrication and low cost are two of these design considerations. Therefore, in **chapter III and chapter IV**, a multifunctional sensing substrate is designed and fabricated using inexpensive materials with a simple approach. Specifically, the commercial glucose test strip composed of a plastic substrate and bimetallic channels (Au and Pd) that are manufactured on the plastic substrate. The bimetallic channels are working as electrodes. To further coat the working electrode/substrate, electrodeposition is used since it is simple. The parameters used for

electrodeposition will decide the morphology, distribution, and size of AgNPs grown on the substrate/electrode. In order to optimize deposition of AgNPs, different electrodeposition parameters are explored. Finally, the optimized AgNP-coated test strip is characterized with test molecules to evaluate its SERS and EC performance.

### 5.1.1 Selection and characterization of the commercial glucose test strip

The selection of inexpensive materials with portability is imperative to build the multifunctional sensing system for PON applications. To address this point, a cheap commercial glucose test strip with conductive channels is utilized to build the support substrate. The working principle, morphological characterization, and how they are beneficial for the establishment of the proposed sensor are discussed here.



**Figure 5.1 Components of Accu-chek aviva test strips:** Photograph of the unmodified test strip before (left) and after (right) peeling off the protecting cover and removing the enzyme (middle)

The test strip is part of the Accu-Chek Aviva system that is used for glucose monitoring. The Accu-Chek Aviva system includes a glucose meter and test strips, which are the strips that are used here. This commercially available system is a EC-based sensing device for glucose monitoring. Accu-Chek Aviva meter is a reliable, sensitive, and user-friendly product that can work in a linear detection range from 0.6 to 33.3 mM for glucose detection in blood sample. A

rapid response time of only a few seconds and a small sample volume down to 0.6  $\mu\text{l}$  are needed for glucose detection using Accu-Chek Aviva meter [119].

The working mechanism is based on enzymatic sensing of glucose oxidation in blood sample on the working electrode. The enzyme used for glucose oxidation is mutant variant of quinoprotein glucose dehydrogenase (Mut. Q-GDH) that is deposited on the exposed sensing area (the yellow area shown in **Figure 5.1**, left), where the blood sample will be dropped on for measurements. As shown in **Figure 5.1 (right)**, the Aviva test strips are composed of several bimetallic channels that are working as electrodes in the EC measuring system with two ends exposed, one of which is the sensing area and the other one is to be connected later with the adapted potentiostat as the glucose meter. During measurements, the sample is dropped on the sensing area [119]. It is then inserted in the glucose meter by the other end, via which a small DC signal is applied and response signal is then collected.

The selected commercial test strip is then characterized with SEM along with EDS to show the morphology and composition of the deposited conductive channels that work as electrodes. As shown in **Figure 5.2**, the channels are composed of Au and Pd and the distribution of each component is confirmed as well (**Figure 5.2B**).

This commercial test strip is built as a EC biosensor for glucose detection. As a commercial product, it offers good portability, stability, and high sensitivity, which unsurprisingly makes it a good choice for EC detection in this work. To make it more specific towards other analytes and make it also work for SERS detection, modification such as the removal of glucose oxidase and the deposition of AgNPs are performed. Moreover, as shown in **Figure 5.2**, this commercial glucose test strip consists of bimetallic Au-Pd channels that offer good electrical conductivity and electrochemical reactivity for EC. Additionally, the conductive layer also makes further electrodeposition possible and simple since electrodeposition has to be performed by applying potential or current on a working electrode in a complete circuit. Therefore, in summary, this glucose test strip is an ideal substrate to build the sensing system for PON sensors due to its existing configuration and low cost.

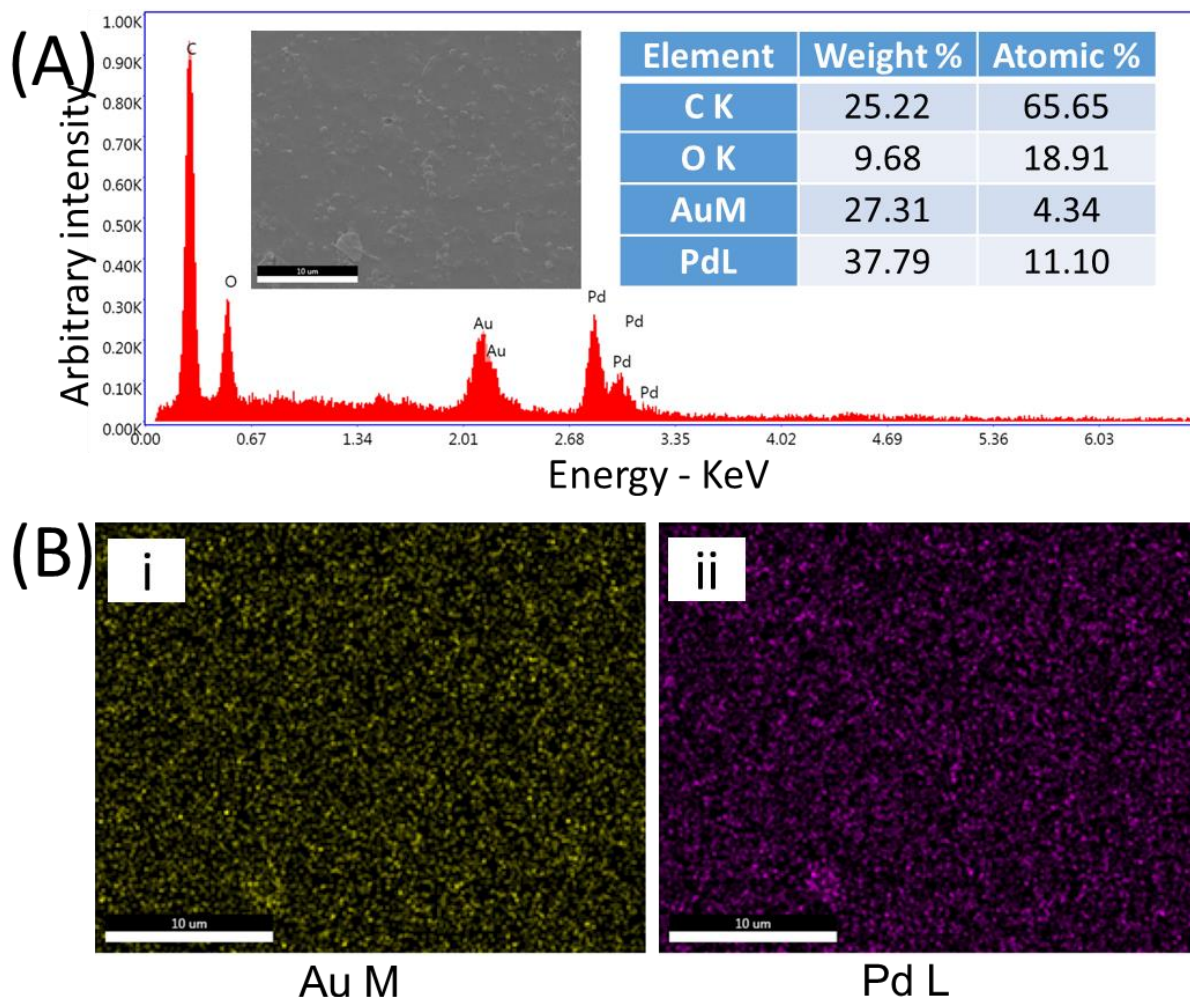


**Figure 5.2 Morphology and elemental characterization of bare strip:** EDS spectrum (A) and EDS mapping (B) of bare commercial glucose test strip.

### 5.1.2 Optimization of parameters used for the electrodeposition of AgNPs

As discussed before, in order to make the selected glucose test strip more specific for other analytes, as well as to make it work for SERS, AgNPs are functionalized on the working electrode of the test strip. Approaches used for deposition of AgNPs are important since they are related with the complexity of fabrication as well as the cost, which are the design considerations that need to be taken account into for developing PON sensors. On the other side, various parameters such as morphology, shape, size, and the distribution of the nanoparticles play important roles in SERS and EC performances since the electrical properties and the plasmonic properties such as the

resonance frequency and the electromagnetic field are related to these factors [120, 121]. Consequently, to achieve improved SERS and EC performance, it is important to explore parameters used for deposition that will affect the abovementioned factors. Therefore, in this section, the deposition methods and the optimization of the deposition parameters are discussed.

Depending on the needs for different applications, various techniques can be considered for the fabrication. Chemical reduction published by Lee and Meisel [122] is one of the most commonly used methods to synthesize AgNPs due to its simplicity and high reproducibility. It can be later used for drop casting modification of AgNPs on the strip, which provides an easy and inexpensive way for coating substrates. It has been reported a lot for AgNP deposition on all kinds of substrates [123-125].

Electrodeposition is another simple technique that combines AgNP synthesis and deposition. It is performed in this work to directly grow AgNPs on the test strip. Based on different conditions applied for electrodeposition, they can be classified into 3 types: constant voltage, pulse electrodeposition, and cyclic voltammetry based. Pulse electrodeposition has been widely explored for AgNP deposition and the size, morphology as well as the distribution can be adjusted by manipulating parameters of the applied pulse such as the amplitude and the frequency, etc.. Pulse electrodeposition is a special kind of electrodeposition that reduces silver salt (the electrolyte) by applying electric energy, i.e., voltage or current on the electrode, followed by the process of nucleation and then growth of metallic nanoparticles of interest [126]. Compared to regular electrodeposition with constant current or voltage, pulse electrodeposition limits the growth of nanoparticles into a certain size by limiting the time for growing stage [127]. As a result, the formation of the nanoparticles can be more controllable, which then affects SERS performance.

In addition to pulse electrodeposition, applying constant voltage or CV is also used frequently as electrodeposition techniques due to their simplicity. Especially when applying a constant voltage to electrochemically deposit metallic nanoparticles, only two key parameters, the value of the voltage and the duration time, are affecting the deposition of nanoparticles. By exploring these two parameters, the deposition protocol can be optimized easily. Compared to pulse electrodeposition, it is more straightforward. Therefore, in this work, a constant voltage is applied for electrodeposition for a certain time to deposit AgNPs on the test strip.

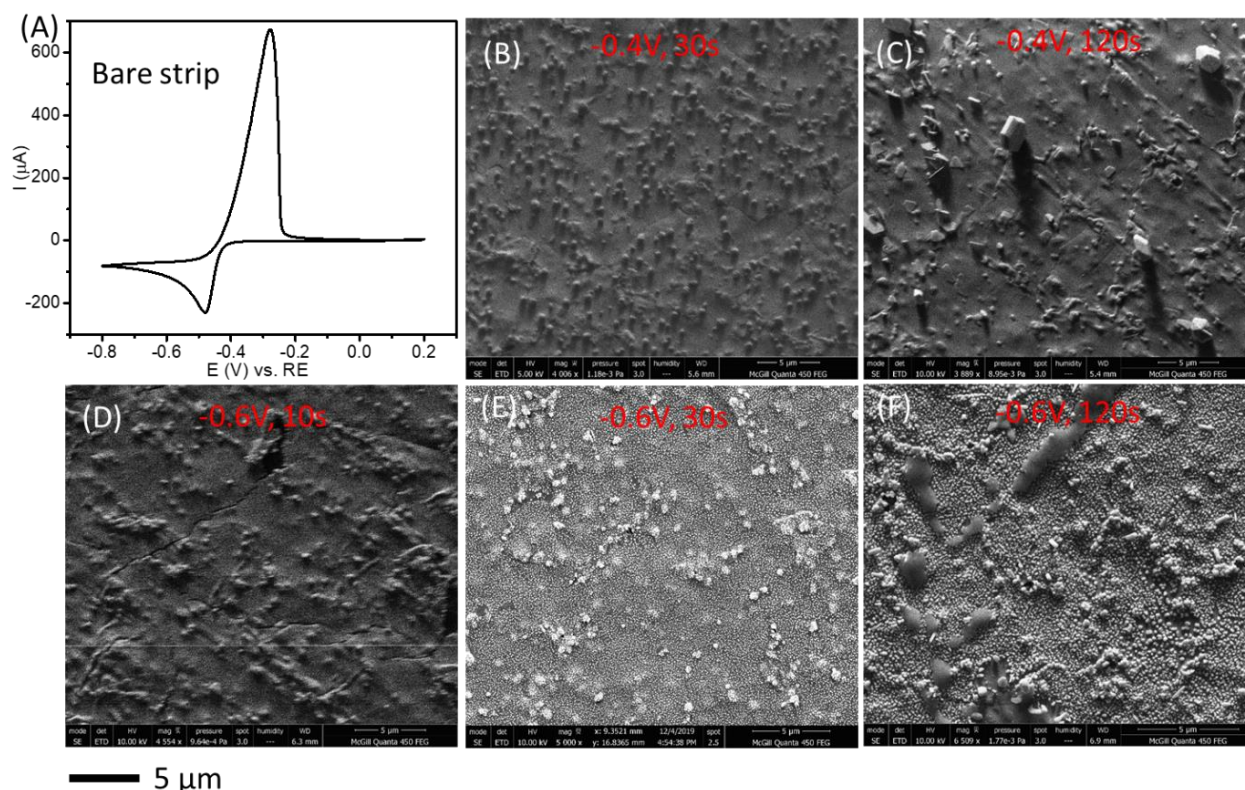


**Figure 5.3 Optimization of parameters used for electrodeposition:** CV response of the bare test strip for silver nitrate (A) and SEM images (B-F) of AgNP-coated test strips via electrodeposition with different applied voltage and duration times.

To study the parameters that have an effect on the formation and deposition of AgNPs regarding morphology and size, different voltages and duration times are explored under same conditions. The used solution for electrodeposition contains silver precursor  $\text{AgNO}_3$  at a concentration of 10 mM and the supporting electrolyte  $\text{KNO}_3$ . To make sure that the applied voltages are high enough to reduce  $\text{AgNO}_3$ , a CV measurement is performed firstly to confirm the critical voltage needed for reduction. As shown in **Figure 5.3A**, the reduction occurs once the voltage reaches -0.4 V. Thus two different voltages at -0.4 V and -0.6 V are explored. On the other side, a series of duration times of 10 s, 30 s, 120 s are applied and explored. Later, to compare the deposition of AgNPs under those conditions, morphology characterization is conducted using SEM.

As shown in **Figure 5.3**, at -0.4 V, less AgNPs are generated on the strip so that the surface of the strip is barely covered. With the increase of time, the size of AgNPs is increasing but the amount doesn't change much. When the applied voltage is -0.6 V, only few AgNPs are grown on the strip

when the duration time is too short (10 s). The number of AgNPs is increased significantly when the duration time is increased to 30 s, leading to a full coverage on the strip. With the same deposition time, compared to -0.4 V, the nanoparticles deposited at -0.6 V are denser and smaller. Besides, it is also worth noticing that the nanoparticles are spherical with uniform size when the voltages at both values are applied for 30 s. However, for both conditions at -0.4 V and -0.6 V, when the duration time is increased to 120 s, some nanoparticles grow into much larger particles or chunks. In addition, the morphologies of the particles also change significantly from sphere to polyhedron. Considering better reproducibility from uniformly distributed nanoparticles and stronger enhancement from silver particles within nanometer range, a final condition at -0.6 V for 30 s is decided for further fabrication of the AgNP-coated test strip.

### 5.1.3 Evaluation of EC and SERS performances on the AgNP-deposited test strip

With the confirmation of successful deposition of AgNPs on the bimetallic test strip, the performances of the AgNP-deposited test strip for EC and SERS are then evaluated respectively with test probes potassium ferricyanide and 4-ATP. For the evaluation of EC behavior, in the presence of potassium ferricyanide in the electrolyte, CV responses are recorded respectively on both AgNP-coated strip electrode and bare test strip electrode without AgNP modification. The collected CV curves are then analyzed and compared. The results show that the AgNP-coated strip electrode shows comparable electrochemical reactivity with similar current response as the bare test strip (**Figure 3.4, Figure 4.2C**). As for the evaluation of SERS performance, SERS measurements for the test molecule 4-ATP are collected on both AgNP-coated test strip and bare test strip. The Raman signal of 4-ATP on AgNP-coated strip is much stronger, while the result on the bare test strip barely shows observable signal (**Figure 4.2D**), indicating a significant enhancing ability from AgNPs. To conclude, the results show that the AgNP-coated test strip is suitable for both EC and SERS, and it can be further used as a sensing platform for dual-modal detection via SERS and EC.

## 5.2 Detection methods based on different transducers

There are various types of sensors depending on the used detection methods. To develop a sensor that is useful at PON, it is important to choose the detection methods since they greatly affect many factors that are crucial for PON applications. For example, the sample preparation, response time,

and the cost can be very different for different types of sensors. This thesis in particular developed a multifunctional sensing platform that works for both SERS and EC, two of the most commonly used sensing techniques. Therefore, this section discusses SERS and EC with emphasis of their suitability for PON sensors.

SERS is a surface technique to enhance Raman scattering on plasmonic substrates such as metallic nanostructures or nanoparticles. Raman spectroscopy is a characteristic technique that fingerprints the chemical and structural information of the target molecule that further enables molecular detection. When target molecules are located within the proximity of a plasmonic substrate, Raman signals can be improved up to  $10^{14}$  order of magnitude, and it is known as SERS. Hence, SERS is a highly sensitive and specific detection method. EC, on the other hand, is a commonly used sensing method for biological molecules such as glucose and urea. Except for high sensitivity and specificity, EC sensors are also widely used as commercial products due to their portability, making them a good choice for PON applications. Therefore, SERS and EC are chosen as detection methods in this work. In addition, the utilization of AgNPs on a conductive test strip also provides an ideal platform for both methods due to their optical and electrical properties. Further, with the evaluation on SERS and EC performance, the AgNP-coated strip has been proven to be a promising dual-modal sensing substrate for SERS and EC measurements. It is further demonstrated for chlorfenapyr detection, where multimodal detection via both EC and SERS is utilized, allowing for characteristic identification via SERS and quantitative analysis via EC.

### **5.3 Applications of the AgNP-deposited test strip**

After the fabrication, characterization, and evaluation of both SERS and EC performance, the AgNP-deposited test strip is explored for the detection of analytes for applications to medical diagnosis and food safety. Its sensing performance for different analytes are discussed here. Sensing parameters like LOD and the linear detection range are discussed in particular since they are important factors to evaluate its potential for applications at PON.

In addition, as discussed previously, AgNPs are deposited on the commercial test strip to achieve specificity and the ability for SERS enhancement. The deposition of AgNPs improves the specificity of the test strip for urea detection because of the catalytic ability of silver. AgNPs can also enhance SERS signals significantly, enabling multimodal detection for chlorfenapyr via both

EC and SERS. Therefore, in this section, the catalytic reactivity of the AgNP-deposited test strip for urea detection is discussed as well by comparing with the bare test strip without deposited AgNPs. On the other hand, its ability for multimodal detection of chlorfenapyr via EC and SERS is also discussed by comparing with a reference substrate, i.e., a test strip coated with AgNPs via drop casting.

### 5.3.1 Urea detection via EC on the AgNP-deposited test strip

In **chapter III**, urea detection is conducted on the fabricated AgNP-coated test strip, and the fabricated platform is explored for urea detection via EC. Urea is not only an important by-product that is involved in metabolism but also a potential additive used in dairy products that are considered to be disqualified. As a result, the detection of urea is of importance for our health not only for disease diagnosis, but also for food safety.

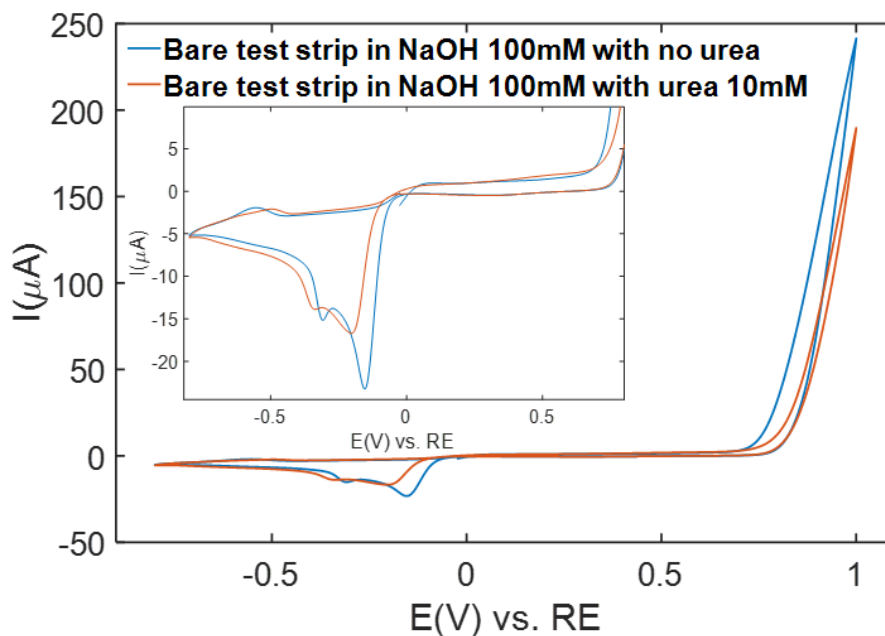


**Figure 5.4.** CV response of the bare test strip (without AgNP deposition) in the absence and presence of urea.

Electrolyte: NaOH 0.1M, scan rate: 20 mV/s

To confirm the function of deposited AgNPs, control experiment of urea detection on bare test strip is conducted before the electrodeposition of AgNPs. As shown in **Figure 5.4**, no oxidation peak corresponding to urea hydrolysis is observed on bare test strip when CV is performed. But urea oxidation is detected on the test strip after modification with AgNPs, indicating that the bare strip is not able to detect urea. Compared with **Figure 3.5A** that shows urea detection on the AgNP-

coated test strip, oxidation peaks corresponding to urea hydrolysis is observed in reverse scan. It is because of the catalytic ability of AgNPs. More specifically, the oxidized AgNPs catalyze the reaction of urea with water, leading to oxidation peaks that are correlated with urea. In other words, the deposition of AgNPs provides the specificity for urea detection.

A series of EC measurements for urea detection using the AgNP-deposited test strip are then performed to explore its sensing performance including the linear detection range, reaction regime, sensitivity, LOD, and other performances that are important for PON applications such as reproducibility. As shown in **Figure 3.5**, the linear relation between the peak current and the square root of scan rates indicates the diffusion controlled mechanism of the reaction. A linear detection range of 1 - 8 mM provides information about its working range as well as sensitivity and LOD. Since the physiological concentration range of urea is within 1 – 8 mM, this platform will be useful for urea detection in medical diagnosis to monitor the health condition. More importantly, its LOD is 141.9  $\mu\text{M}$ , which is comparable with other reported biosensors for urea detection, but our substrate shows advantages of low cost and simple fabrication over the other biosensors.

Further, more parameters for urea detection on this substrate are explored to evaluate its potential for applications at PON. In specific, reproducibility that indicates its variation, reliability, reusability, stability that is vital for the shelf life, and the selectivity are explored (**Figure 4.3**). The result of selectivity shows that this sensing platform is exclusively working for urea and won't be affected in the presence of interference molecules like glucose. The stability test shows it can last for at least 10 days without much variation in detected signals, which needs to be further explored with longer time for future applications as a commercial product. The reusability shows decrease with multiple cycles, but it is acceptable since this strip can be made disposable to maintain high accuracy. And results on different strips for urea detection at same concentration show that the AgNP-coated strip is reproducible.

For practical applications, it is important to evaluate the ability of the platform to work for urea detection in real samples. Therefore, real sample analysis is also explored by detecting urea that is added in reconstituted plasma and milk samples. Based on the calibration plot obtained before, the theoretical concentration found in the samples are calculated and compared to the added amount, thus the recovery rates for urea detection in real samples are obtained (**Table 4.2, Figure 5.5**). The results show better recovery of urea in milk compared to plasma sample. However, for both

samples, it is expected to further improve the accuracy for recovery, which can be explored from sample preparation as well as improving the sensitivity of the platform.

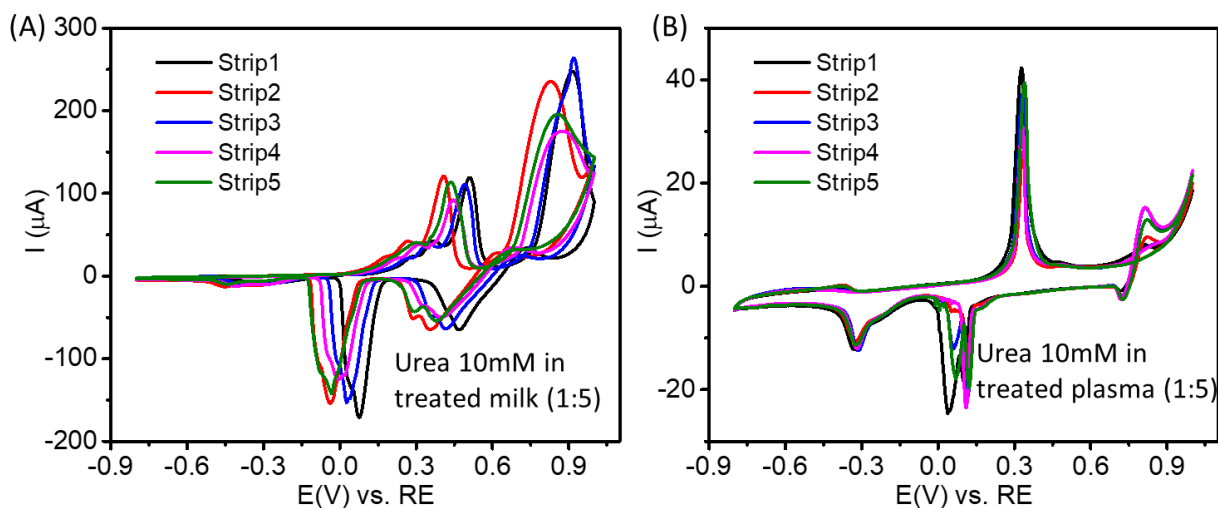


**Figure 5.5. Urea detection in real samples on the AgNP-coated test strip:** CV response for the detection of urea in milk (A) and plasma (B) samples

### 5.3.2 Chlorfenapyr detection via EC and SERS on the AgNP-deposited test strip

Urea detection using this platform demonstrates its potential for EC detection. Further, its ability to work as a multimodal sensor is investigated with a different analyte, chlorfenapyr, an insecticide that is used in plants such as in chives. It is a potential food contaminant that is toxic for human. The detection of chlorfenapyr is performed via both SERS and EC. It is the first time to report analytical detection of chlorfenapyr via EC, and SERS is combined to complement characteristic identification.

For EC detection, CV measurements are performed in the presence of a probe molecule, potassium ferricyanide. When CV responses of the probe molecule at the same concentration on the AgNP-coated strip are compared in the presence and in the absence of chlorfenapyr, a shift in the potential of the oxidation peak of ferricyanide is observed (**Figure 4.4**). Linear detection is obtained from the concentration 20 ppm to 50 ppm with a LOD at 4.2 ppm. Although it is not as low as other traditional techniques such as HPLC that can reach much a lower LOD in  $10^{-3}$  ppm range, the

linear detection range and LOD fulfill the demand for the detection of tolerable chlorfenapyr residues in vegetables such as chive according to federal regulations code in the U.S.

Further, the potential of the substrate for the use in real applications is explored by detecting chlorfenapyr mixed with chive supernatants. Considering that the tolerance concentration of chlorfenapyr residue for chive is 20 ppm, a final concentration of 20 ppm is prepared in the supernatants of chive leafs. The recovery rates are then calculated to be ~98% (**Table 4.1**), indicating the ability of this method to and detect and recover chlorfenapyr from real samples with high accuracy. For a further implementation into industrial level, more work will need to be done to improve reproducibility.

Although the detection of chlorfenapyr via EC shows quantitative results, characteristic detection that confirms the unique fingerprint of chlorfenapyr is still needed to improve the reliability. Therefore, SERS is utilized as a complementary detection method on the same sensing platform to validate the presence of chlorfenapyr since SERS can fingerprint analytes by providing Raman peaks corresponding to chemical bonds. As mentioned before, the platform is designed for a multimodal detection. The modification with AgNPs enables significant enhancement for SERS detection. Chlorfenapyr has a  $C\equiv N$  group that distinguishes it from other insecticides, thus it can be used as the characteristic “fingerprint”. Its corresponding peak via SERS is at  $2230\text{ cm}^{-1}$ . As a result, the characteristic peak for chlorfenapyr is identified at  $2230\text{ cm}^{-1}$ . On the AgNP-coated strip, the characteristic peak is detected and a limit of detection at 7 ppm is obtained when exploring different concentrations of chlorfenapyr. However, due to the fact that SERS signal is significantly dependent on the location and alignment of analyte on the SERS substrate, SERS detection on this substrate may not be suitable for quantitative identification. The combination with EC detection compensates for this disadvantage since EC provides quantitative measurements. Therefore, this substrate provides a multifunctional platform that combines both SERS and EC to realize the identification and quantification of chlorfenapyr.

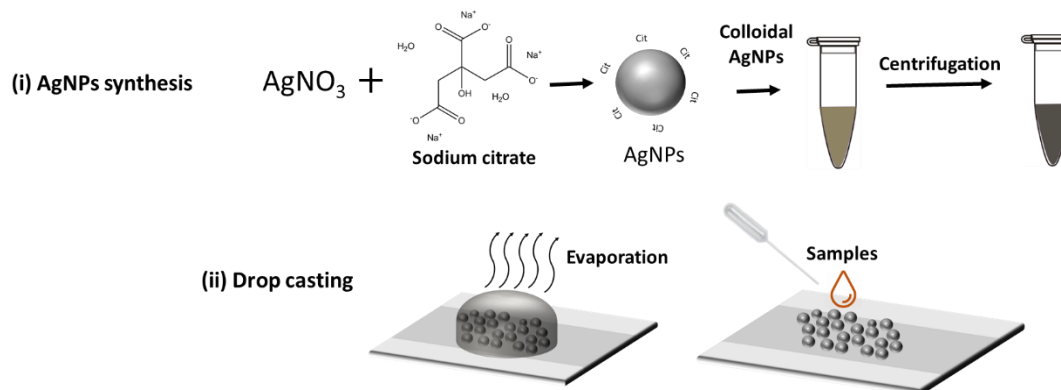


**Figure 5.6** Schematic representation of the fabrication of AgNP-coated test strips via drop casting colloidal AgNPs. (i) The synthesis and concentration of the colloidal AgNPs; (ii) The deposition of colloidal AgNPs on the test strip via drop casting

Additionally to the AgNP coated test strip prepared by electrodeposition (electrodeposited AgNP-coated test strip), a reference substrate prepared by drop casting AgNPs on a test strip is also fabricated and utilized for chlorfenapyr detection (**Figure 5.6**). Colloidal AgNPs are synthesized via chemical reduction. They are then characterized via UV-vis spectroscopy and SEM (**Figure 5.7**). The absorbance spectra indicates the uniform distribution of the size of AgNPs at near 50-60 nm and SEM further confirms the distribution of size and also demonstrates their spherical morphology.

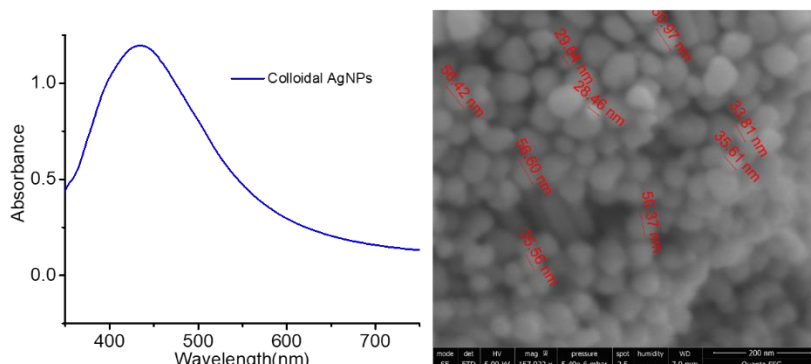


**Figure 5.7** Morphology characterization of colloidal AgNPs. (Left) Absorbance spectrum of colloidal AgNPs reduced by sodium citrate; (Right) SEM image of colloidal AgNPs reduced by sodium citrate

After characterization, the colloidal AgNPs are drop cast on the test strip and then used to run CV and SERS measurements for chlorfenapyr detection (**Figure 4.4B**, **Figure 4.3D**). However, it is not able to detect chlorfenapyr via EC, even though there is no problem for SERS detection. As a

result, to achieve analytical detection for chlorfenapyr, electrodeposition of AgNPs on the test strip is preferred for the fabrication of multimodal AgNP-deposited test strip.

## Chapter VI: Conclusions and perspectives

### 6.1 Conclusions

In conclusion, to develop sensors for applications at PON, comprehensive exploration of different sensor parameters are presented. A multi-functional sensing platform is established, characterized, and explored for applications to health care and food safety are studied to demonstrate its potential for PON applications. This platform is serving as an EC sensor as well as a SERS sensor that provides accurate and rapid detection of multiple analytes. In addition to that, the sensor is developed in a simple way at low cost, which is very important for the applications at PON. In detail, the proposed sensor is built from a unique nanocomposite material consisting of metallic nanoparticles and a bimetallic strip and it is then explored for applications to diagnostics and food safety. Specifically, two objectives are achieved. First, novel nanocomposite based electrode/substrate for molecular detection is developed and characterized. This substrate is composed of AgNPs and modified commercial glucose test strips that are composed of bimetallic Au-Pd electrodes. Second, the substrate is used for molecular detection of two analytes, which are potential biomarker and food contaminant that are related to human health and food safety.

As described in this thesis, applications at PON are closely related to our life. Sensors that are developed for PON applications provide a powerful tool to monitor our health condition or the food quality which is significant for our health. This thesis offers a comprehensive exploration on the parameters that are important for the development of sensors for applications at PON in chapter II, where I reviewed the fundamentals, materials, sensing performance such as sensitivity and so on in the field of plasmonic biosensors. I discussed the effects and the importance of each factor with correlation to specific applications. The discussion on fundamentals, commonly used materials with different properties, structures and how they affect the optical properties, as well as the detection methods and the working principles on how they are implemented for specific applications provides an in-depth understanding of the perspective on the design and fabrication of biosensors. Further, this chapter presents the current status, potential, and challenges for the development of plasmonic biosensors at PON, opening up novel avenues for the development of PON sensors, especially for plasmonic biosensors that require specialized equipment and how they can be expanded out of laboratories to point of need.

Therefore, based on the discussion about the design specifications such as the sensitivity, portability, as well as the simplicity of the sensing device, I developed a novel multimodal sensing platform via EC and SERS used it for the detection of molecules that are relevant for health care and food safety at PON. Two analytes, urea and chlorfenapyr, are detected using this platform. More specifically, I detected urea via EC, and detected chlorfenapyr via EC and SERS to achieve complimentary detection. Within the physiological concentration, I measured a linear detection range for urea detection. Further, I conducted real sample analysis of urea in reconstituted plasma and milk samples, and showed that the fabricated substrate has the potential to be used in practical applications to health monitoring at PON, such as a home test assay kit. On the other hand, I measured a linear detection range for chlorfenapyr within the practical concentration range via EC, and achieved characteristic determination of chlorfenapyr via SERS. In addition, I performed real sample analysis of chlorfenapyr in a vegetable sample chive and evaluated the potential for practical applications. The results for both analytes detection demonstrate the promising potential of the substrate for various applications at PON.

The development of this substrate based on a modified commercial test strip with electrodeposition of AgNPs demonstrates a novel way for the design of a sensing platform regarding the selection of the components and materials that can be easily obtained and modified with built-in EC system, as well as the manufacturing methods that is simple and suitable for the selected platform. For the detection of urea using this substrate, with the systematic exploration and evaluation on the sensing performance for urea, it provides a prototype for a home test assay kit to monitor urea, which allows for the regular monitoring of urea level, especially for people who are suffering from kidney related diseases. As for the multimodal detection of chlorfenapyr, it opens up a new way for chlorfenapyr detection via electrochemistry. In addition, the combination of SERS and EC utilizing the fabricated substrate shows a strategy of how to design and make use of composite materials for specific applications. Further, this system also demonstrates possibilities for PON applications using different detection methods. To conclude, the work accomplished in this thesis opens up the way for the development of sensing platforms that is highly accurate and cost effective.

## 6.2 Outlook

With more and more attention being paid to PON applications that are highly connected with our life, the demand for sensors developed for the use in applications at PON is also increasing. Therefore, it is imperative to fully understand the mechanism of the techniques involved as well as the key factors that play an important role in PON applications. In this thesis, a multifunctional substrate is established for different applications to health care and food safety with consideration of the key factors that are important for PON applications. Specifically, as discussed in **Chapter III and IV**, after fabrication of the sensing substrate, it was used and adapted into different applications to urea and chlorfenapyr detection. Since it is modified from a low cost commercial test strip that is portable, it is beneficial for the applications at PON. The evaluation of the substrate for urea and chlorfenapyr detection paves the first step for further implementation in practical applications. Based on different applications demonstrated in **chapter III and IV**, future work to improve the substrate in specific applications are still needed and it is discussed here.

For urea detection on this substrate, the whole test strip including three electrodes (RE, CE, and WE) is utilized and the working electrode is modified with AgNPs to achieve the catalytic functionality. When it is used for EC detection, a drop of the sample is deposited on the tip of the strip, covering the area that is in contact with three electrodes. On the other end of the test strip, these three electrodes are connected to the potentiostat, which provides space for the implementation of a portable potentiostat and a reader. Regarding the techniques used for measurements, in addition to CV, it can also be simplified to applying a constant voltage to reduce the response time. Based on the target analyte, a calibration plot can be obtained. Thus, the concentration of the target analyte in the detected sample can be calculated based on the relation between the concentration and the output signal. The whole detection system including the strip and the simplified potentiostat and reading screen is not complicated, which makes it a suitable device for home test assay or personal use.

In this thesis, the substrate has been applied to urea detection, within a linear detection range from 1 – 8 mM that is in the physiological range. The calibration plot is also obtained based on the measurements of urea at different concentrations. Moreover, other performance of the platform for urea detection including reproducibility, stability has also been evaluated. The results demonstrate the ability of this system to be further used in practical applications. To further implement the

AgNP-coated test strip into a commercial sensing device that can be used in home test assay kit or for personnel, it can be integrated with a portable simplified potentiostat combined with a reader or micro-computer to process data and display results. However, the sensing performances such as reproducibility and stability will need to be further improved and validated so the sensor can reach the industrial standard before commercialization.

The other application of the developed substrate is for chlorfenapyr detection. Chlorfenapyr is an insecticide that can be used on plants such as cottons and some vegetables, which brings potential food contamination that is harmful for human health. This thesis provides the first step for further application. Differently from urea detection, when used for chlorfenapyr detection, the AgNP-coated strip substrate is cut from the whole strip. The cut part AgNP-coated substrate is then used as a dual functional substrate: as SERS substrate and also as EC working electrode. Then chlorfenapyr is detected using this substrate via both EC and SERS. When it is detected via EC, the substrate is used as a working electrode, and the experiment is performed in a glass cell, together with a reference electrode (Ag/AgCl) and a counter electrode (Pt). Compared to the setup on the whole strip, this setup is less portable. On the other hand, the identification of chlorfenapyr is accomplished via SERS while EC detection provides analytical measurements. Compared to its utilization for urea detection, this application requires Raman spectrometer, which is not suitable for personal use due to the fact that it is expensive, big, and training demanding. Consequently, this substrate for chlorfenapyr detection is not appropriate for home test or personal uses as it was the case for urea detection demonstrated in **chapter III**. However, it shows promising potential for food quality control in settings that handle food or grocery in large scale such as grocery store due to its low cost and simple fabrication compared to the traditional techniques used for chlorfenapyr detection that require lab settings.

## References

1. Liu, J., et al., *Are plasmonic optical biosensors ready for use in point-of-need applications?* Analyst, 2020. **145**(2): p. 364-384.
2. Liu, J., et al., *An AgNP-deposited commercial electrochemistry test strip as a platform for urea detection.* Scientific Reports, 2020. **10**(1): p. 9527.
3. Liu, J., et al., *Multimodal electrochemical and SERS platform for chlorfenapyr detection.* Applied Surface Science, 2021. **566**: p. 150617.
4. Chao, J., et al., *Nanostructure-based surface-enhanced Raman scattering biosensors for nucleic acids and proteins.* Journal of Materials Chemistry B, 2016. **4**(10): p. 1757-1769.
5. Zheng, J. and L. He, *Surface-Enhanced Raman Spectroscopy for the Chemical Analysis of Food.* Comprehensive reviews in food science and food safety, 2014. **13**(3): p. 317-328.
6. Bantz, K.C., et al., *Recent progress in SERS biosensing.* Physical Chemistry Chemical Physics, 2011. **13**(24): p. 11551-11567.
7. Avella-Oliver, M., et al., *Label-free SERS analysis of proteins and exosomes with large-scale substrates from recordable compact disks.* Sensors and Actuators B: Chemical, 2017. **252**: p. 657-662.
8. Kahraman, M., et al., *Fabrication and characterization of flexible and tunable plasmonic nanostructures.* Scientific reports, 2013. **3**: p. 3396.
9. Grieshaber, D., et al., *Electrochemical biosensors-sensor principles and architectures.* Sensors, 2008. **8**(3): p. 1400-1458.
10. Hammond, J.L., et al., *Electrochemical biosensors and nanobiosensors.* Essays in biochemistry, 2016. **60**(1): p. 69-80.
11. Kahraman, M., et al., *Fundamentals and applications of SERS-based bioanalytical sensing.* Nanophotonics, 2017. **6**(5): p. 831-852.
12. Luo, X., et al., *Application of nanoparticles in electrochemical sensors and biosensors.* Electroanalysis, 2006. **18**(4): p. 319-326.
13. Heller, A. and B. Feldman, *Electrochemical Glucose Sensors and Their Applications in Diabetes Management.* Chemical Reviews, 2008. **108**(7): p. 2482-2505.
14. Kong, X.M., et al., *Detecting explosive molecules from nanoliter solution: A new paradigm of SERS sensing on hydrophilic photonic crystal biosilica.* Biosensors & Bioelectronics, 2017. **88**: p. 63-70.
15. Sanati, A., et al., *A review on recent advancements in electrochemical biosensing using carbonaceous nanomaterials.* Microchimica Acta, 2019. **186**(12): p. 773.
16. Ronkainen, N.J., H.B. Halsall, and W.R. Heineman, *Electrochemical biosensors.* Chem Soc Rev, 2010. **39**(5): p. 1747-63.
17. McMurry, J., R.C. Fay, and J.K. Robinson, *Chemistry.* 2015.
18. Allen J. Bard, L.R.F., *Electrochemical Methods: Fundamentals and Applications, New York: Wiley, 2001, 2nd ed.* Russian Journal of Electrochemistry, 2002. **38**(12): p. 1364-1365.
19. Shinwari, M.W., et al., *Microfabricated Reference Electrodes and their Biosensing Applications.* Sensors, 2010. **10**(3).
20. Zhang, J.X.J. and K. Hoshino, *Chapter 4 - Electrical transducers: Electrochemical sensors and semiconductor molecular sensors, in Molecular Sensors and Nanodevices (Second Edition), J.X.J. Zhang and K. Hoshino, Editors. 2019, Academic Press. p. 181-230.*
21. Zoski, C.G., *Handbook of electrochemistry.* 2006: Elsevier.
22. Elgrishi, N., et al., *A practical beginner's guide to cyclic voltammetry.* 2018. **95**(2): p. 197-206.
23. Li, X., et al., *A nonenzymatic hydrogen peroxide sensor based on Au-Ag nanotubes and chitosan film.* Journal of Electroanalytical Chemistry, 2014. **735**: p. 19-23.

24. Oliveira, G.C.M., et al., *Flexible platinum electrodes as electrochemical sensor and immunosensor for Parkinson's disease biomarkers*. Biosens Bioelectron, 2020. **152**: p. 112016.
25. Yang, P., et al., *A method for determination of glucose by an amperometric bienzyme biosensor based on silver nanocubes modified Au electrode*. Sensors and Actuators B: Chemical, 2014. **194**: p. 71-78.
26. Shao, Y., et al., *Graphene Based Electrochemical Sensors and Biosensors: A Review*. Electroanalysis, 2010. **22**(10): p. 1027-1036.
27. Song, N.-n., et al., *A novel electrochemical biosensor for the determination of dopamine and ascorbic acid based on graphene oxide /poly(aniline-co-thionine) nanocomposite*. Journal of Electroanalytical Chemistry, 2020. **873**: p. 114352.
28. Zhang, Y., et al., *A laccase based biosensor on AuNPs-MoS<sub>2</sub> modified glassy carbon electrode for catechol detection*. Colloids and Surfaces B: Biointerfaces, 2020. **186**: p. 110683.
29. Hrapovic, S., et al., *Electrochemical Biosensing Platforms Using Platinum Nanoparticles and Carbon Nanotubes*. Analytical Chemistry, 2004. **76**(4): p. 1083-1088.
30. Wall, S., *The history of electrokinetic phenomena*. Current Opinion in Colloid & Interface Science, 2010. **15**(3): p. 119-124.
31. Helmholtz, H., *Ueber einige Gesetze der Vertheilung elektrischer Ströme in körperlichen Leitern mit Anwendung auf die thierisch-elektrischen Versuche*. Annalen der Physik, 1853. **165**(6): p. 211-233.
32. Brownson, D.A. and C.E. Banks, *Interpreting electrochemistry*, in *The handbook of graphene electrochemistry*. 2014, Springer. p. 23-77.
33. del Caño, R., et al., *Hemoglobin becomes electroactive upon interaction with surface-protected Au nanoparticles*. Talanta, 2018. **176**: p. 667-673.
34. Zhu, H., et al., *Effects of cyclic voltammetric scan rates, scan time, temperatures and carbon addition on sulphation of Pb disc electrodes in aqueous H<sub>2</sub>SO<sub>4</sub>*. Materials Technology, 2016: p. 1-6.
35. Scholz, F., *Electroanalytical methods*. Vol. 1. 2010: Springer.
36. Scholz, F., *Voltammetric techniques of analysis: the essentials*. ChemTexts, 2015. **1**(4): p. 17.
37. Macdonald, J.R. and E. Barsoukov, *Impedance spectroscopy: theory, experiment, and applications*. History, 2005. **1**(8): p. 1-13.
38. Chooto, P., *Cyclic voltammetry and its applications*, in *Voltammetry*. 2019, IntechOpen.
39. Elgrishi, N., et al., *A Practical Beginner's Guide to Cyclic Voltammetry*. Journal of Chemical Education, 2018. **95**(2): p. 197-206.
40. Chang, B.-Y. and S.-M. Park, *Electrochemical Impedance Spectroscopy*. Annual Review of Analytical Chemistry, 2010. **3**(1): p. 207-229.
41. Khan, M.Z.H., et al., *Ultrasensitive detection of pathogenic viruses with electrochemical biosensor: State of the art*. Biosensors and Bioelectronics, 2020. **166**: p. 112431.
42. Mishra, G.K., et al., *Food Safety Analysis Using Electrochemical Biosensors*. Foods, 2018. **7**(9).
43. Rassaei, L., et al., *Nanoparticles in electrochemical sensors for environmental monitoring*. TrAC Trends in Analytical Chemistry, 2011. **30**(11): p. 1704-1715.
44. Wang, J., *Electrochemical Sensors*, in *Analytical Electrochemistry*. 2006. p. 201-243.
45. Stevenson, H., et al., *A Rapid Response Electrochemical Biosensor for Detecting Thc In Saliva*. Scientific Reports, 2019. **9**(1): p. 12701.
46. Wang, Z. and Z. Dai, *Carbon nanomaterial-based electrochemical biosensors: an overview*. Nanoscale, 2015. **7**(15): p. 6420-6431.
47. Otero, F. and E. Magner, *Biosensors—Recent Advances and Future Challenges in Electrode Materials*. Sensors, 2020. **20**(12).

48. Malekzad, H., et al., *Noble metal nanoparticles in biosensors: recent studies and applications*. Nanotechnology Reviews, 2017. **6**(3): p. 301-329.
49. Xiao, X., P. Si, and E. Magner, *An overview of dealloyed nanoporous gold in bioelectrochemistry*. Bioelectrochemistry, 2016. **109**: p. 117-126.
50. Wittstock, A., A. Wichmann, and M. Bäumer, *Nanoporous Gold as a Platform for a Building Block Catalyst*. ACS Catalysis, 2012. **2**(10): p. 2199-2215.
51. Chen, L.Y., et al., *Nanoporous gold for enzyme-free electrochemical glucose sensors*. Scripta Materialia, 2011. **65**(1): p. 17-20.
52. Xia, Y., et al., *Nonenzymatic amperometric response of glucose on a nanoporous gold film electrode fabricated by a rapid and simple electrochemical method*. Biosensors and Bioelectronics, 2011. **26**(8): p. 3555-3561.
53. Vassilyev, Y.B., O.A. Khazova, and N.N. Nikolaeva, *Kinetics and mechanism of glucose electrooxidation on different electrode-catalysts: Part I. Adsorption and oxidation on platinum*. Journal of Electroanalytical Chemistry and Interfacial Electrochemistry, 1985. **196**(1): p. 105-125.
54. Hwang, D.-W., et al., *Recent advances in electrochemical non-enzymatic glucose sensors – A review*. Analytica Chimica Acta, 2018. **1033**: p. 1-34.
55. Xiao, X., et al., *Nanoporous Gold-Based Biofuel Cells on Contact Lenses*. ACS Applied Materials & Interfaces, 2018. **10**(8): p. 7107-7116.
56. Masuda, H., et al., *Highly ordered nanochannel-array architecture in anodic alumina*. Applied Physics Letters, 1997. **71**(19): p. 2770-2772.
57. Szamocki, R., et al., *Tailored mesostructuring and biofunctionalization of gold for increased electroactivity*. Angew Chem Int Ed Engl, 2006. **45**(8): p. 1317-21.
58. Hu, K., et al., *Electrochemical DNA Biosensor Based on Nanoporous Gold Electrode and Multifunctional Encoded DNA–Au Bio Bar Codes*. Analytical Chemistry, 2008. **80**(23): p. 9124-9130.
59. Xiao, X., et al., *Nanoporous gold assembly of glucose oxidase for electrochemical biosensing*. Electrochimica Acta, 2014. **130**: p. 559-567.
60. Meng, F., et al., *Nanoporous gold as non-enzymatic sensor for hydrogen peroxide*. Electrochimica Acta, 2011. **56**(12): p. 4657-4662.
61. Maduraiveeran, G., M. Sasidharan, and V. Ganesan, *Electrochemical sensor and biosensor platforms based on advanced nanomaterials for biological and biomedical applications*. Biosensors and Bioelectronics, 2018. **103**: p. 113-129.
62. Hu, T., et al., *Colorimetric sandwich immunosensor for Aβ(1-42) based on dual antibody-modified gold nanoparticles*. Sensors and Actuators B: Chemical, 2017. **243**: p. 792-799.
63. Li, J., X. Wei, and Y. Yuan, *Synthesis of magnetic nanoparticles composed by Prussian blue and glucose oxidase for preparing highly sensitive and selective glucose biosensor*. Sensors and Actuators B: Chemical, 2009. **139**(2): p. 400-406.
64. Yuan, Y., et al., *A signal-on electrochemical probe-label-free aptasensor using gold–platinum alloy and stearic acid as enhancers*. Biosensors and Bioelectronics, 2010. **26**(2): p. 881-885.
65. Shabalina, A.V., et al., *Copper Nanoparticles for Ascorbic Acid Sensing in Water on Carbon Screen-printed Electrodes*. Analytical Sciences, 2017. **33**(12): p. 1415-1419.
66. Jamkhande, P.G., et al., *Metal nanoparticles synthesis: An overview on methods of preparation, advantages and disadvantages, and applications*. Journal of Drug Delivery Science and Technology, 2019. **53**: p. 101174.
67. Antuña-Jiménez, D., et al., *Screen-Printed Electrodes Modified with Metal Nanoparticles for Small Molecule Sensing*. Biosensors, 2020. **10**(2).
68. Nasirpouri, F., et al., *Chapter 24 - Electrodeposition of anticorrosion nanocoatings*, in *Corrosion Protection at the Nanoscale*, S. Rajendran, et al., Editors. 2020, Elsevier. p. 473-497.

69. McCreery, R.L., *Advanced Carbon Electrode Materials for Molecular Electrochemistry*. Chemical Reviews, 2008. **108**(7): p. 2646-2687.
70. Vestergaard, M.d., et al., *A Rapid Label-Free Electrochemical Detection and Kinetic Study of Alzheimer's Amyloid Beta Aggregation*. Journal of the American Chemical Society, 2005. **127**(34): p. 11892-11893.
71. Geim, A.K. and K.S. Novoselov, *The rise of graphene*. Nature Materials, 2007. **6**(3): p. 183-191.
72. Geim, A.K. and K.S. Novoselov, *The rise of graphene*, in *Nanoscience and Technology*. 2009, Co-Published with Macmillan Publishers Ltd, UK. p. 11-19.
73. Lee, C., et al., *Measurement of the elastic properties and intrinsic strength of monolayer graphene*. Science, 2008. **321**(5887): p. 385-8.
74. Stoller, M.D., et al., *Graphene-Based Ultracapacitors*. Nano Letters, 2008. **8**(10): p. 3498-3502.
75. Wu, J., W. Pisula, and K. Müllen, *Graphenes as Potential Material for Electronics*. Chemical Reviews, 2007. **107**(3): p. 718-747.
76. Novoselov, K.S., et al., *Electric Field Effect in Atomically Thin Carbon Films*. Science, 2004. **306**(5696): p. 666.
77. Somani, P.R., S.P. Somani, and M. Umeno, *Planer nano-graphenes from camphor by CVD*. Chemical Physics Letters, 2006. **430**(1): p. 56-59.
78. Kim, K.S., et al., *Large-scale pattern growth of graphene films for stretchable transparent electrodes*. Nature, 2009. **457**(7230): p. 706-710.
79. Datta, S.S., et al., *Crystallographic Etching of Few-Layer Graphene*. Nano Letters, 2008. **8**(7): p. 1912-1915.
80. Gass, M.H., et al., *Free-standing graphene at atomic resolution*. Nature Nanotechnology, 2008. **3**(11): p. 676-681.
81. Huc, V., et al., *Large and flat graphene flakes produced by epoxy bonding and reverse exfoliation of highly oriented pyrolytic graphite*. Nanotechnology, 2008. **19**(45): p. 455601.
82. Shukla, A., et al., *Graphene made easy: High quality, large-area samples*. Solid State Communications, 2009. **149**(17): p. 718-721.
83. Choi, W., et al., *Synthesis of Graphene and Its Applications: A Review*. Critical Reviews in Solid State and Materials Sciences, 2010. **35**(1): p. 52-71.
84. Jenkins, G.M., A. Jenkins, and K. Kawamura, *Polymeric carbons: carbon fibre, glass and char*. 1976: Cambridge University Press.
85. Engstrom, R.C. and V.A. Strasser, *Characterization of electrochemically pretreated glassy carbon electrodes*. Analytical Chemistry, 1984. **56**(2): p. 136-141.
86. Van der Linden, W.E. and J.W. Dieker, *Glassy carbon as electrode material in electro-analytical chemistry*. Analytica Chimica Acta, 1980. **119**(1): p. 1-24.
87. Monerris, M.J., et al., *Electrochemical immunosensor based on gold nanoparticles deposited on a conductive polymer to determine estrone in water samples*. Microchemical Journal, 2016. **129**: p. 71-77.
88. Alim, S., et al., *Enhanced direct electron transfer of redox protein based on multiporous SnO<sub>2</sub> nanofiber-carbon nanotube nanocomposite and its application in biosensing*. International Journal of Biological Macromolecules, 2018. **114**: p. 1071-1076.
89. Huang, K.-J., et al., *Electrochemical biosensor based on silver nanoparticles-polydopamine-graphene nanocomposite for sensitive determination of adenine and guanine*. Talanta, 2013. **114**: p. 43-48.
90. Monošík, R., M. Stred'anský, and E. Šturdík, *Application of Electrochemical Biosensors in Clinical Diagnosis*. Journal of Clinical Laboratory Analysis, 2012. **26**(1): p. 22-34.
91. Ivnitski, D., et al., *Application of Electrochemical Biosensors for Detection of Food Pathogenic Bacteria*. Electroanalysis, 2000. **12**(5): p. 317-325.

92. Badihi-Mossberg, M., V. Buchner, and J. Rishpon, *Electrochemical Biosensors for Pollutants in the Environment*. *Electroanalysis*, 2007. **19**(19-20): p. 2015-2028.
93. Rishpon, J., *Electrochemical biosensors for environmental monitoring*. *Rev Environ Health*, 2002. **17**(3): p. 219-47.
94. Sun, A., et al. *A low-cost smartphone-based electrochemical biosensor for point-of-care diagnostics*. in *2014 IEEE Biomedical Circuits and Systems Conference (BioCAS) Proceedings*. 2014.
95. LaGier, M.J., et al., *An electrochemical RNA hybridization assay for detection of the fecal indicator bacterium Escherichia coli*. *Marine pollution bulletin*, 2005. **50**(11): p. 1251-1261.
96. Mollarasouli, F., S. Kurbanoglu, and S.A. Ozkan, *The Role of Electrochemical Immunosensors in Clinical Analysis*. *Biosensors*, 2019. **9**(3): p. 86.
97. Thatikayala, D., et al., *Progress of Advanced Nanomaterials in the Non-Enzymatic Electrochemical Sensing of Glucose and H<sub>2</sub>O<sub>2</sub>*. *Biosensors*, 2020. **10**(11).
98. Wang, G., et al., *Non-enzymatic electrochemical sensing of glucose*. *Microchimica Acta*, 2013. **180**(3): p. 161-186.
99. Ismail, B.P. and S.S. Nielsen, *Analysis of Food Contaminants, Residues, and Chemical Constituents of Concern*, in *Food Analysis*, S.S. Nielsen, Editor. 2017, Springer International Publishing: Cham. p. 573-597.
100. Singh, C., et al., *Functionalized MoS<sub>2</sub> nanosheets assembled microfluidic immunosensor for highly sensitive detection of food pathogen*. *Sensors and Actuators B: Chemical*, 2018. **259**: p. 1090-1098.
101. Jiang, X., et al., *Immunosensors for detection of pesticide residues*. *Biosensors and Bioelectronics*, 2008. **23**(11): p. 1577-1587.
102. Anirudhan, T.S. and S. Alexander, *Design and fabrication of molecularly imprinted polymer-based potentiometric sensor from the surface modified multiwalled carbon nanotube for the determination of lindane ( $\gamma$ -hexachlorocyclohexane), an organochlorine pesticide*. *Biosensors and Bioelectronics*, 2015. **64**: p. 586-593.
103. Kahraman, M., et al., *Fundamentals and applications of SERS-based bioanalytical sensing*, in *Nanophotonics*. 2017. p. 831.
104. Raman, C.V. and K.S. Krishnan, *A New Type of Secondary Radiation*. *Nature*, 1928. **121**(3048): p. 501-502.
105. Rayleigh, L., X. *On the electromagnetic theory of light*. *The London, Edinburgh, and Dublin Philosophical Magazine and Journal of Science*, 1881. **12**(73): p. 81-101.
106. Ellis, D.I. and R. Goodacre, *Metabolic fingerprinting in disease diagnosis: biomedical applications of infrared and Raman spectroscopy*. *Analyst*, 2006. **131**(8): p. 875-885.
107. Movasaghi, Z., S. Rehman, and I.U. Rehman, *Raman Spectroscopy of Biological Tissues*. *Applied Spectroscopy Reviews*, 2007. **42**(5): p. 493-541.
108. Sharma, B., et al., *SERS: materials, applications, and the future*. *Materials today*, 2012. **15**(1): p. 16-25.
109. Hao, B., et al., *Determination of Hg<sup>2+</sup> in water based on acriflavine functionalized AgNPs by SERS*. *Microchemical Journal*, 2020. **155**: p. 104736.
110. Perumal, J., et al., *Towards a point-of-care SERS sensor for biomedical and agri-food analysis applications: a review of recent advancements*. *Nanoscale*, 2021. **13**(2): p. 553-580.
111. Suarasan, S., et al., *Superhydrophobic bowl-like SERS substrates patterned from CMOS sensors for extracellular vesicle characterization*. *Journal of Materials Chemistry B*, 2020. **8**(38): p. 8845-8852.
112. Fortuni, B., et al., *In situ synthesis of Au-shelled Ag nanoparticles on PDMS for flexible, long-life, and broad spectrum-sensitive SERS substrates*. *Chemical Communications*, 2017. **53**(82): p. 11298-11301.
113. Leonardo, S., B. Prieto-Simón, and M. Campàs, *Past, present and future of diatoms in biosensing*. *TrAC Trends in Analytical Chemistry*, 2016. **79**: p. 276-285.

114. Chamuah, N., et al., *A naturally occurring diatom frustule as a SERS substrate for the detection and quantification of chemicals*. Journal of Physics D: Applied Physics, 2017. **50**(17): p. 175103.
115. Dolatabadi, J.E.N. and M. de la Guardia, *Applications of diatoms and silica nanotechnology in biosensing, drug and gene delivery, and formation of complex metal nanostructures*. TrAC Trends in Analytical Chemistry, 2011. **30**(9): p. 1538-1548.
116. Rojalin, T., et al., *Hybrid Nanoplasmonic Porous Biomaterial Scaffold for Liquid Biopsy Diagnostics Using Extracellular Vesicles*. ACS Sensors, 2020. **5**(9): p. 2820-2833.
117. Justino, C.I., T.A. Rocha-Santos, and A.C. Duarte, *Review of analytical figures of merit of sensors and biosensors in clinical applications*. TrAC Trends in Analytical Chemistry, 2010. **29**(10): p. 1172-1183.
118. Špačková, B., et al., *Optical Biosensors Based on Plasmonic Nanostructures: A Review*. Proceedings of the IEEE, 2016. **104**(12): p. 2380-2408.
119. Guselnikova, O., et al., *Pretreatment-free selective and reproducible SERS-based detection of heavy metal ions on DTPA functionalized plasmonic platform*. Sensors and Actuators B: Chemical, 2017. **253**: p. 830-838.
120. Jain, P.K., et al., *Calculated Absorption and Scattering Properties of Gold Nanoparticles of Different Size, Shape, and Composition: Applications in Biological Imaging and Biomedicine*. The Journal of Physical Chemistry B, 2006. **110**(14): p. 7238-7248.
121. Kelly, K.L., et al., *The Optical Properties of Metal Nanoparticles: The Influence of Size, Shape, and Dielectric Environment*. The Journal of Physical Chemistry B, 2003. **107**(3): p. 668-677.
122. Lee, P.C. and D. Meisel, *Adsorption and surface-enhanced Raman of dyes on silver and gold sols*. The Journal of Physical Chemistry, 1982. **86**(17): p. 3391-3395.
123. Karaballi, R.A., et al., *Development of an electrochemical surface-enhanced Raman spectroscopy (EC-SERS) aptasensor for direct detection of DNA hybridization*. Physical Chemistry Chemical Physics, 2015. **17**(33): p. 21356-21363.
124. Greene, B.H.C., et al., *Electrochemical-Surface Enhanced Raman Spectroscopic (EC-SERS) Study of 6-Thiouric Acid: A Metabolite of the Chemotherapy Drug Azathioprine*. The Journal of Physical Chemistry C, 2017. **121**(14): p. 8084-8090.
125. Goodall, B.L., A.M. Robinson, and C.L. Brosseau, *Electrochemical-surface enhanced Raman spectroscopy (E-SERS) of uric acid: a potential rapid diagnostic method for early preeclampsia detection*. Physical Chemistry Chemical Physics, 2013. **15**(5): p. 1382-1388.
126. Kahl, M., et al., *Periodically structured metallic substrates for SERS*. Sensors and Actuators B: Chemical, 1998. **51**(1): p. 285-291.
127. Miranda-Hernández, M., et al., *Identification of different silver nucleation processes on vitreous carbon surfaces from an ammonia electrolytic bath*. Journal of Electroanalytical Chemistry, 1998. **443**(1): p. 81-93.